Lecture 22

A. The third Paradigm in HQA

B. Generalized pilot-wave framework

The state-of-the-art theoretical model of Bauyrzhan Primkulov

- goes beyond variable-phase model by fully treating vertical dynamics

Vertical dynamics:

$$\ddot{z}_p = F_N(\tau) - Bo$$

Horizontal dynamics:

$$\ddot{\mathbf{x}}_p + (\mathscr{D}_h F_N(\tau) + \mathscr{D}_a)\dot{\mathbf{x}}_p = -F_N(\tau)\nabla h$$

Normal force:

$$F_N(\tau) = -\mathscr{H}(-z_p + z_b + h)[\mathscr{D}_v(\dot{z}_p - \dot{z}_b - \dot{h}) + \mathscr{C}_v(z_p - z_b - h)]$$

Linear drag

Surface tension: linear spring

Pilot wave:

$$h(\mathbf{x},\tau) = \cos(\Omega\tau/2)\sum_{i=1}^{n} A_i e^{-\frac{\tau-\tau_i}{\tau_F Me}}(\tau-\tau_i)^{-1/2} J_0(k_F r)[1 + (\xi r K_1(\xi r) - 1)e^{-r^{-2}}]$$

where $A_i = \frac{4}{3}\sqrt{2\pi Oh_e}\frac{k_F^3}{3k_F^2 + Bo}\int_{\tau_c} F_N(s)\sin(\Omega s/2)ds$

Impact time, position:

$$\tau_i = \frac{\int_{\tau_c} F_N(s)s\,ds}{\int_{\tau_c} F_N(s)ds}, \quad \mathbf{x}_i = \frac{\int_{\tau_c} F_N(s)\mathbf{x}_p(s)ds}{\int_{\tau_c} F_N(s)ds}$$

- captures a number of phenomena that have to date eluded rationalization

Nonresonant effects not captured with strobe models

Swaying start-up

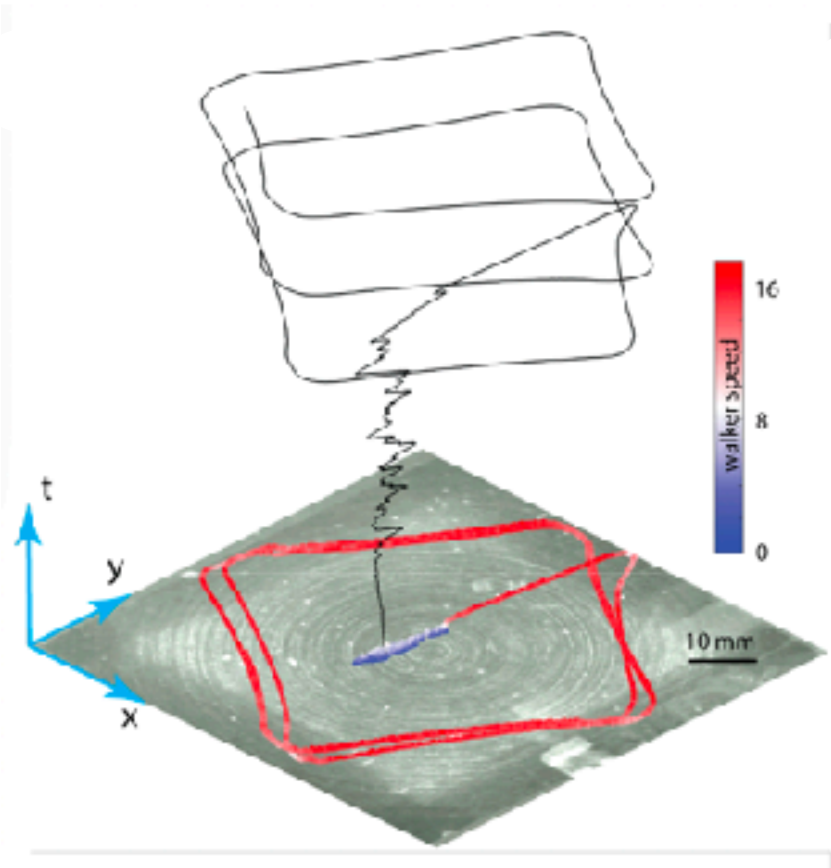

Intermittent walking

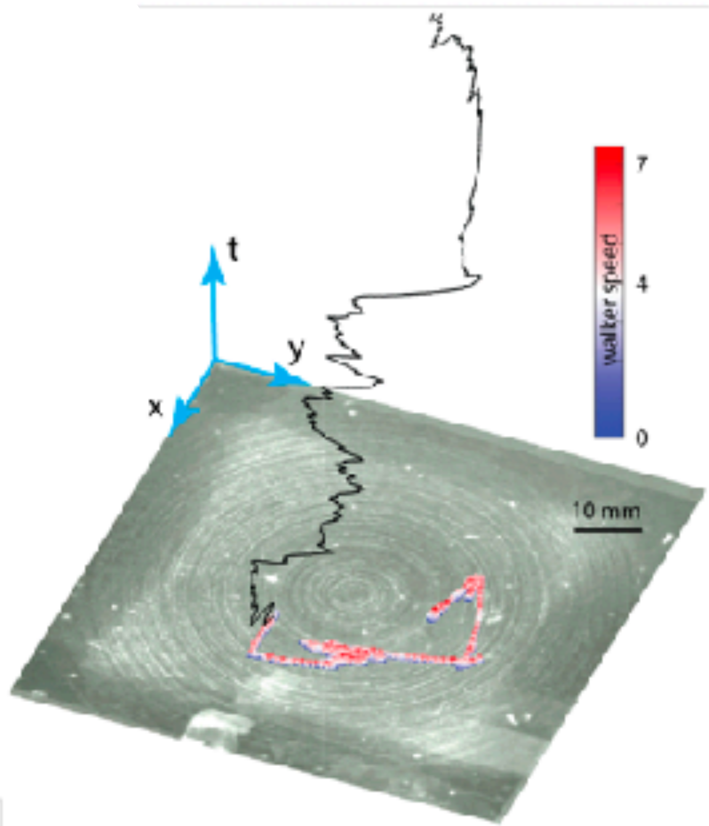

Mode switching

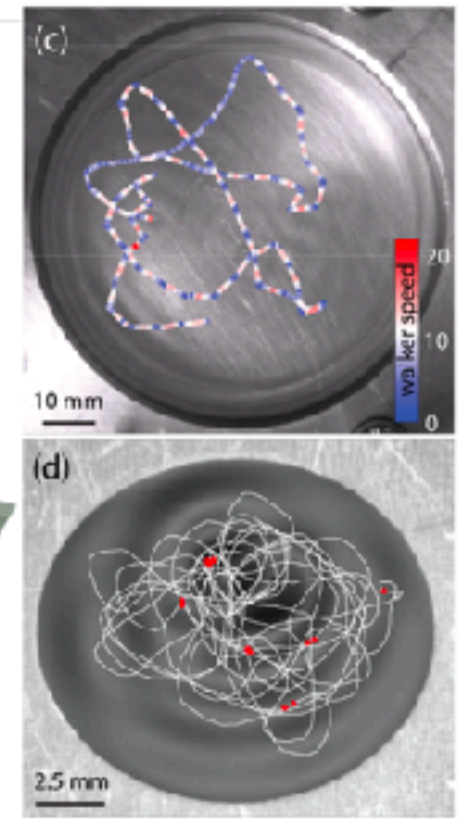

Phase flipping

Swaying start-up

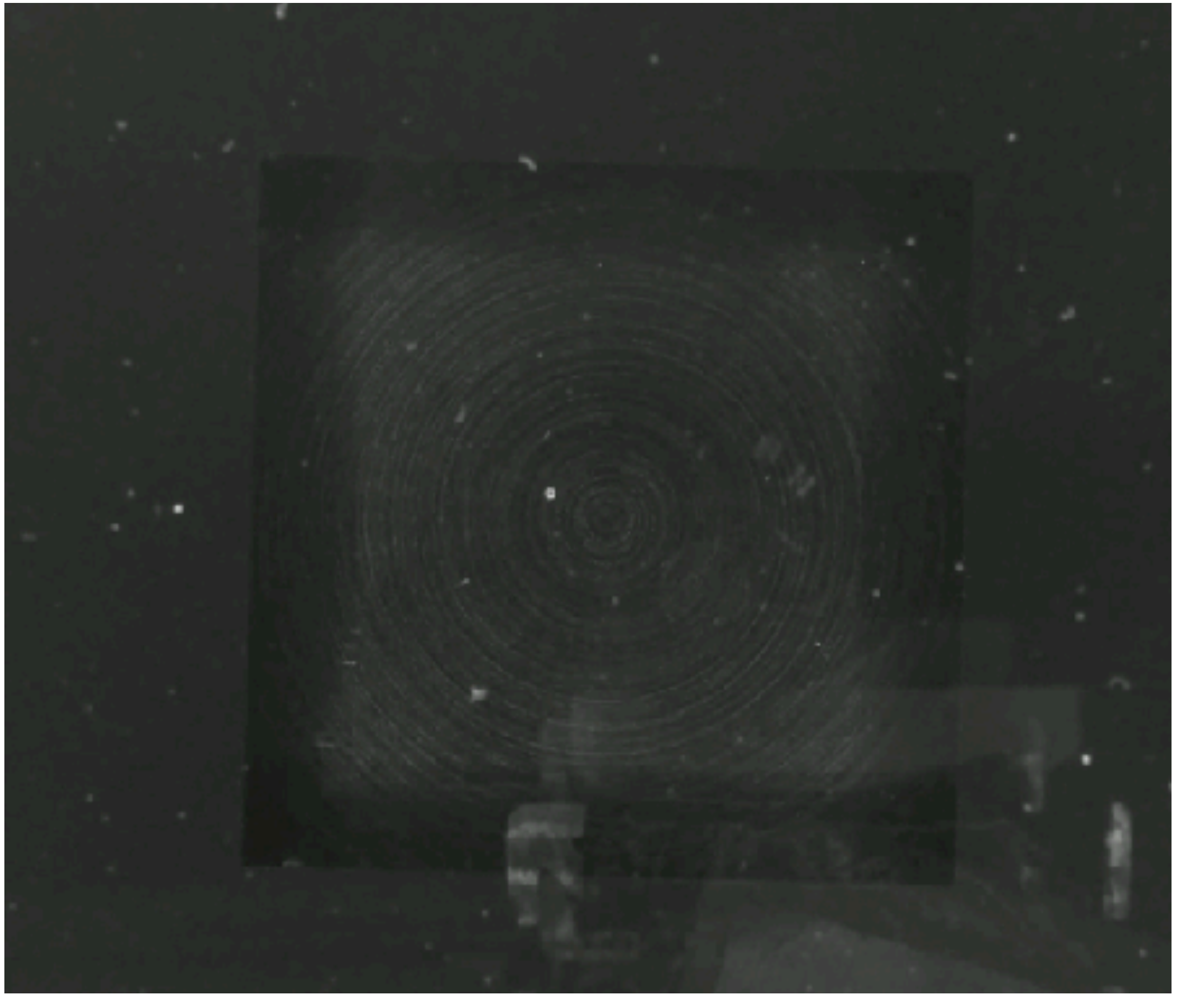

$f = 70$ Hz and 20 cSt

$f = 70$ Hz and 20 cSt

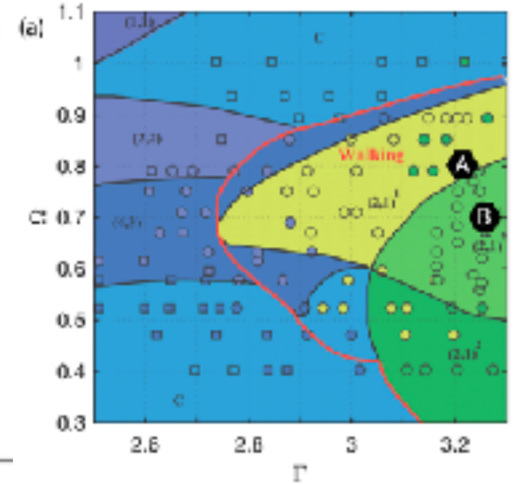

The swaying start-up of the (2,1) walker: Simulation

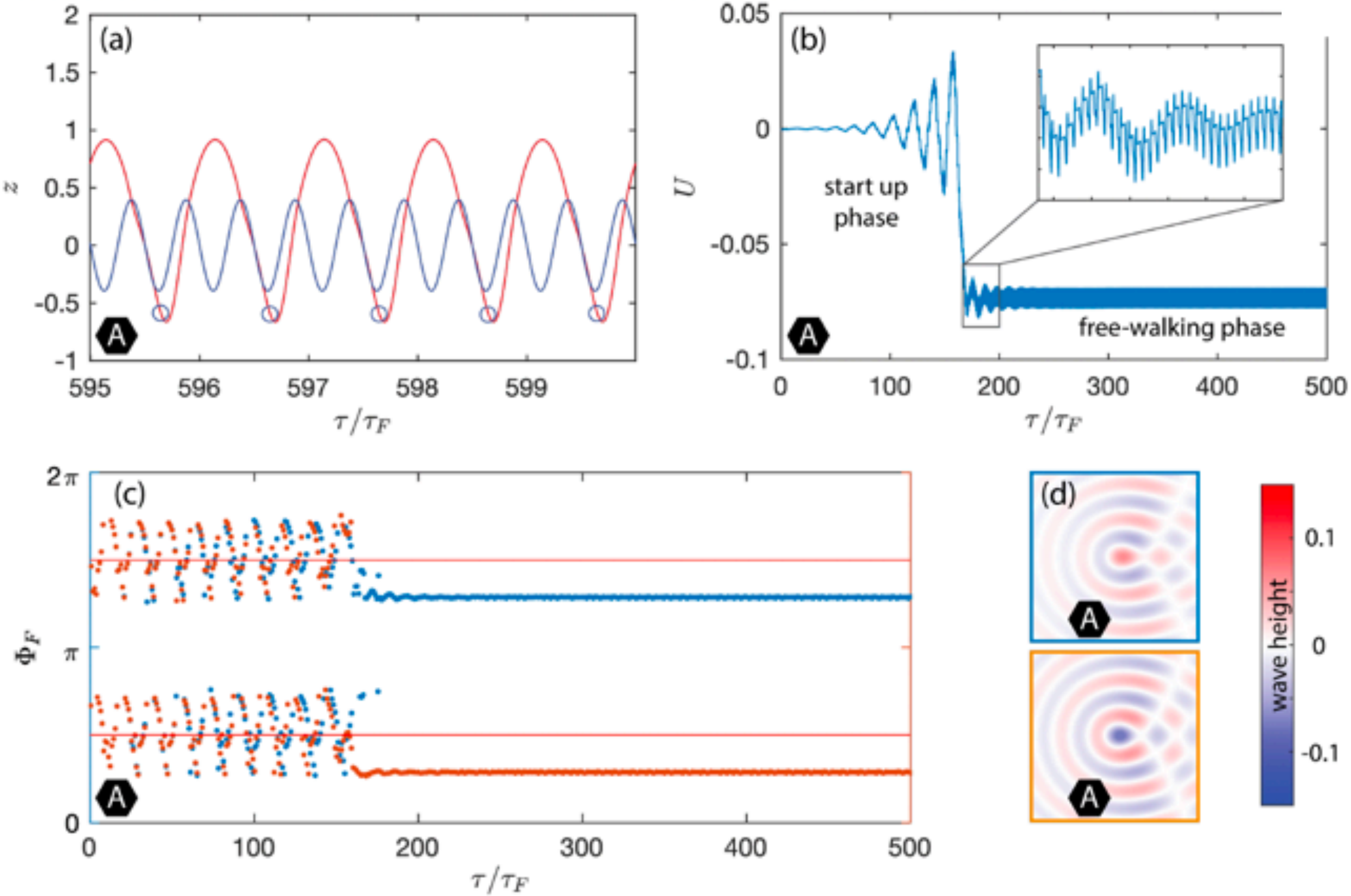

Mixed-state, `mode-switching' walkers

Experiments

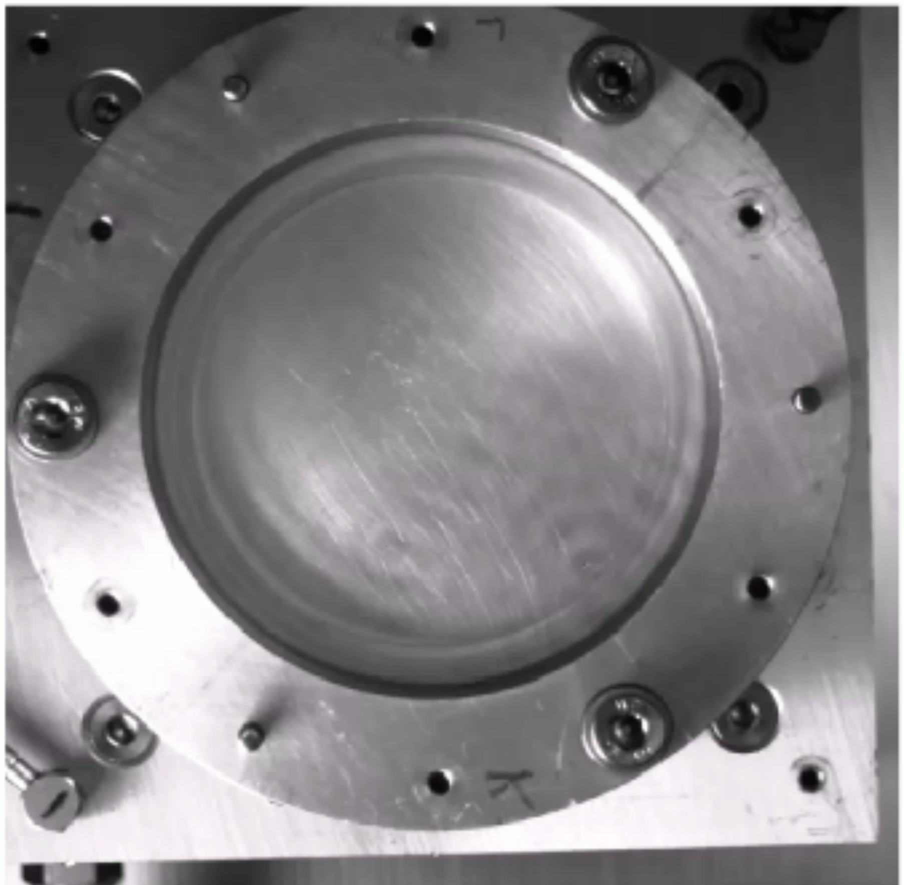

Simulations

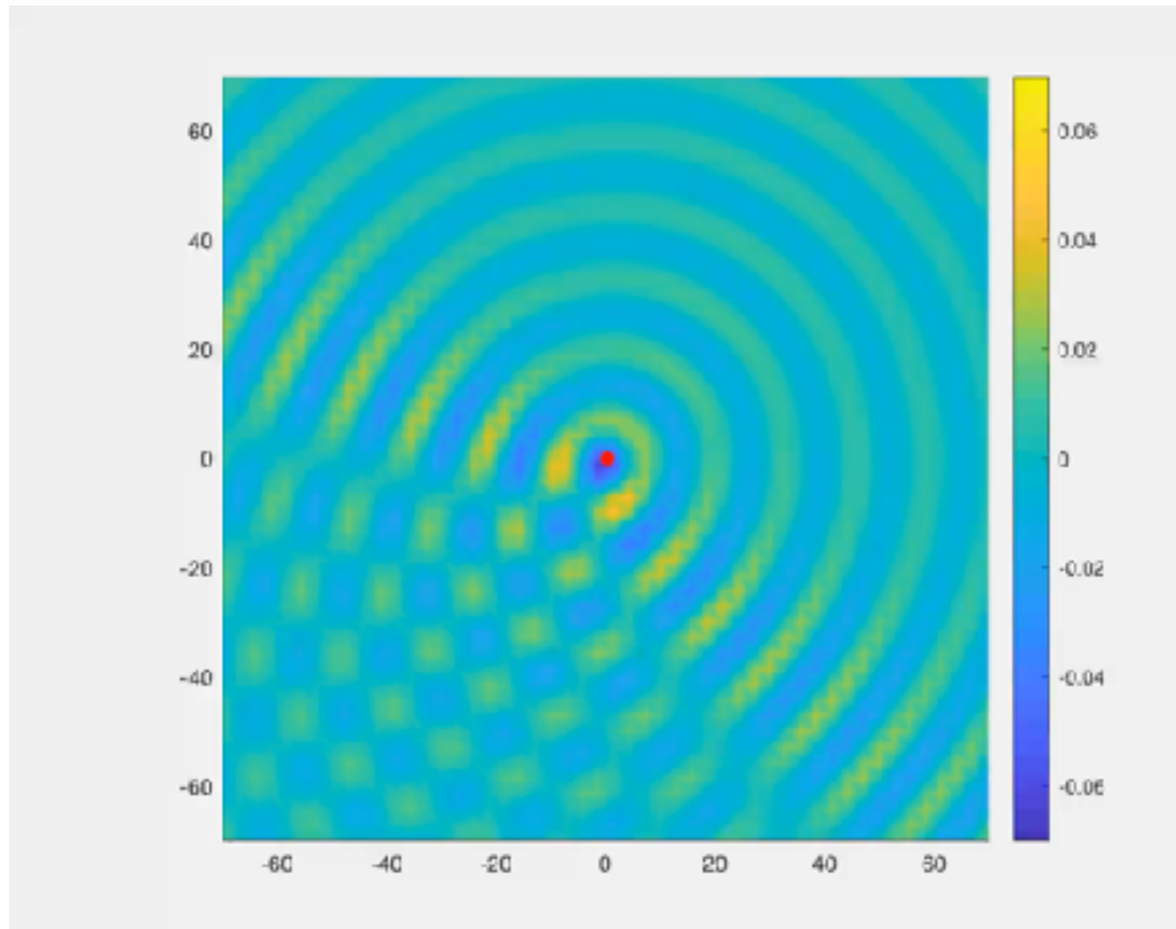

- what we thought was periodic switching between $(2,1)^1$ and $(2,1)^2$ modes is actually a …

  … (22,11) mode!

$f = 70$ Hz and 20 cSt

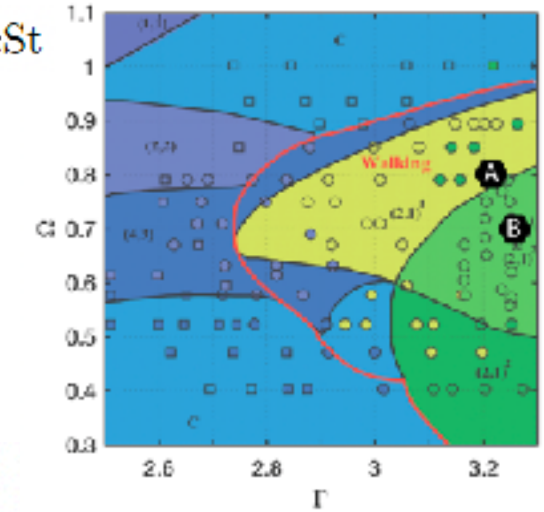

Mixed-state, `mode-switching' walkers

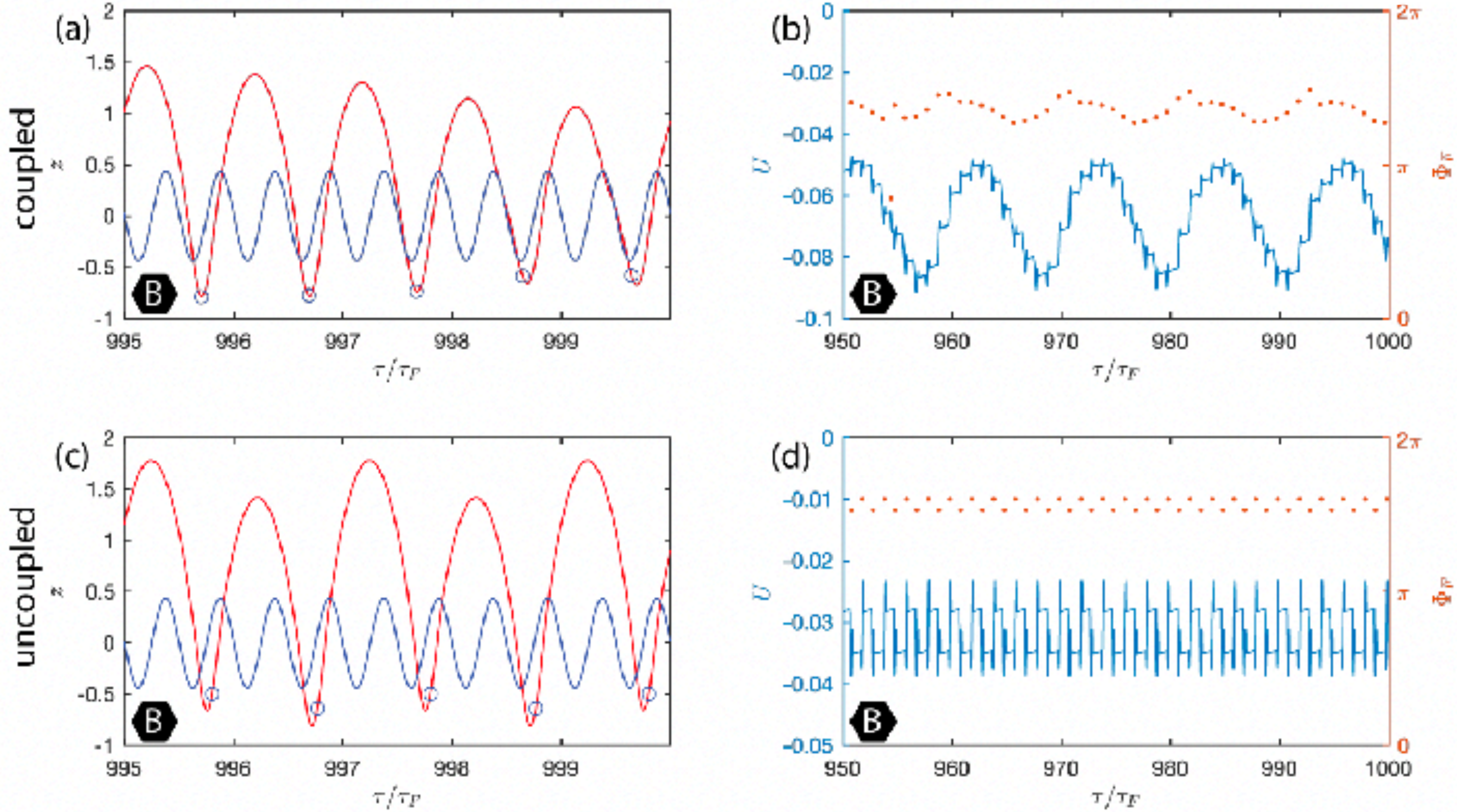

Intermittent walking

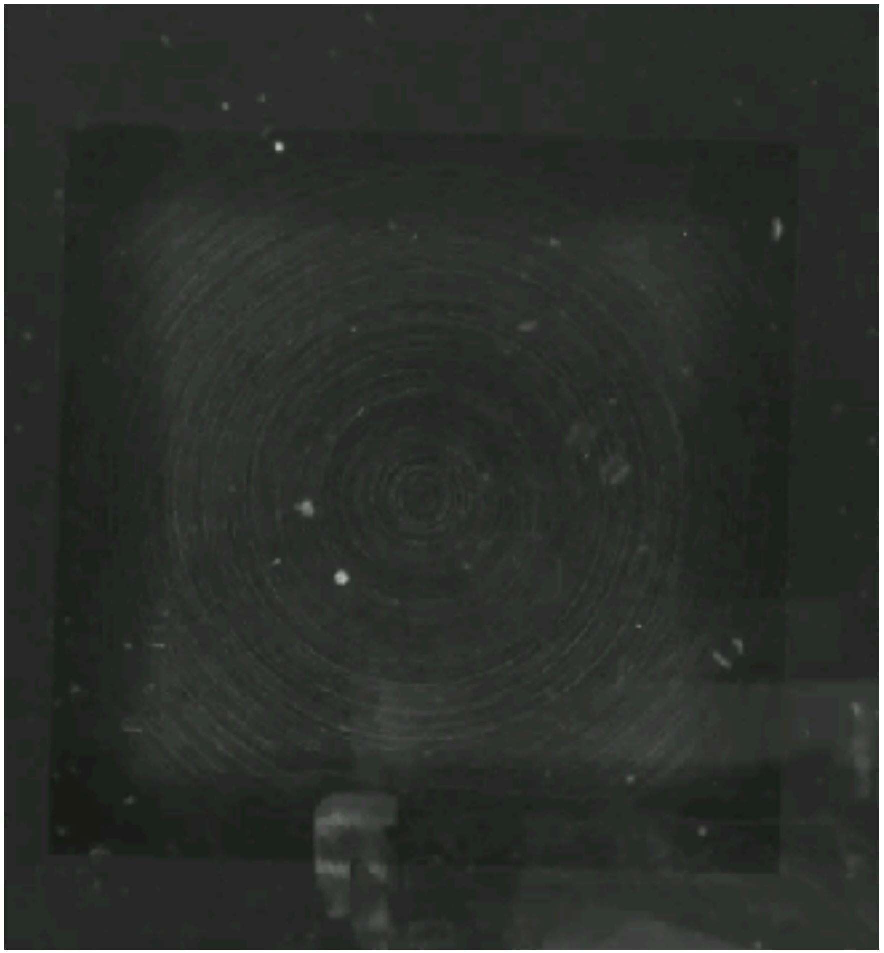

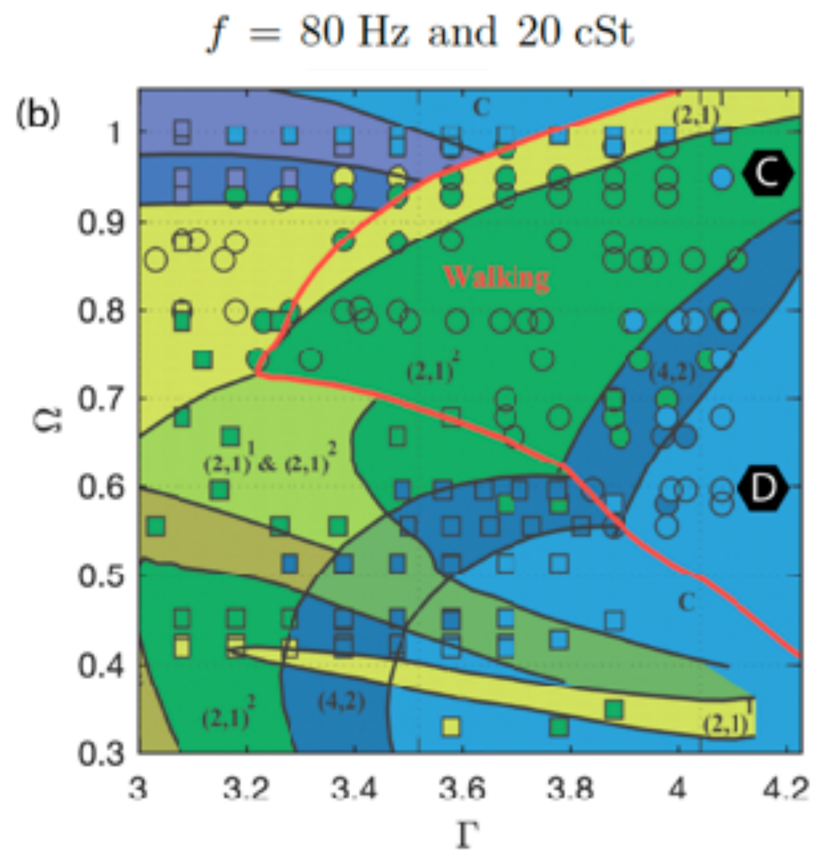

$f = 80$ Hz and 20 cSt

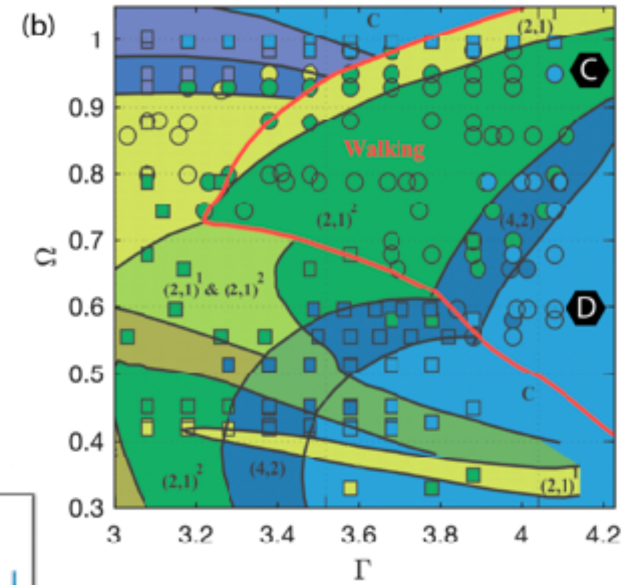

Intermittent walker

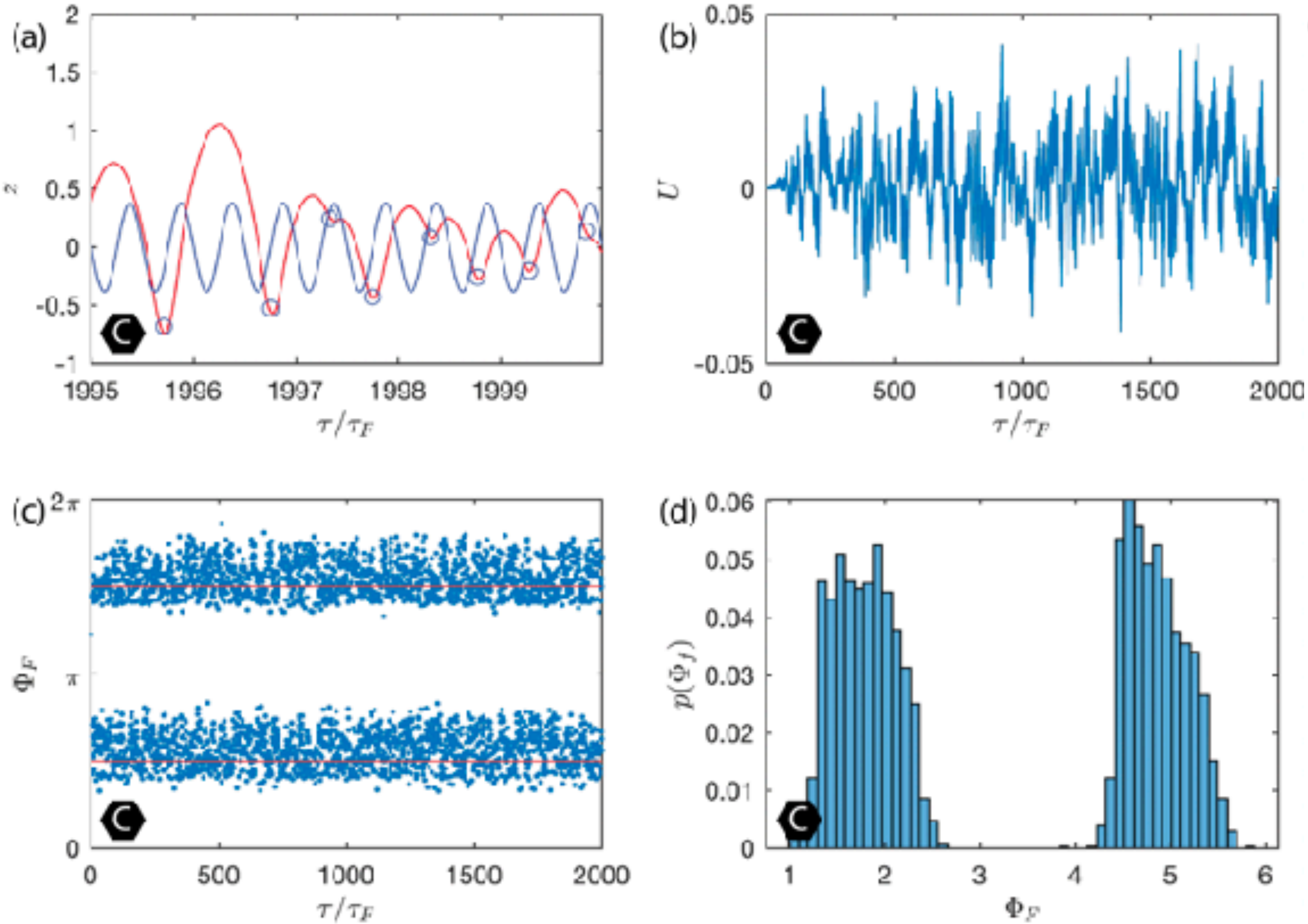

Chaotic walker

$f = 80$ Hz and 20 cSt

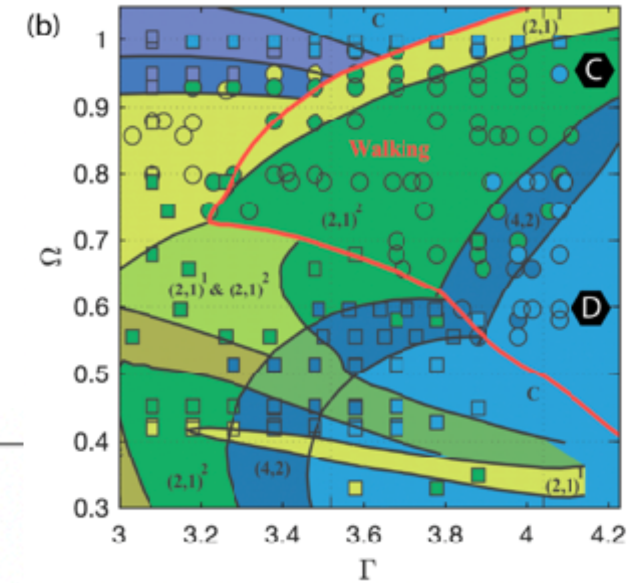

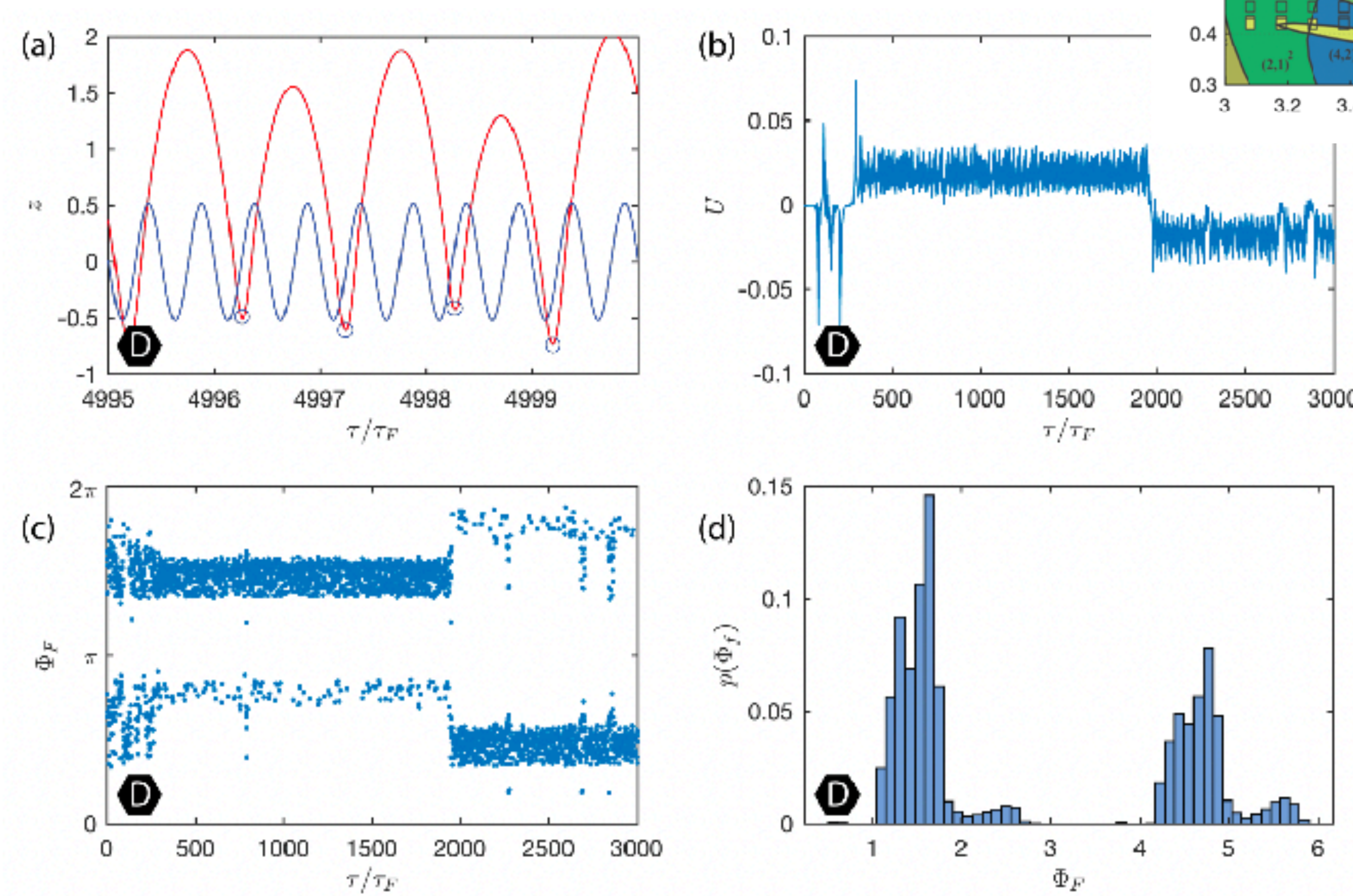

`Corrals': confine with central potential

- captures mode-switching apparent at high Me, marked by reversals in direction

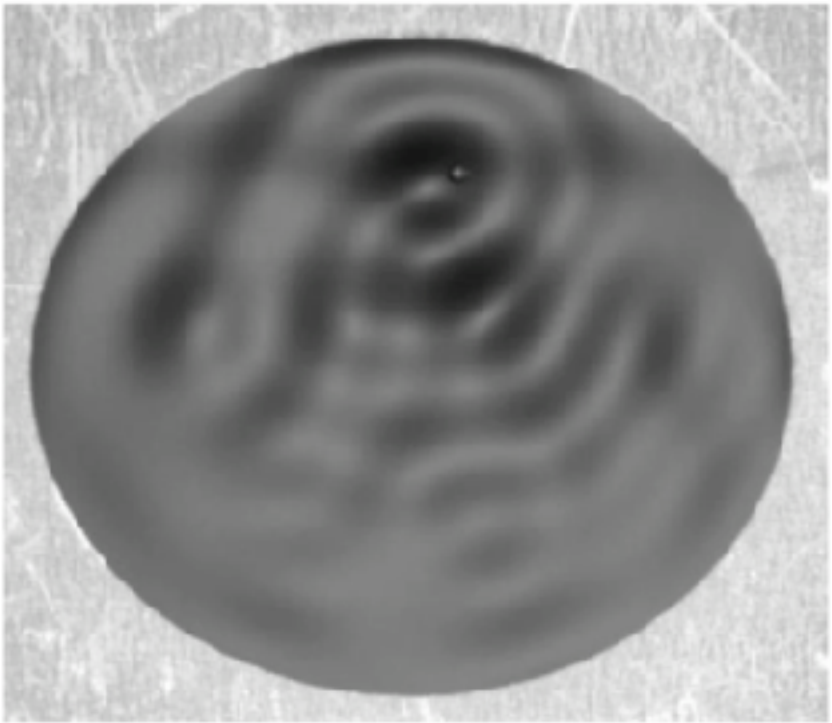

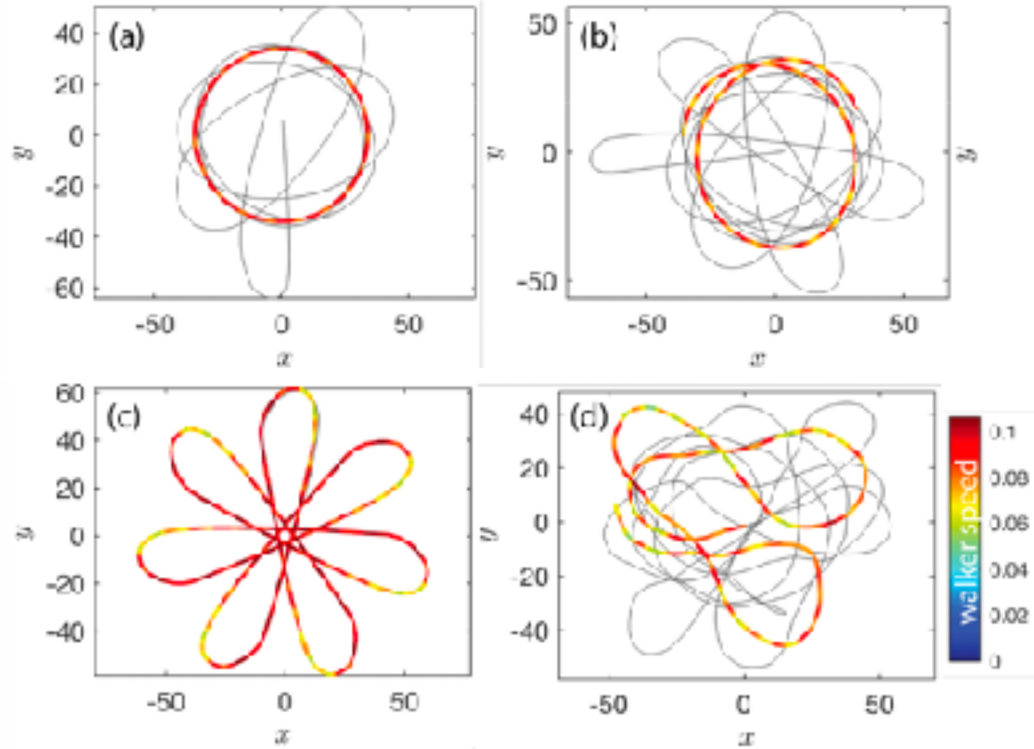

Mode switches

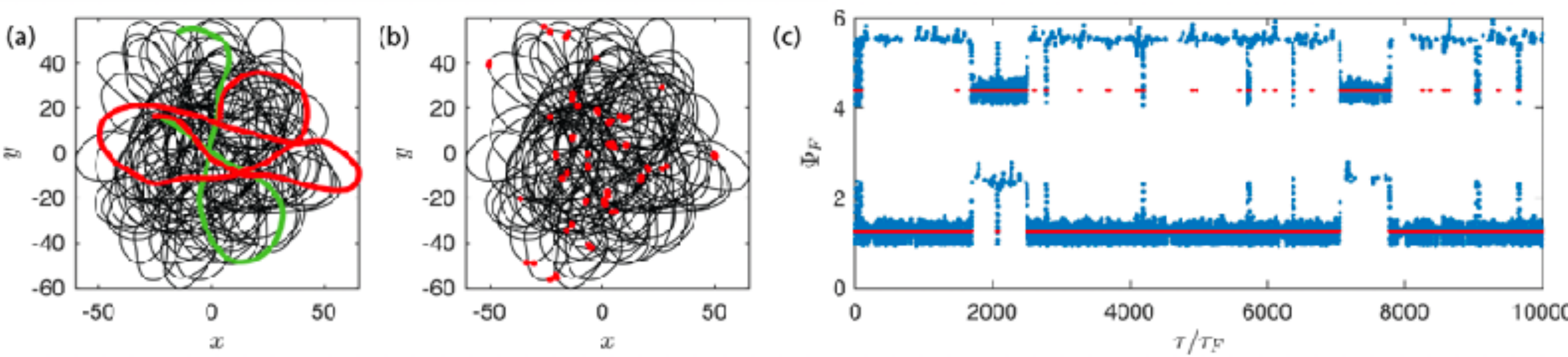

A hydrodynamic analog of the Kapitza-Dirac effect

B.K. Primkulov, V. Frumkin, D.J. Evans, P.J. Sáenz, J.W.M. Bush

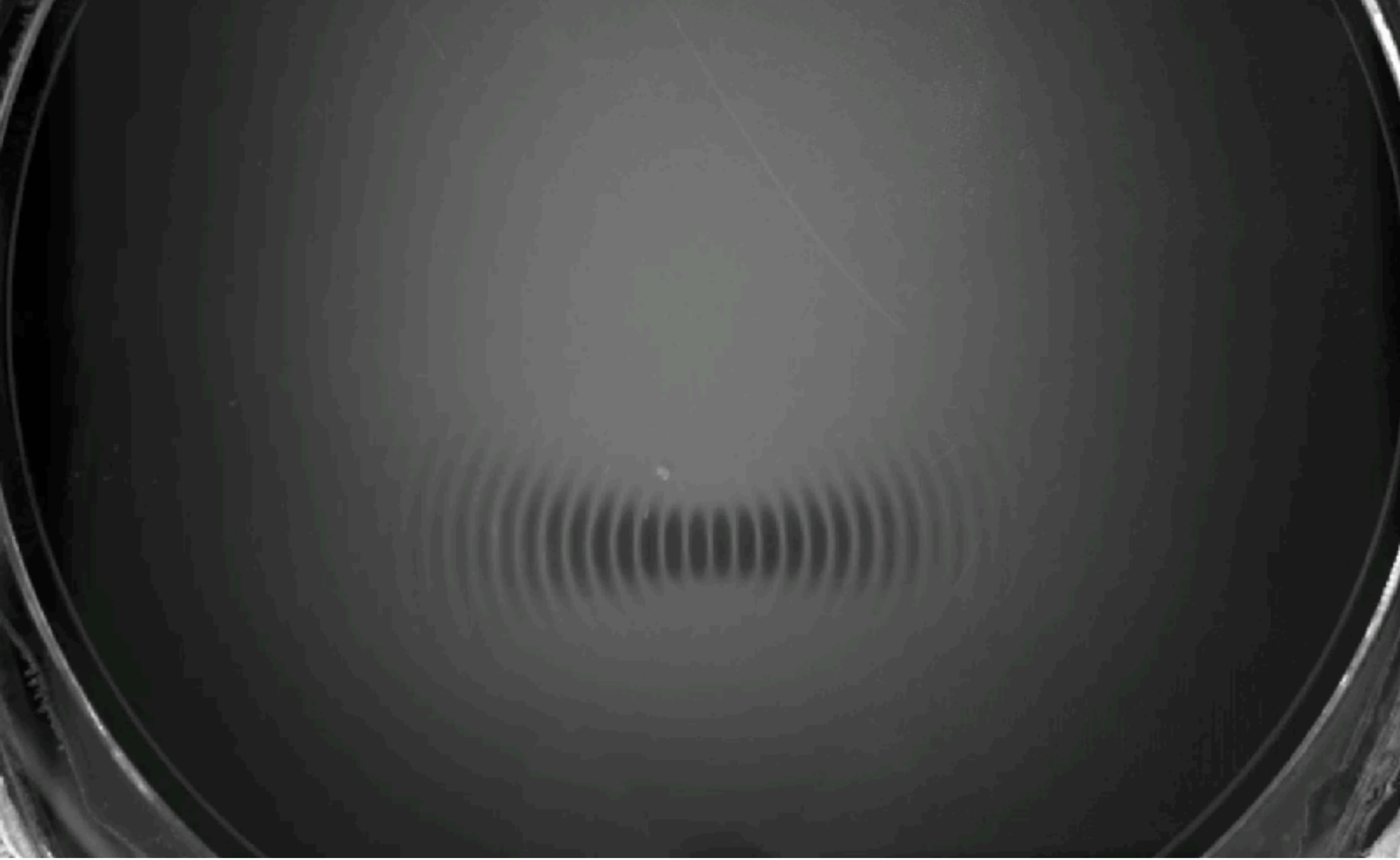

Kapitza-Dirac Effect (1933)

Batelaan, Rev. Mod. Phys. (2007)

- classic diffraction is the bending of light by matter
- the KD-effect is the diffraction of matter by light

  e.g. electrons by a laser-induced standing wave

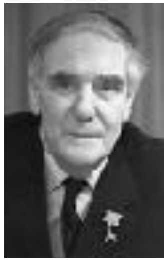

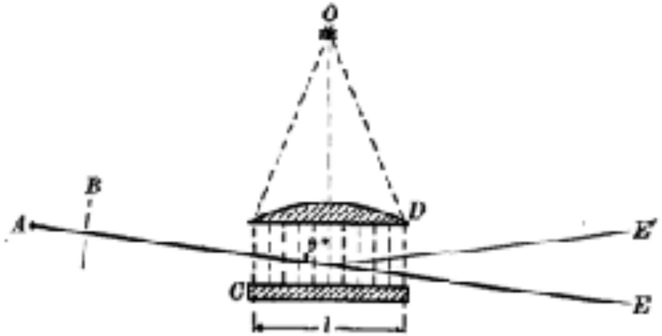

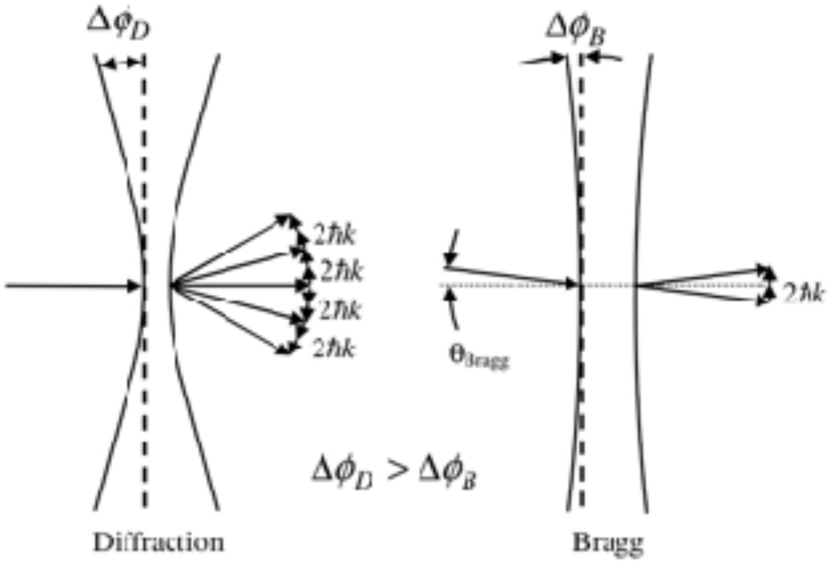

FIG. 1. Comparing two regimes of the Kapitza-Dirac effect. Electrons passing through a narrow laser waist (left) are exposed to photons with larger angular uncertainty, allowing for diffraction into many different orders. For a wide laser waist (right), momentum and energy can be conserved only for Bragg scattering.

Freimund et al., Nature 2001

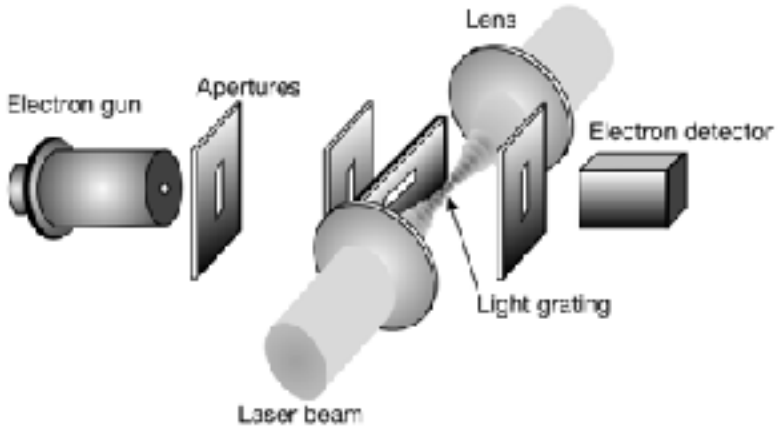

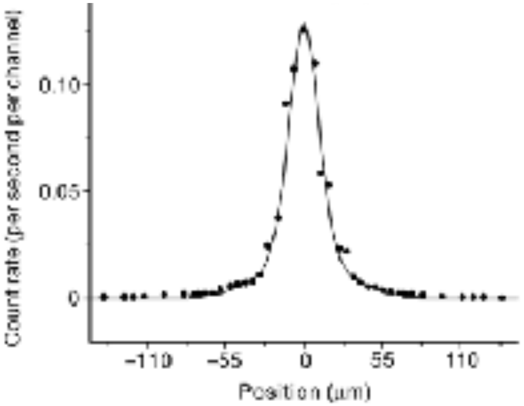

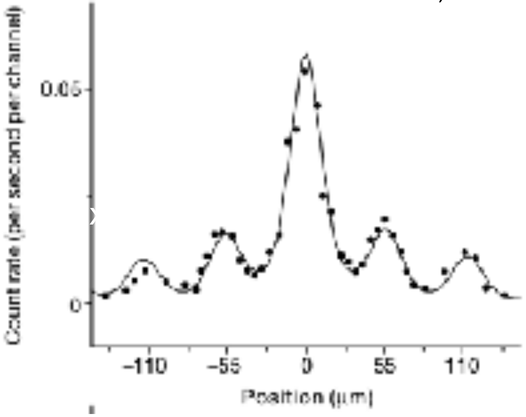

The hydrodynamic analog

- a walker traverses a deep region (above threshold) with a standing Faraday wave field

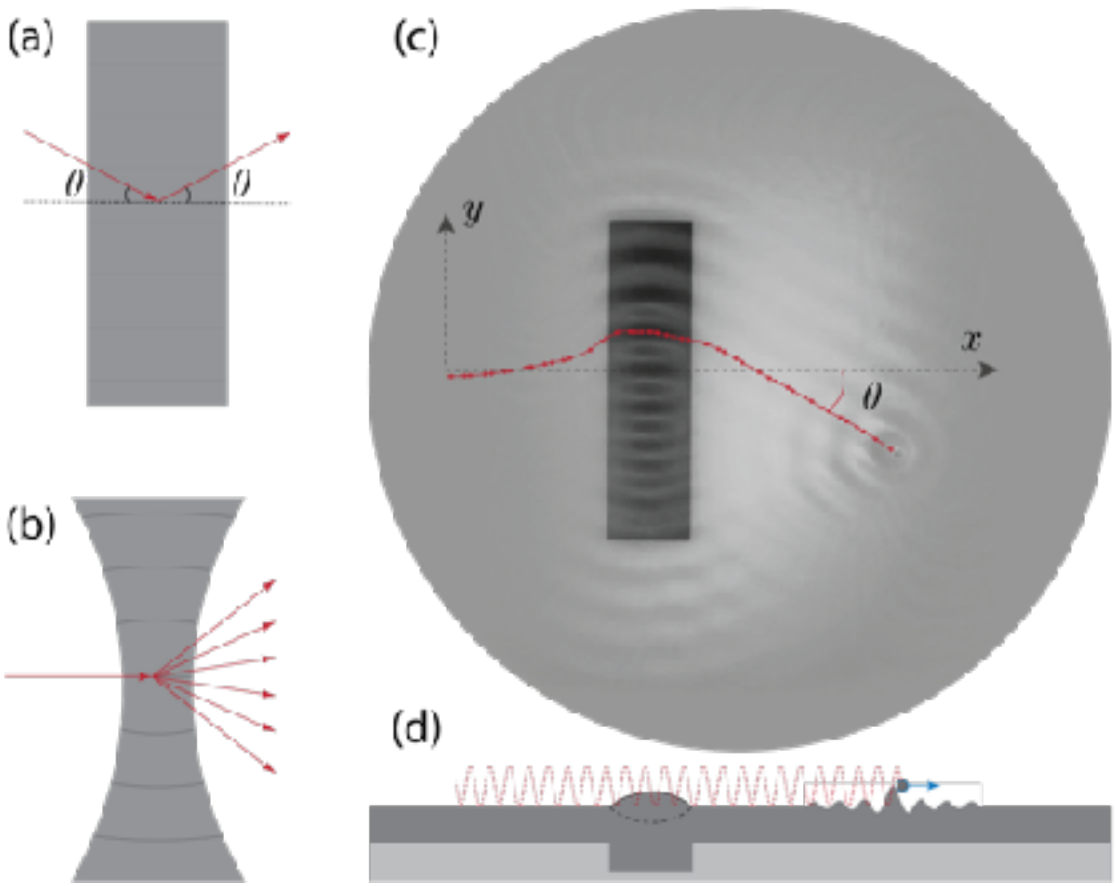

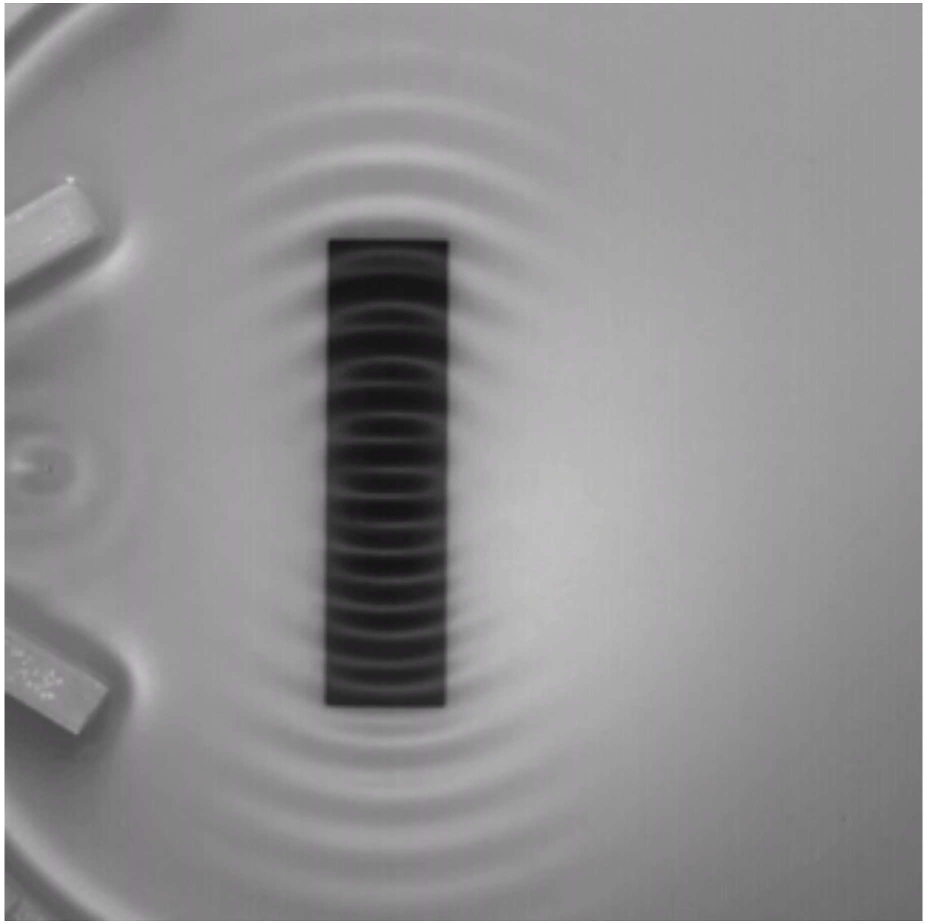

Bauyrzhan Primkulov

Observations

Resonant, fast

↑

Non-resonant, slow

↑

Resonant, fast

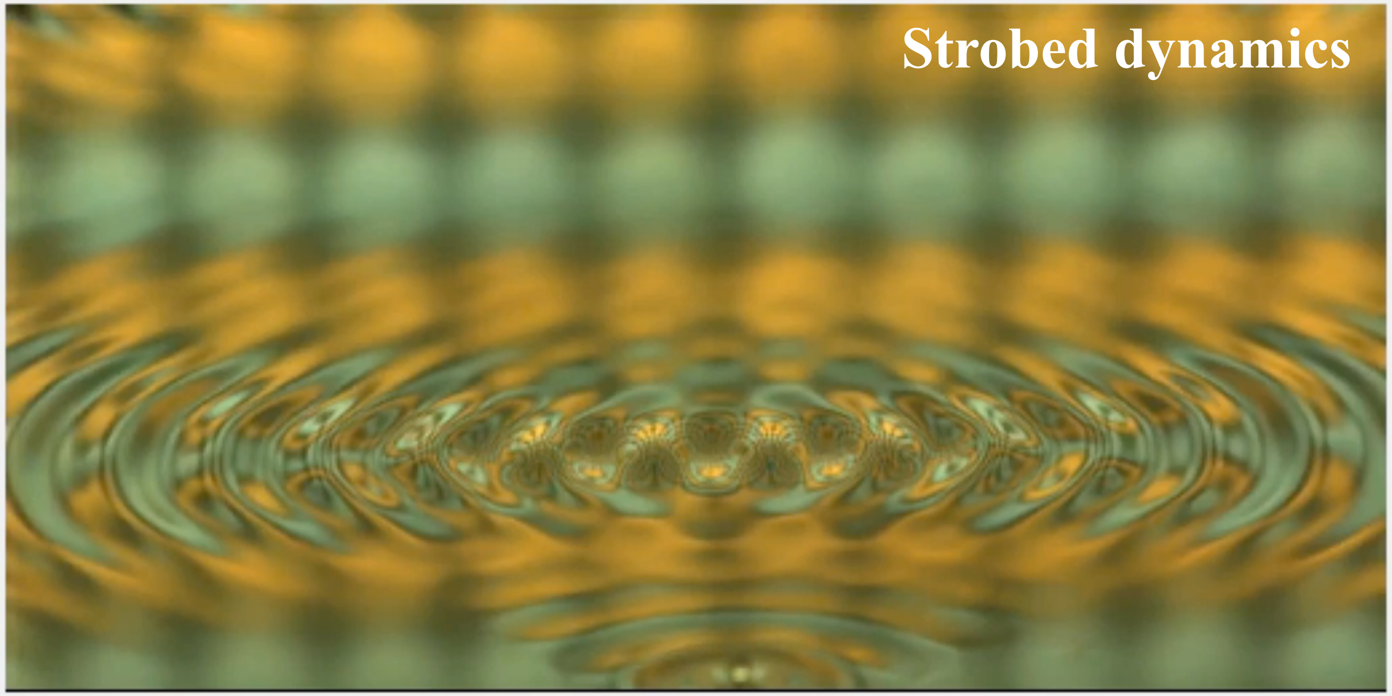

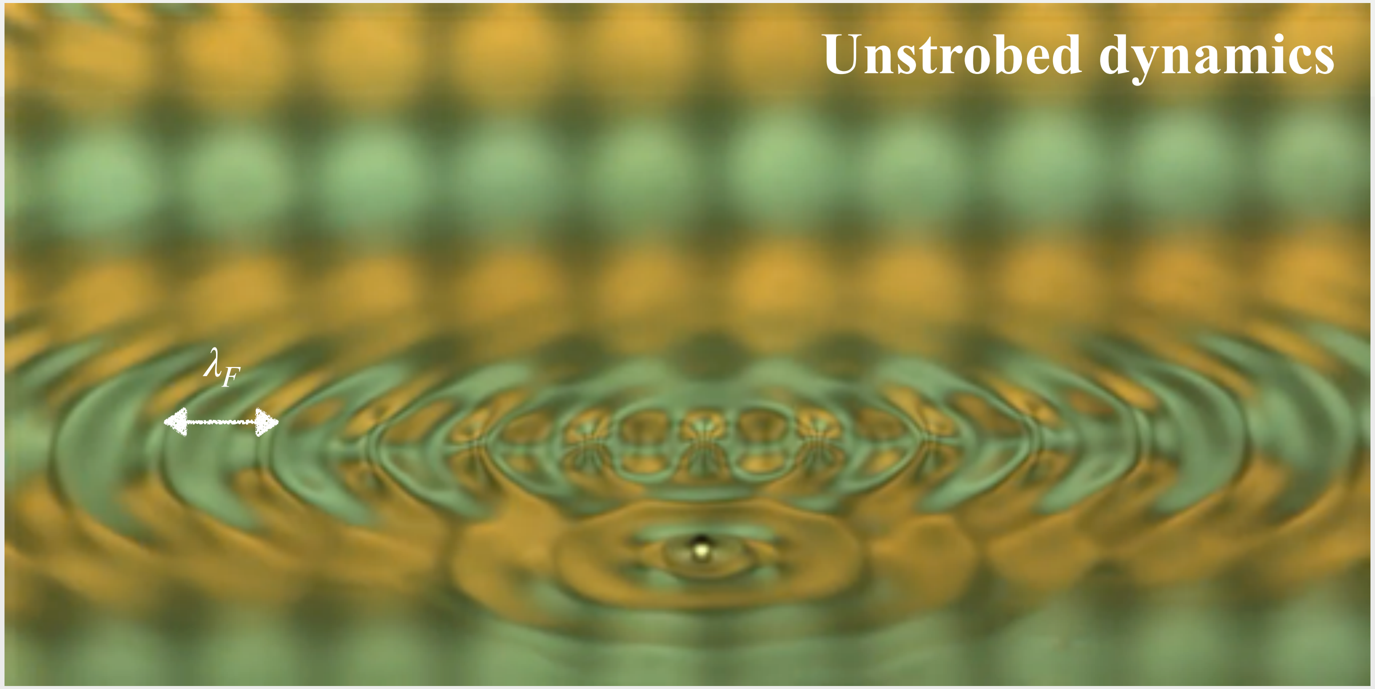

Analog of the KD effect

Resonant, fast Non-resonant, slow Resonant, fast

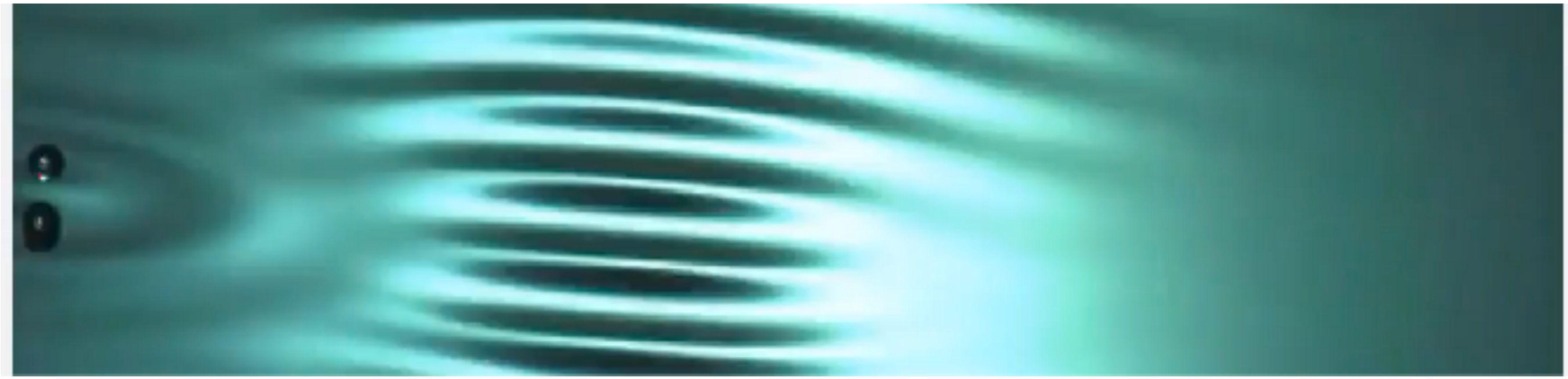

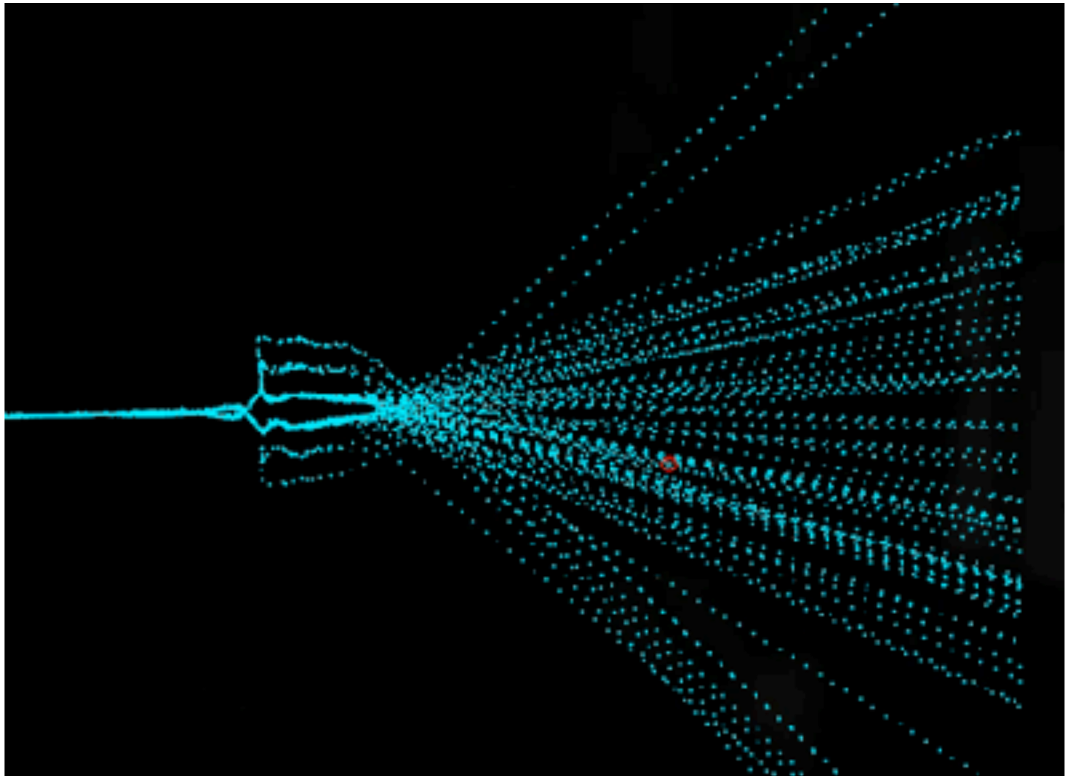

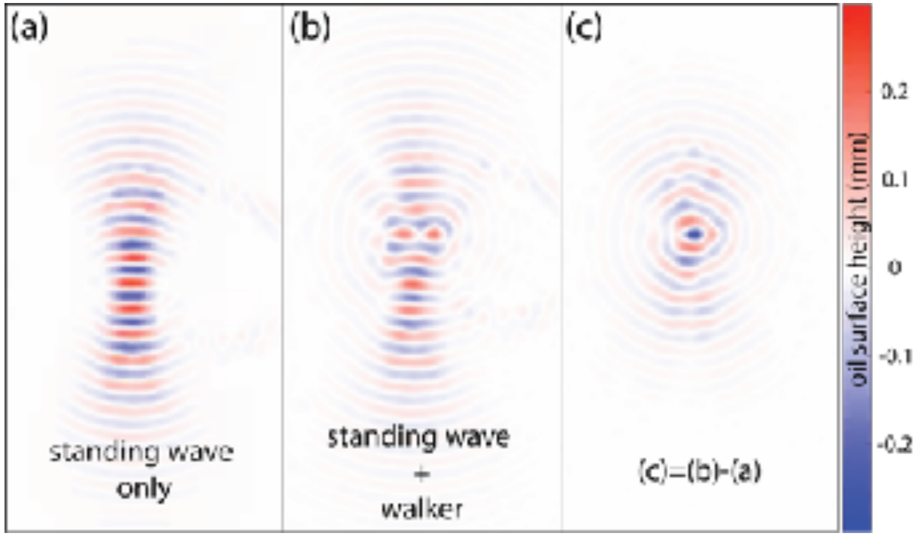

Observations

- resonance of walkers disrupted above deep region, leading to relatively slow motion
- over the deep region, the walkers are sorted according to phase, channel, cross in a trough
- because walkers may have one of two phases, channels spaced by $\lambda_F/2$
- downstream of deep region, motion marked by speed oscillations with wavelength ~ λ_F
- a number of diffraction angles are preferred

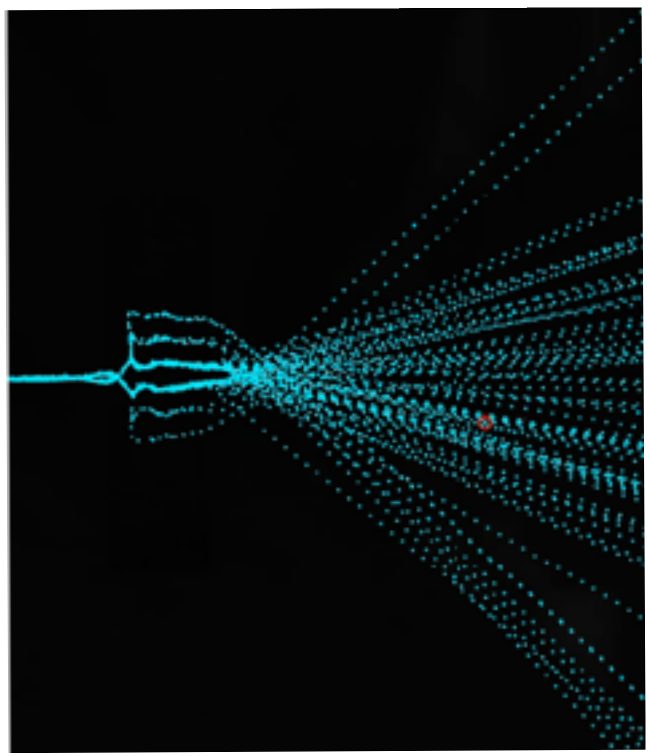

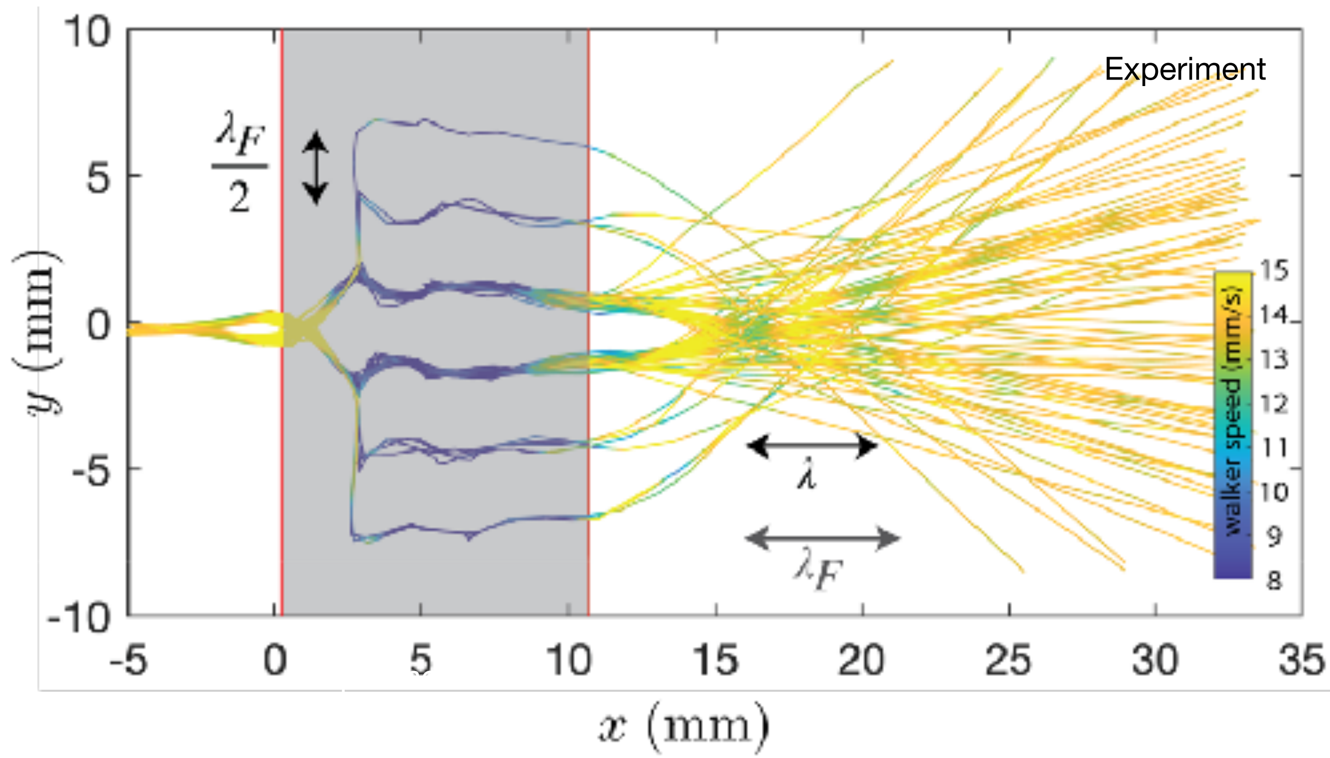

Channeling: sorting according to bouncing phase

- over the deep region, the walkers are sorted according to phase, channel, cross in a trough
- because walkers may have one of two phases, channels spaced by $\lambda_F/2$

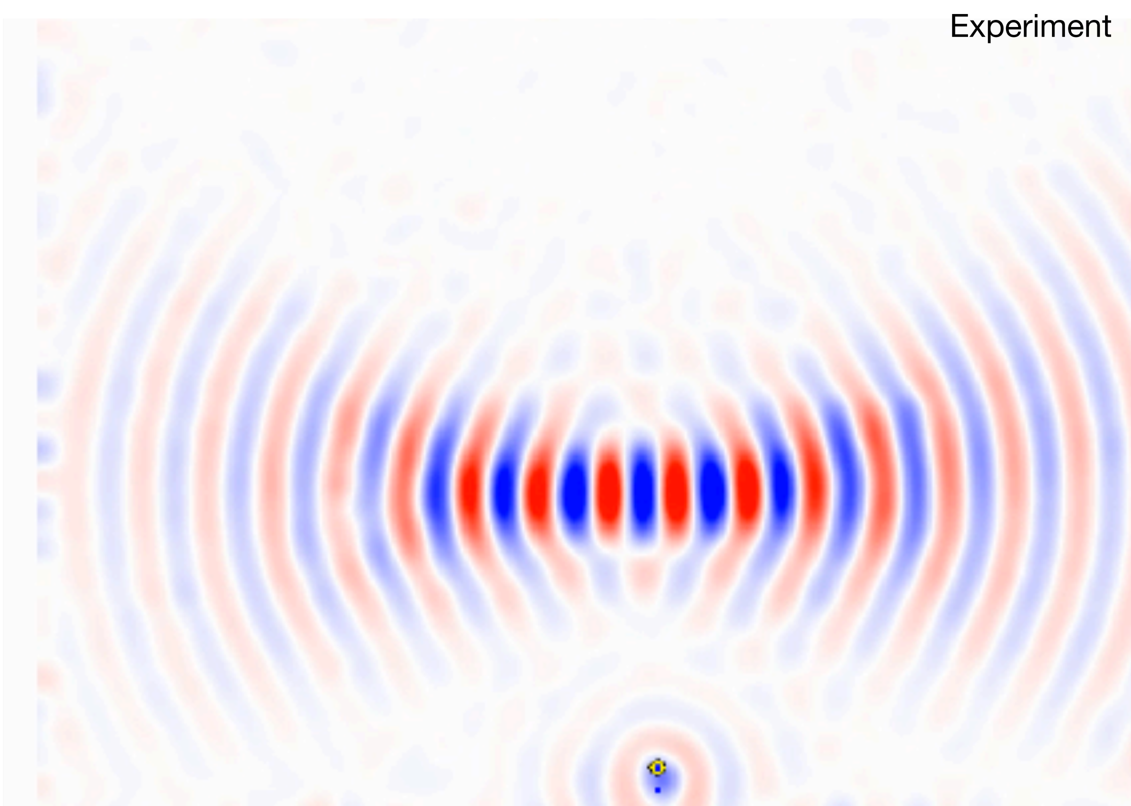

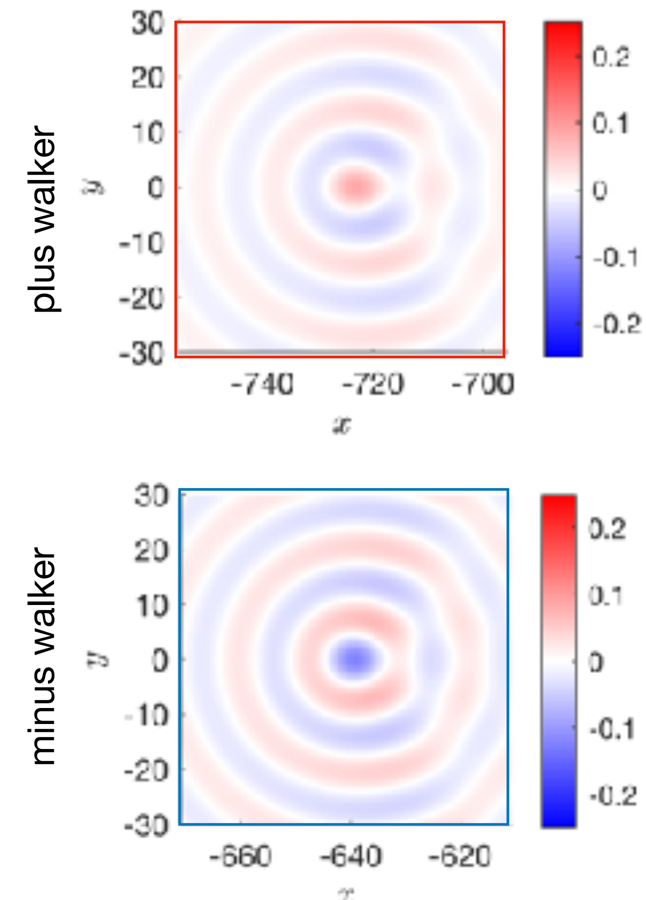

Preferred diffraction angles

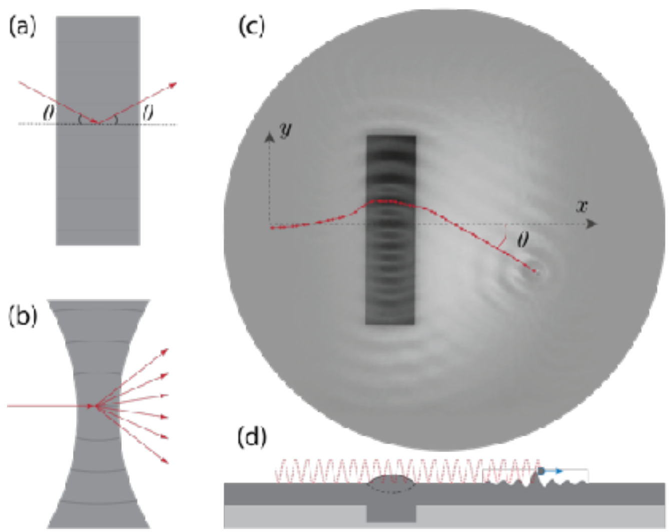

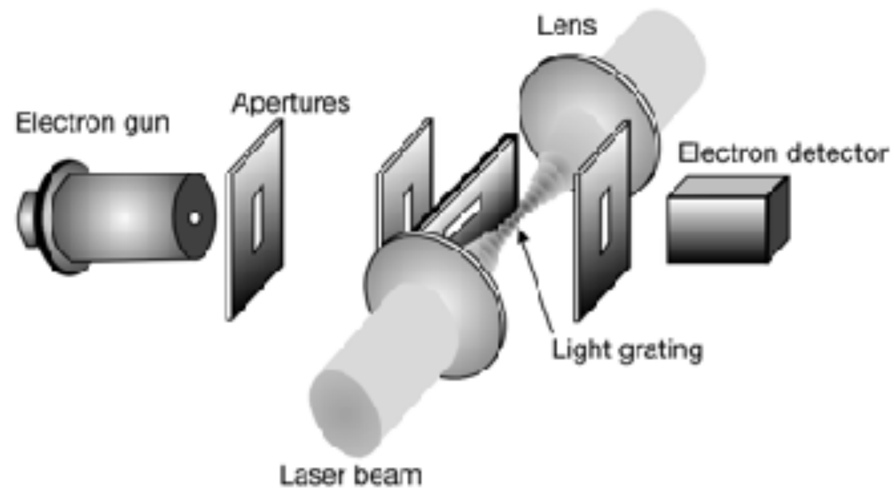

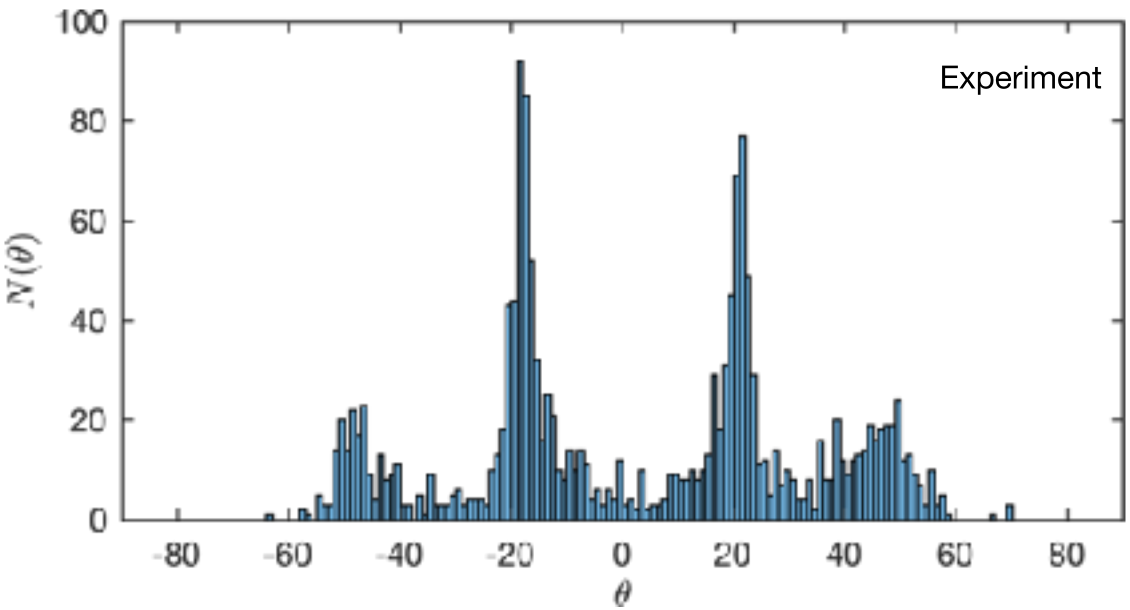

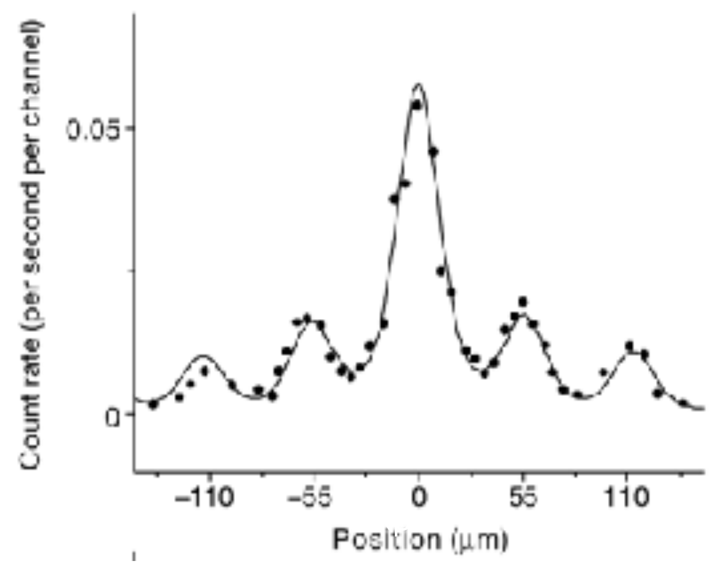

- a number of diffraction angles are preferred, qualitatively similar to that in KD diffraction

Simulations

$$\ddot{z}_p = F_N(\tau) - Bo \qquad \ddot{\mathbf{x}}_p + (\mathscr{D}_h F_N(\tau) + \mathscr{D}_a)\dot{\mathbf{x}}_p = -F_N(\tau)\nabla(h+H)$$

$$F_N(\tau) = -\mathscr{H}(-z_p + z_b + h)[\mathscr{D}_v(\dot{z}_p - \dot{z}_b - \dot{h}) + \mathscr{C}_v(z_p - z_b - h)]$$

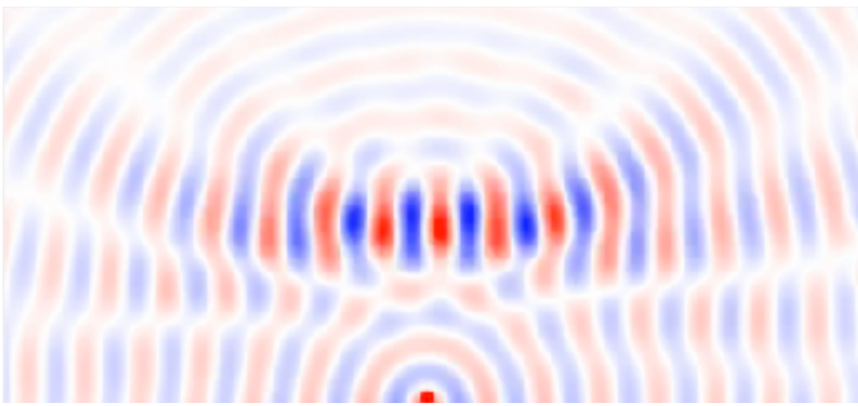

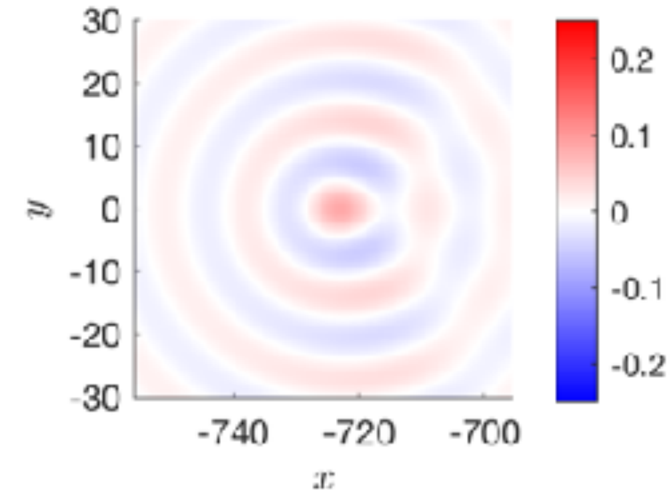

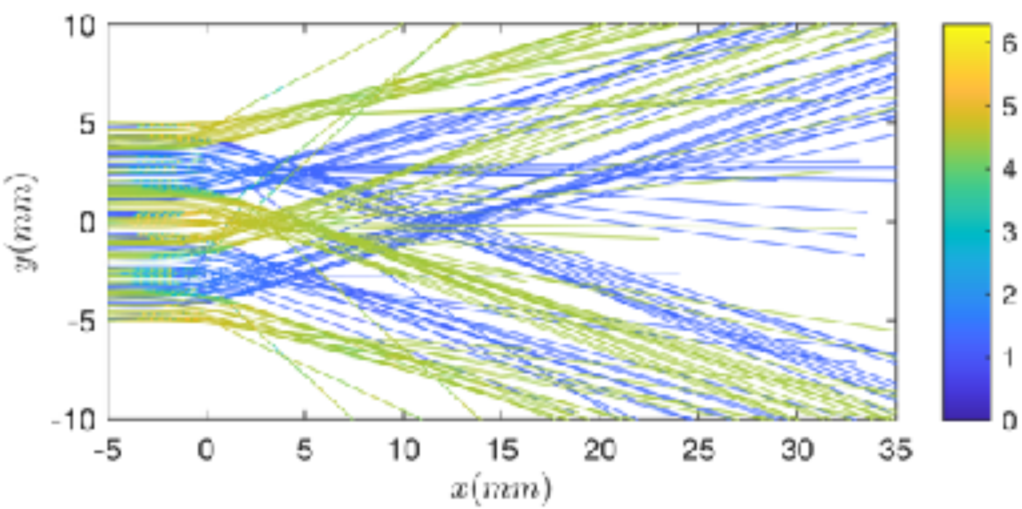

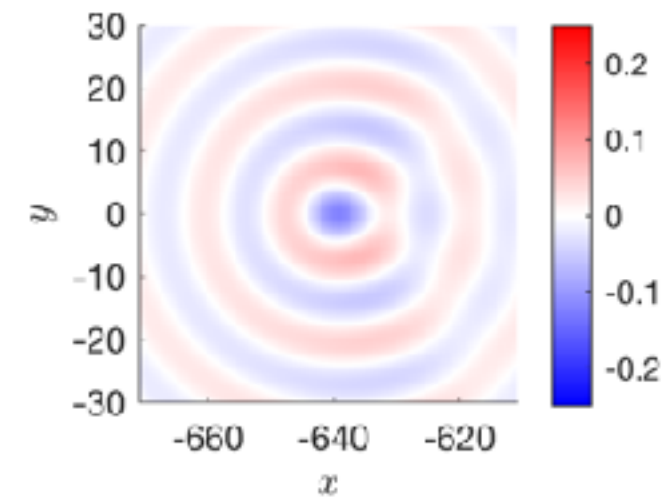

Crossing the wave field

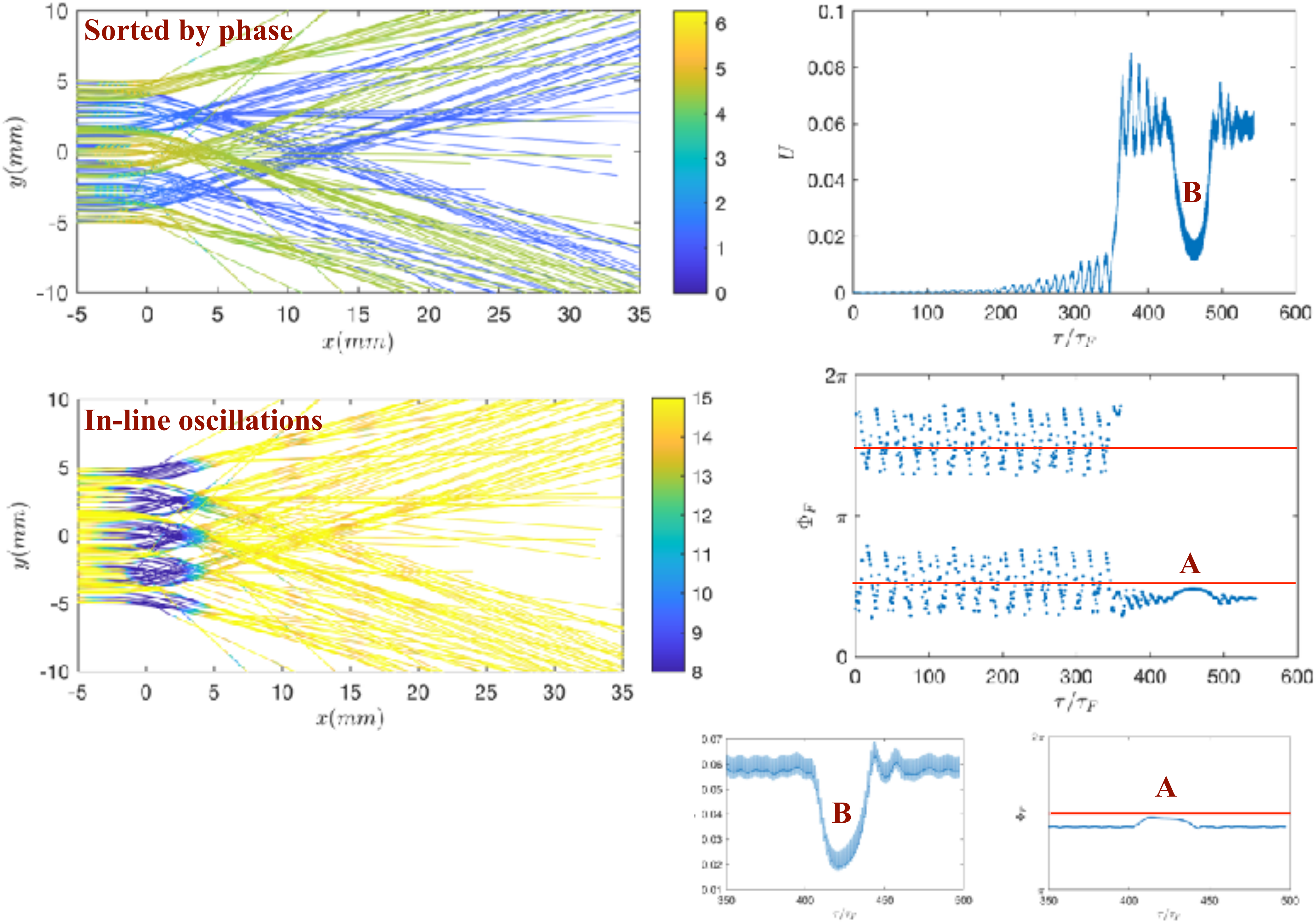

Diffraction pattern

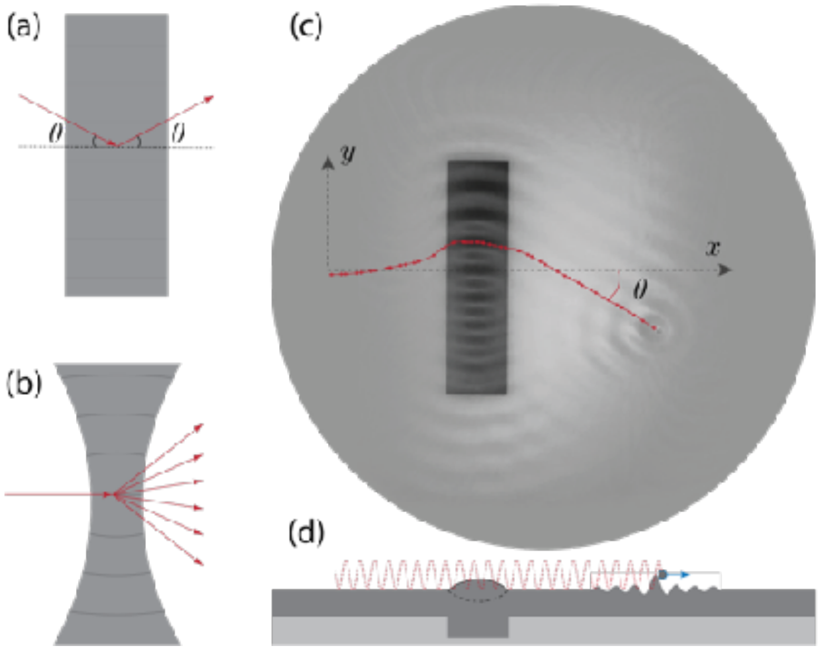

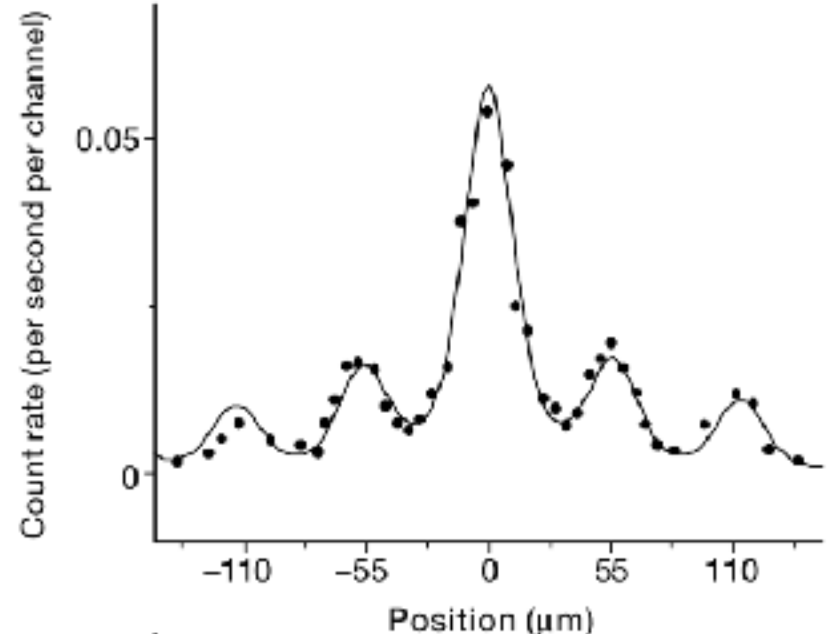

Experiment

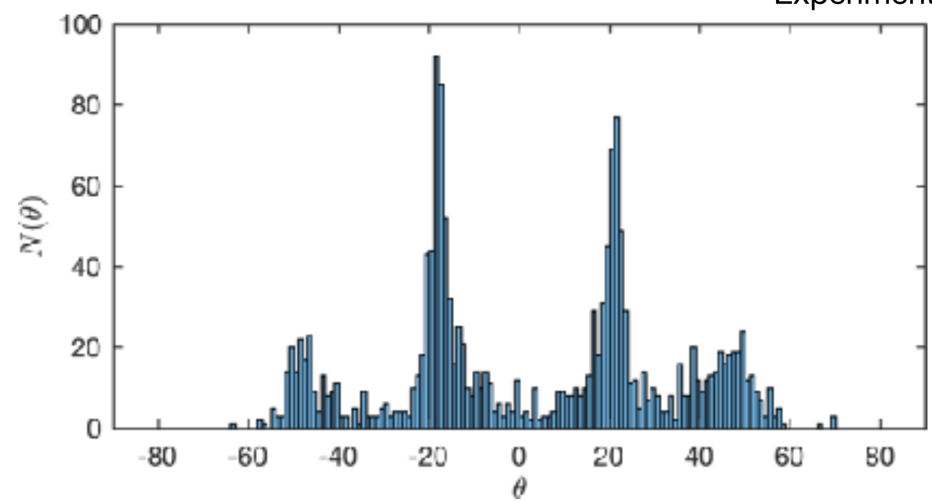

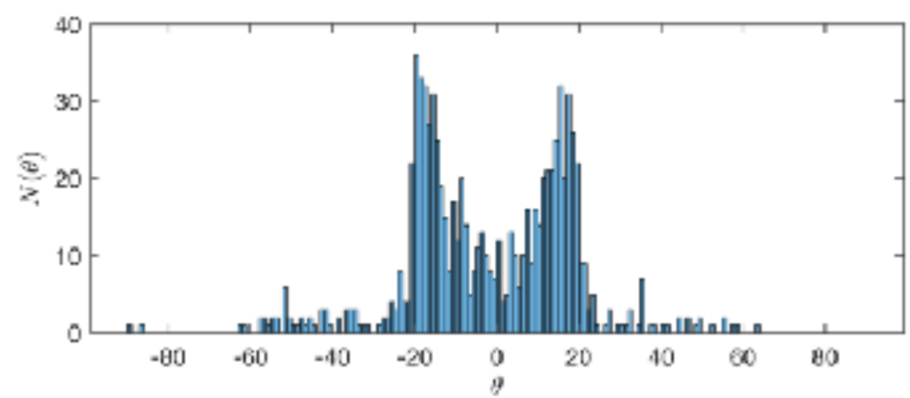

- simulations capture only central peaks

Ponderomotive Forces in Pilot-Wave Hydrodynamics

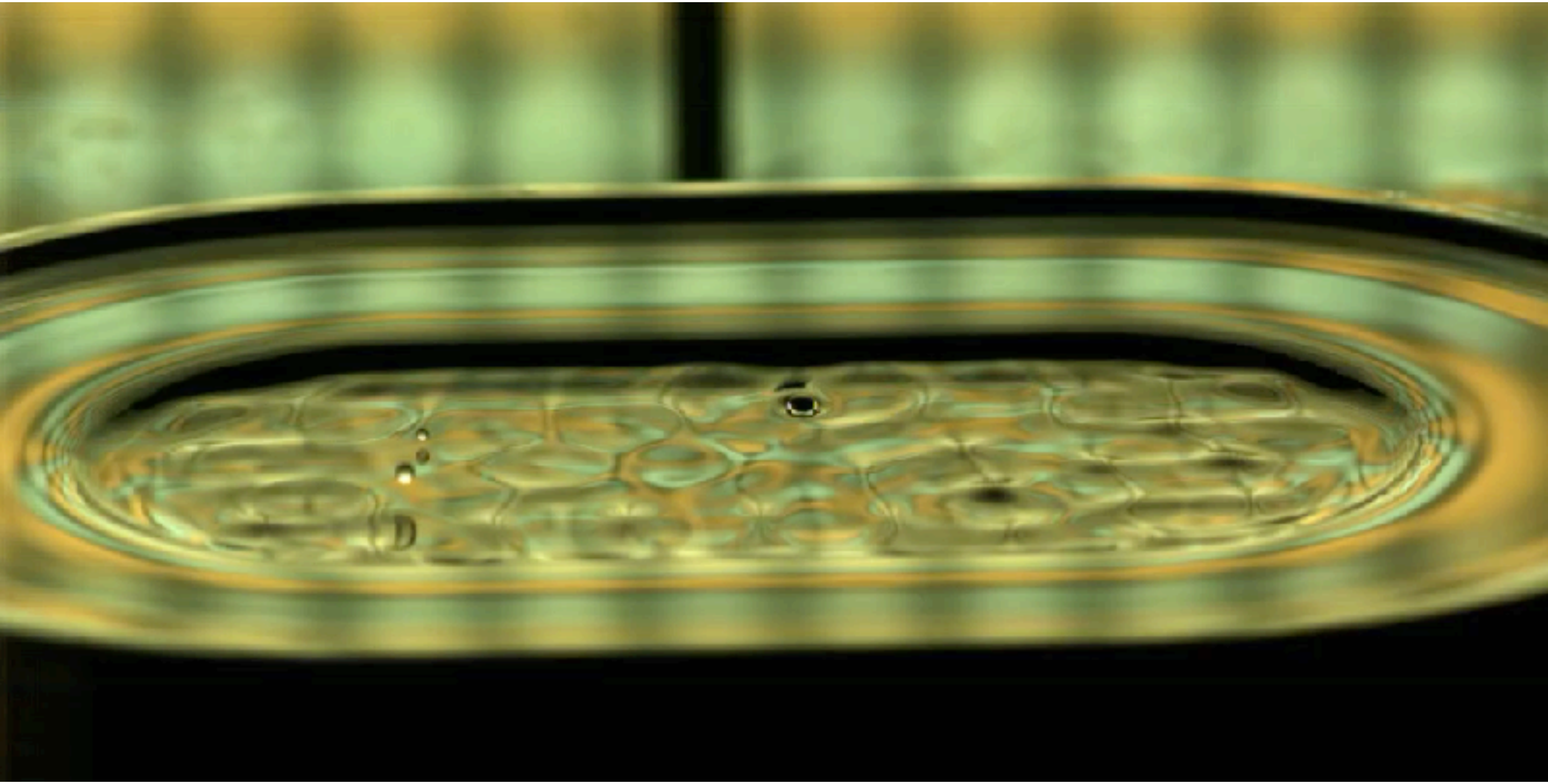

The thesis work of Davis Evans

Mechanism for the coherent emergent statistics at hight Me?

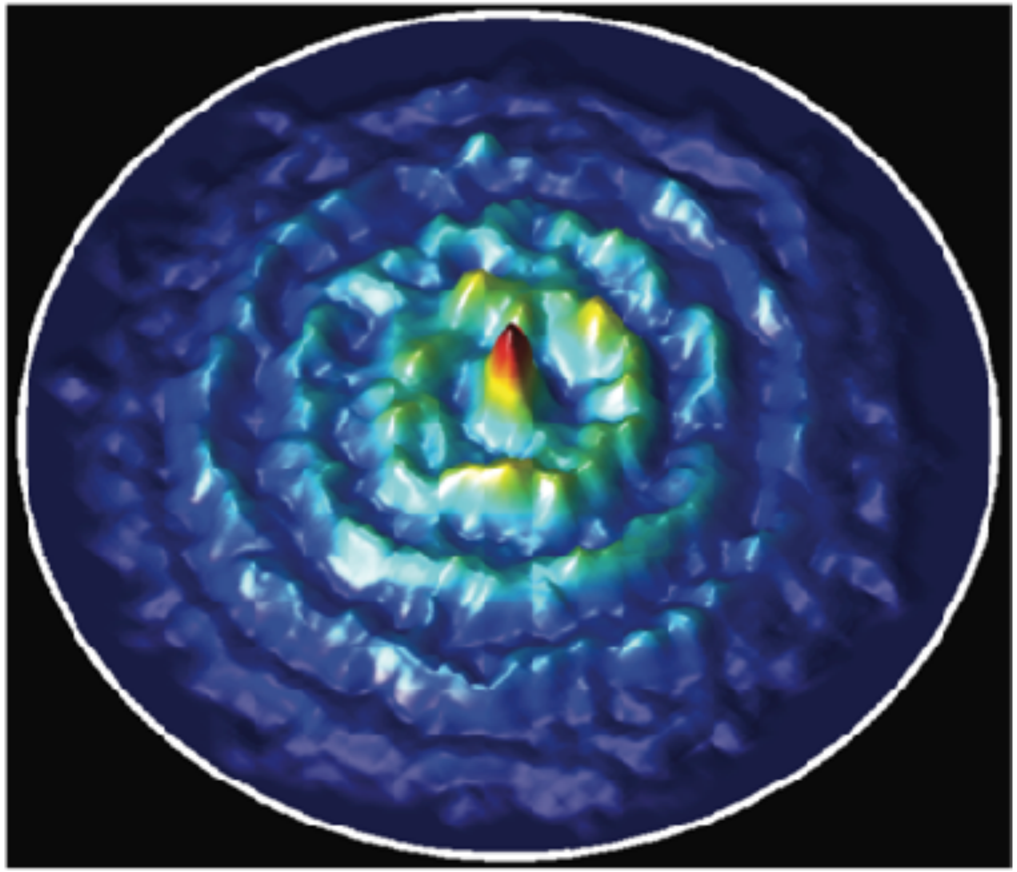

- two possible mechanisms have been proposed
- based on the 2 existing HQA paradigms
- their shortcomings have prompted the development of Paradigm III

Paradigm I: suggested by orbital dynamics

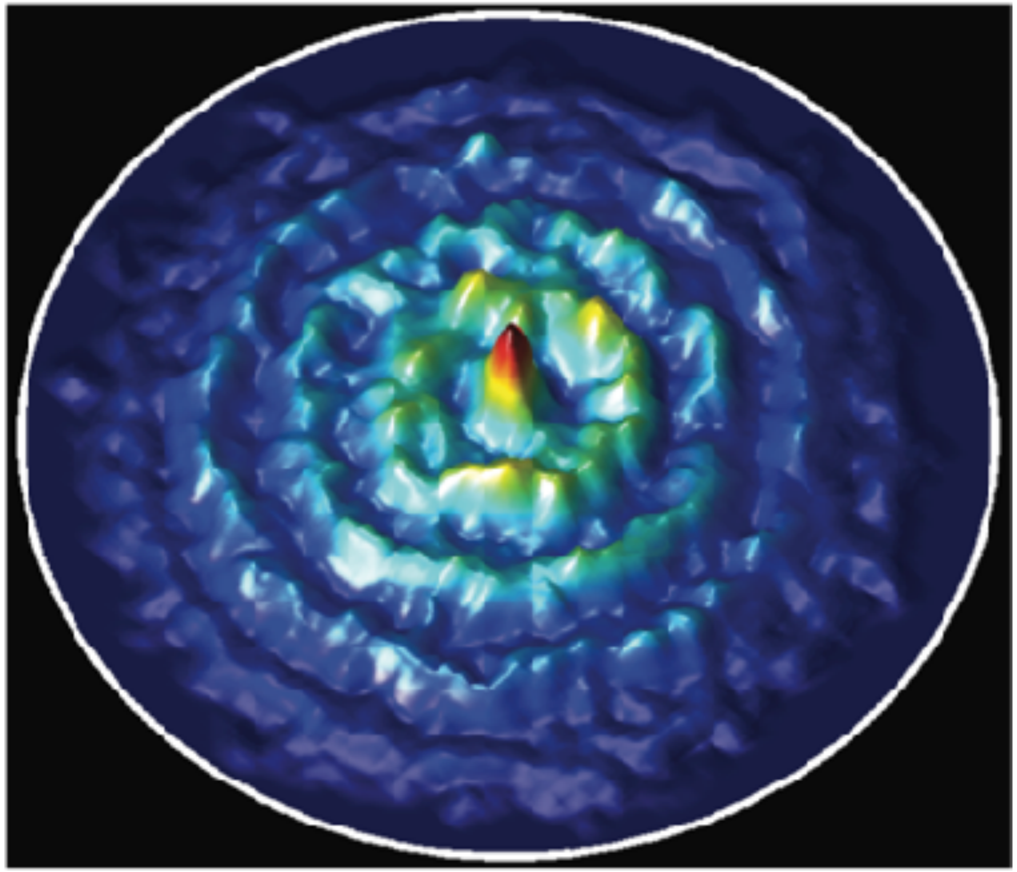

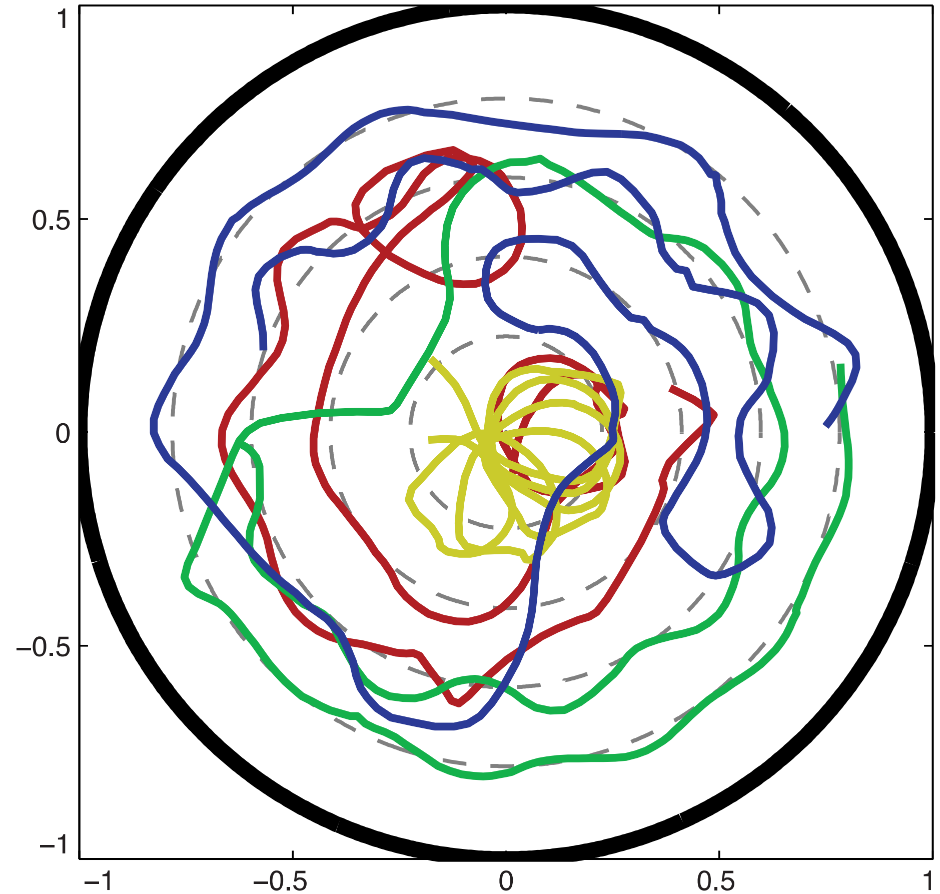

- at low memory, circular orbits along extrema of cavity mode are stable
- at higher memory, these orbits destabilize, yield to chaotic pilot-wave dynamics
- intermittent switching between periodic states results in multimodal statistics

Harris et al. (2013)

Paradigm II: Friedel oscillations from the outer boundaries

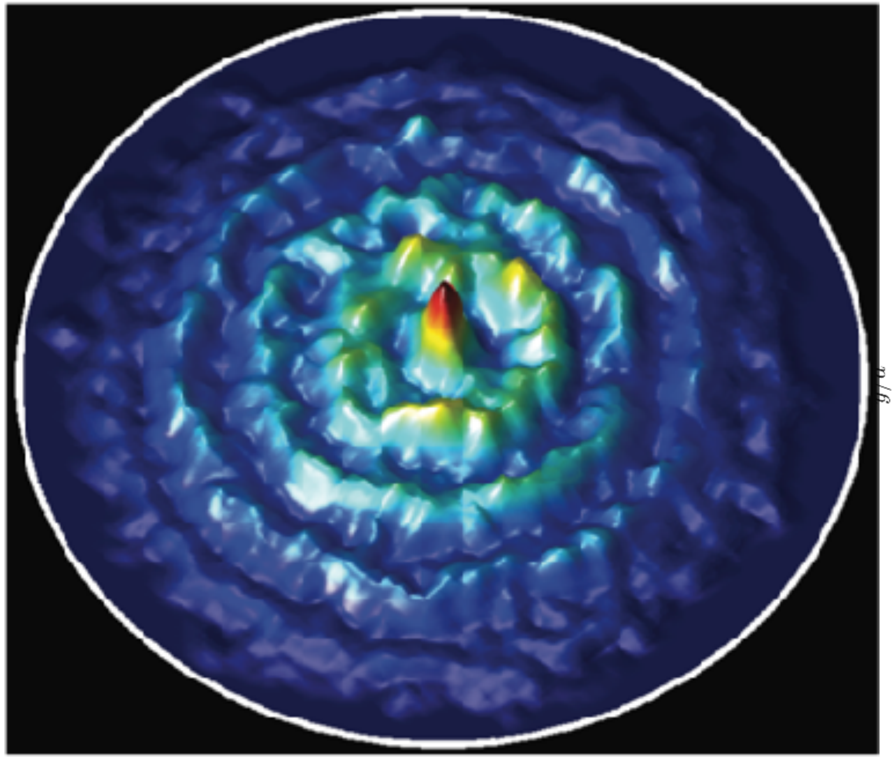

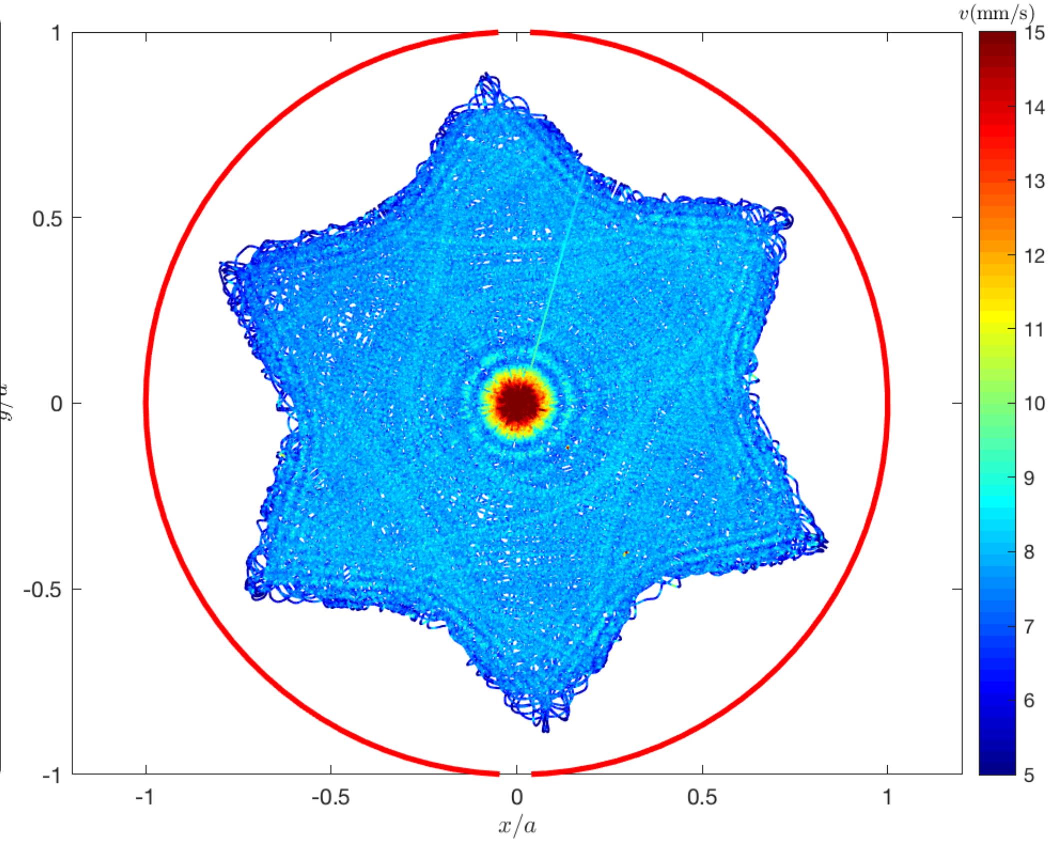

- in-line oscillations with λ_F excited at corral's edge
- preferred reflection angle of $\theta_R = 60^0$ gives rise to statistical signature with wavelength

$$\lambda_F \cos \pi/3 = \lambda_F/2$$

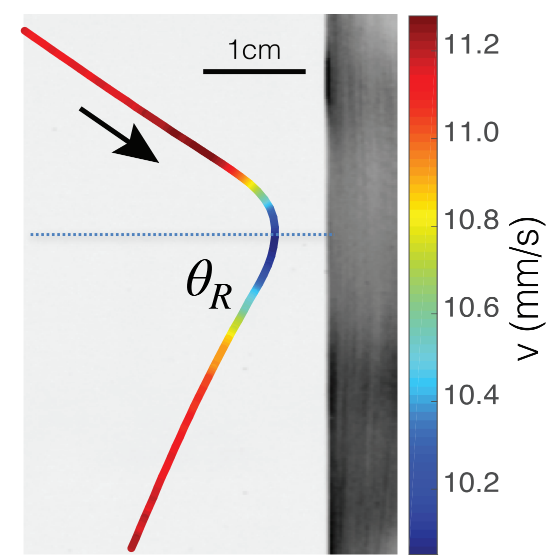

Paradigm II: Friedel oscillations from the outer boundaries

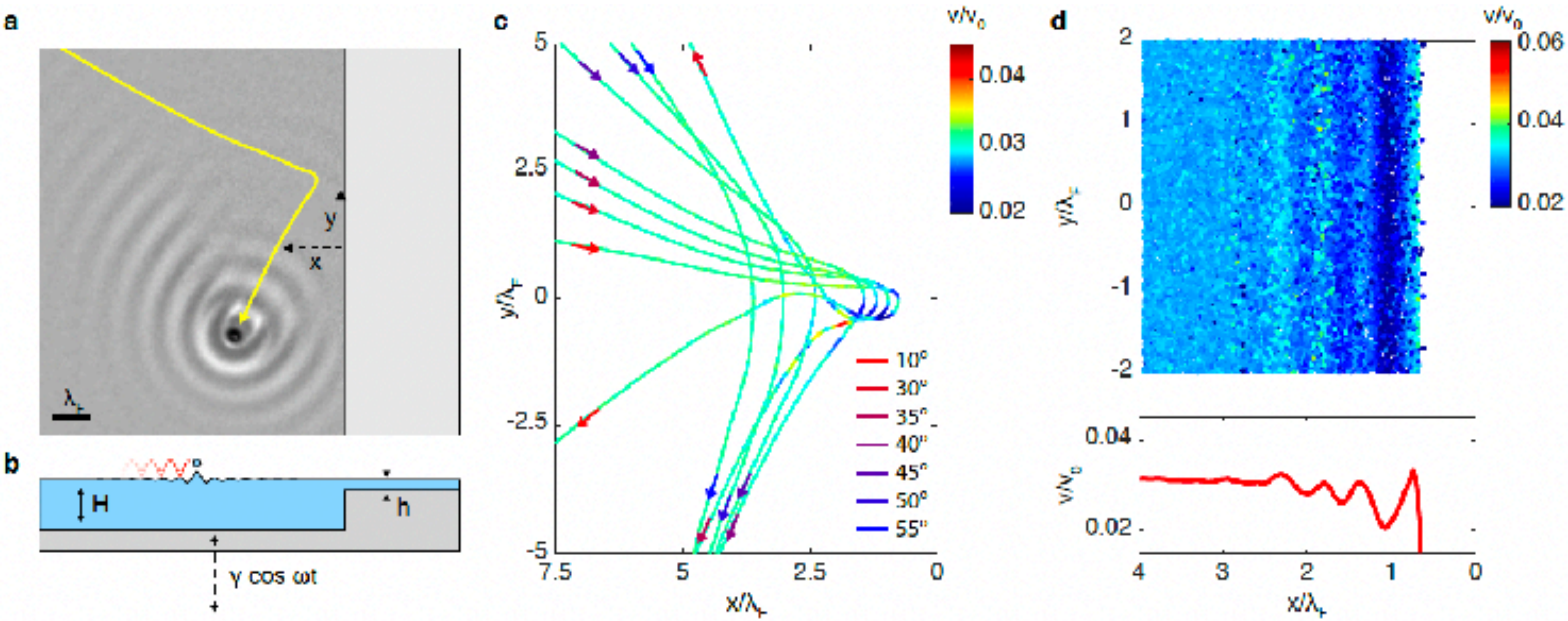

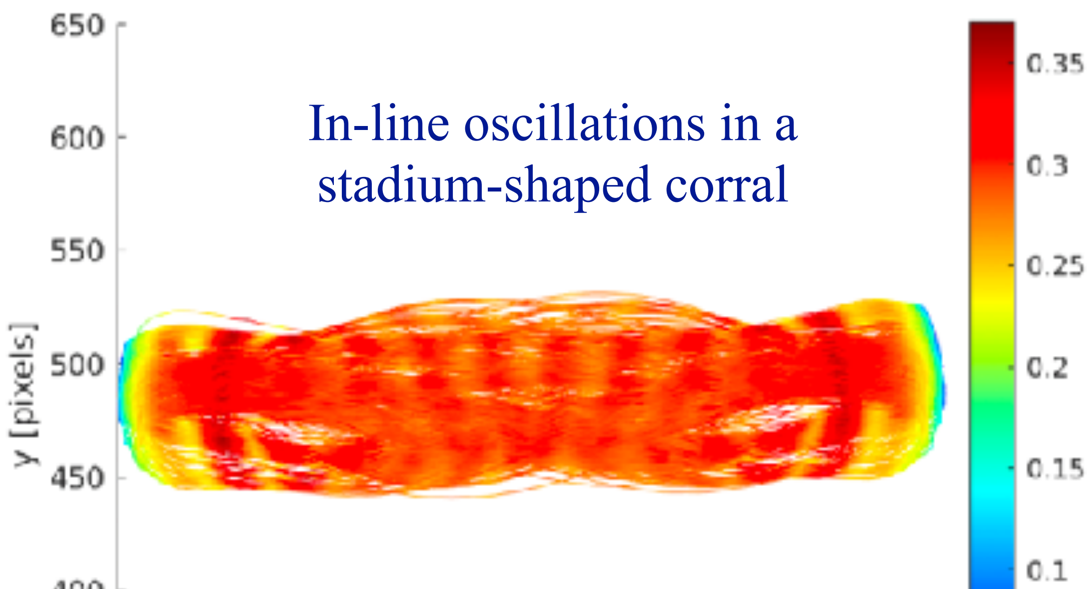

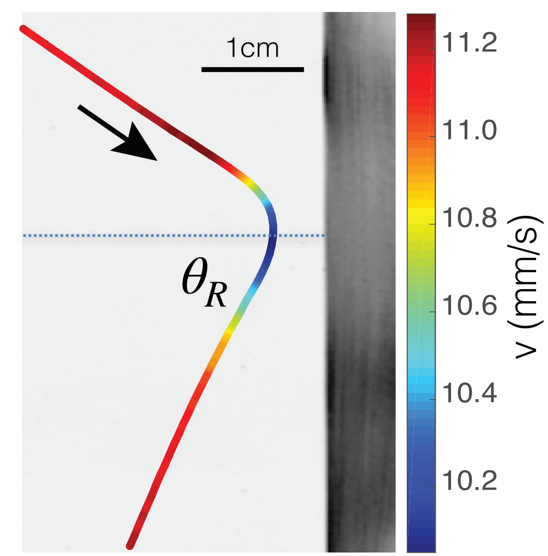

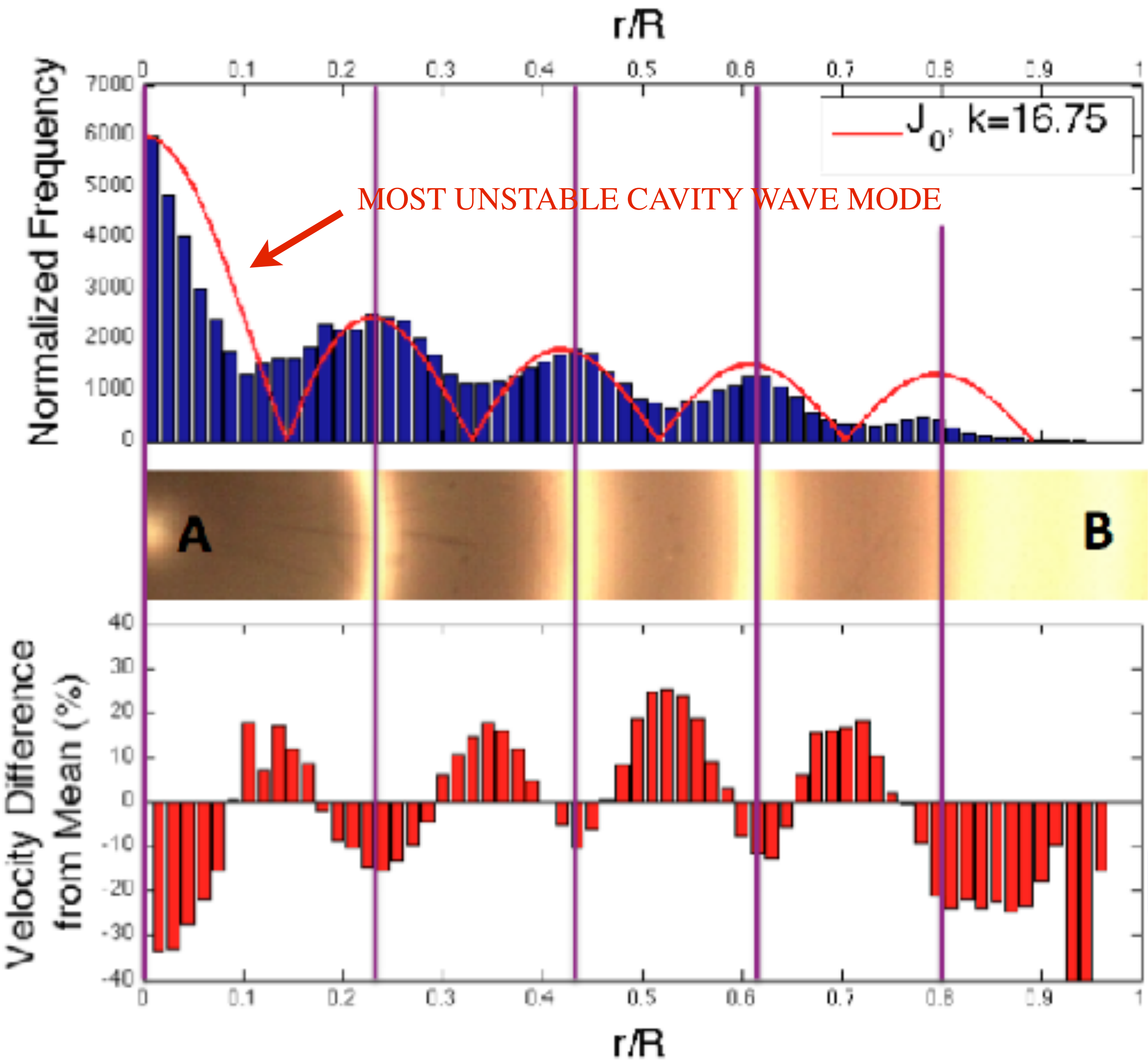

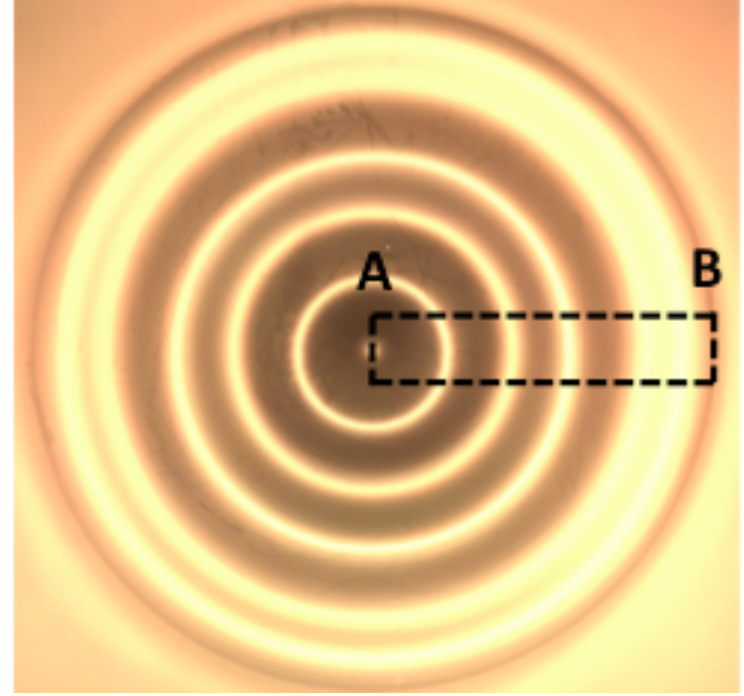

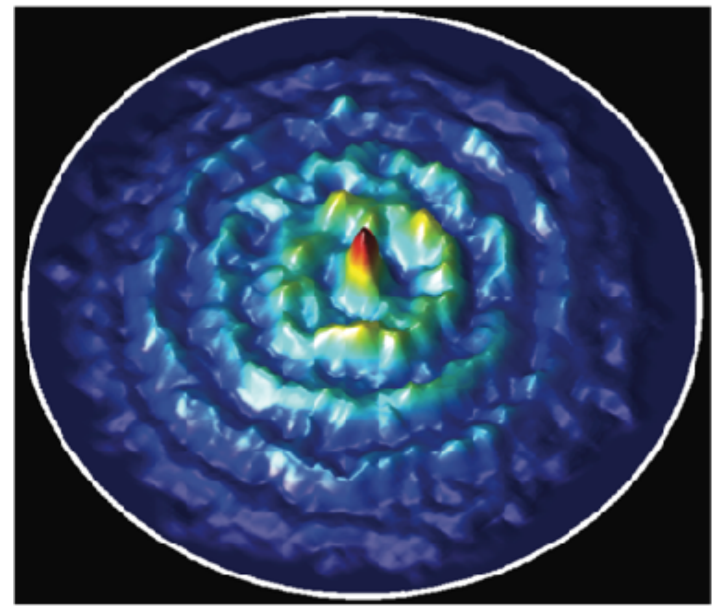

- max in surface perturbation amplitude correspond to peaks in pdf, spaced at $\lambda_F/2$
- pdf prescribed by amplitude of the most unstable resonant wave mode of the cavity

Ponderomotive forces

- emerge when a particle is subject to a rapidly oscillating force field

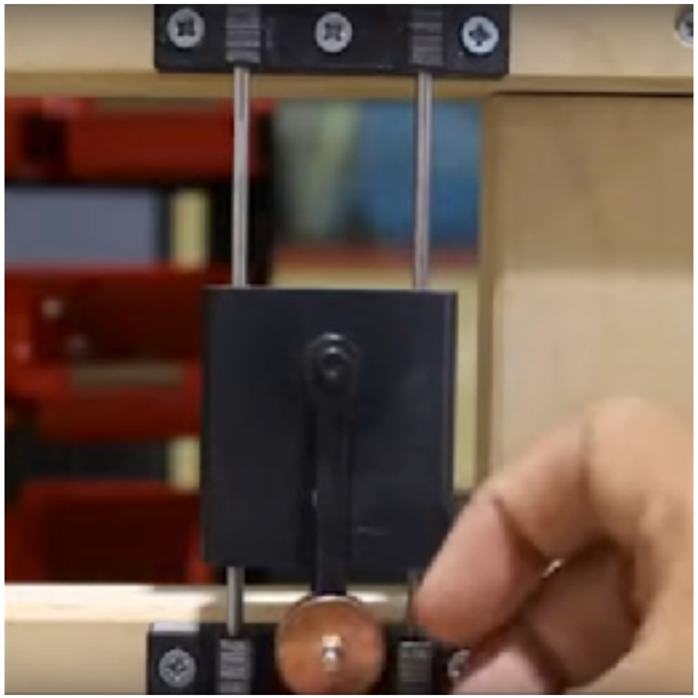

Rapidly oscillating force

$$F(x,t) = -\nabla U(x)\cos(\omega t)$$

$\xrightarrow{\text{Average}}$

Mean ponderomotive force

$$F_{avg} \sim -\nabla|\nabla U|^2$$

- particles driven to extrema in potential (MAX *or* MIN), where $\nabla U = 0$

E.g. Charge is a rapidly oscillating electric field: $\mathbf{F}_{\text{p}} = -\frac{e^2}{4m\omega^2}\nabla(E^2)$

Ponderomotive forces

- stroboscopic models assume resonance between droplet and wave, fail to capture corral statistics (Durey et al. 2021)

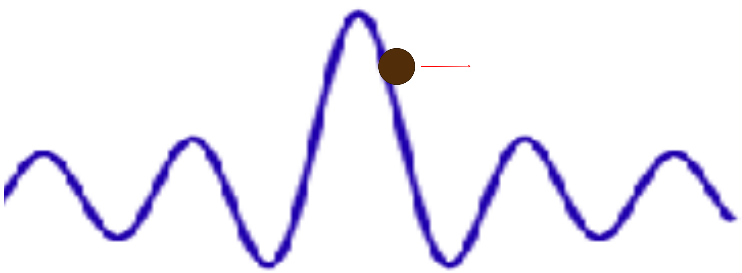

Resonant: bounces at same phase each period : "Strobed" wavefield serves as a self-potential

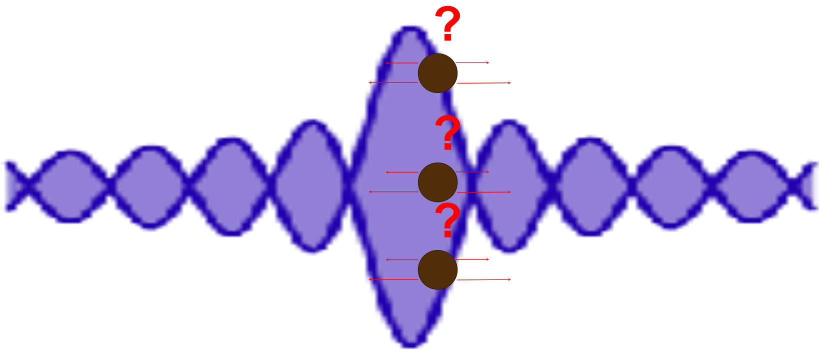

Non-resonant: variable bouncing phase.
Must we truly model each bounce?
Can we infer an effective force?

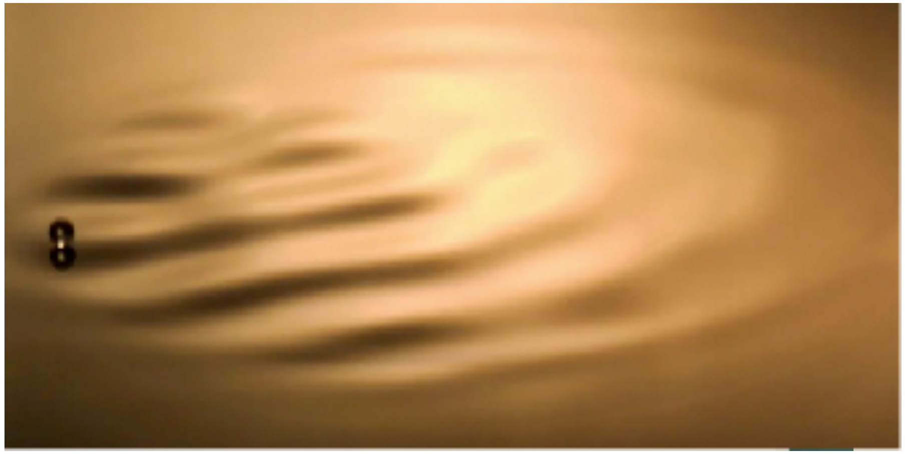

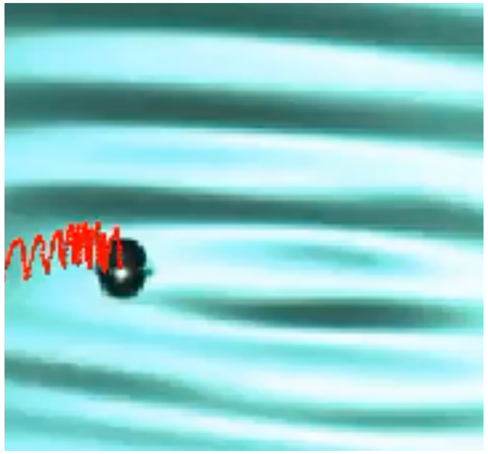

Walker in a corral

- non-resonant effects evident in velocity variations, and sporadic phase flips

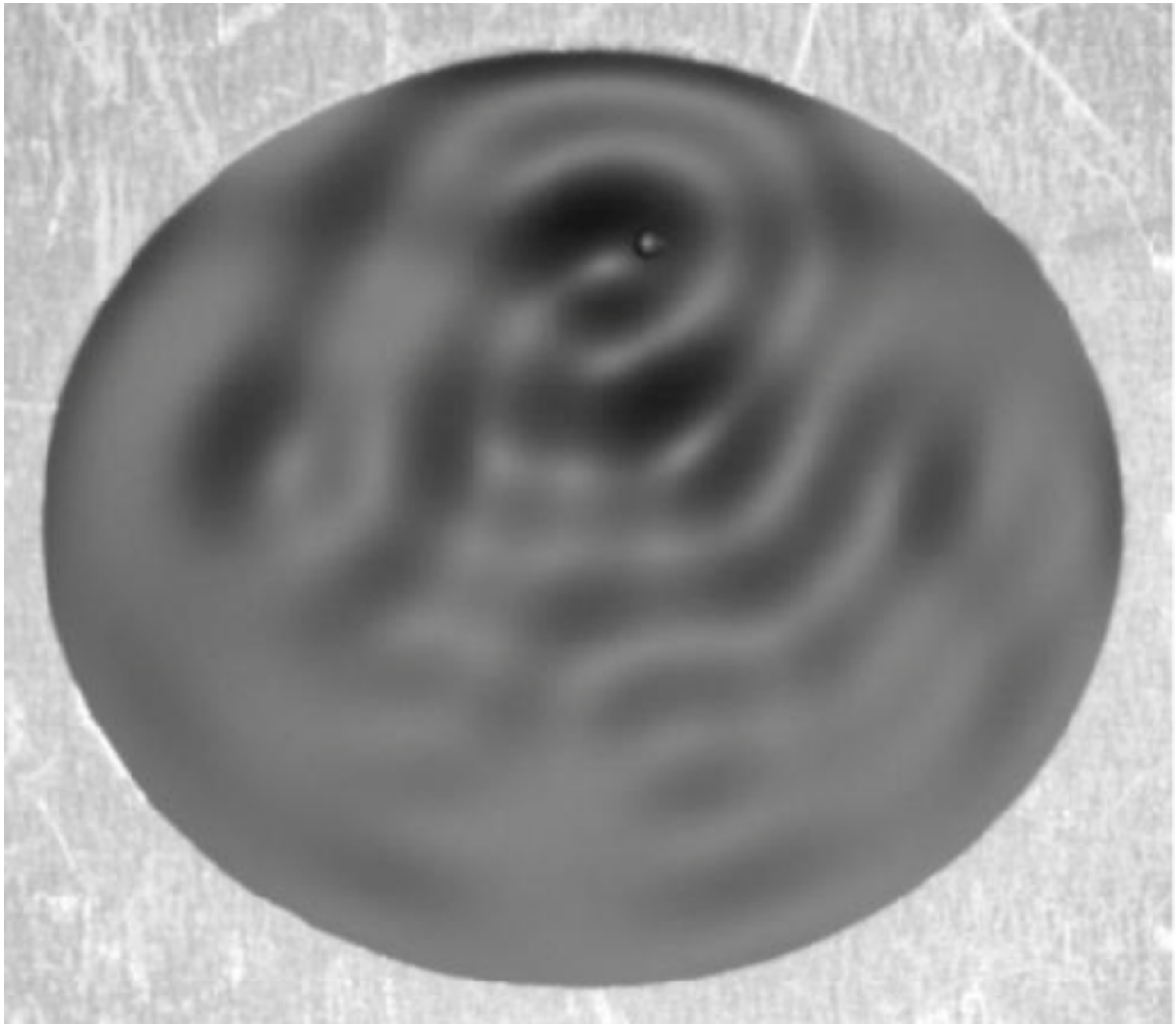

Walker in a corral

- explores its own pilot-wave field
- variations of bouncing phase induced by its pilot-wave field
- dynamics, statistics *not* captured by the stroboscopic model

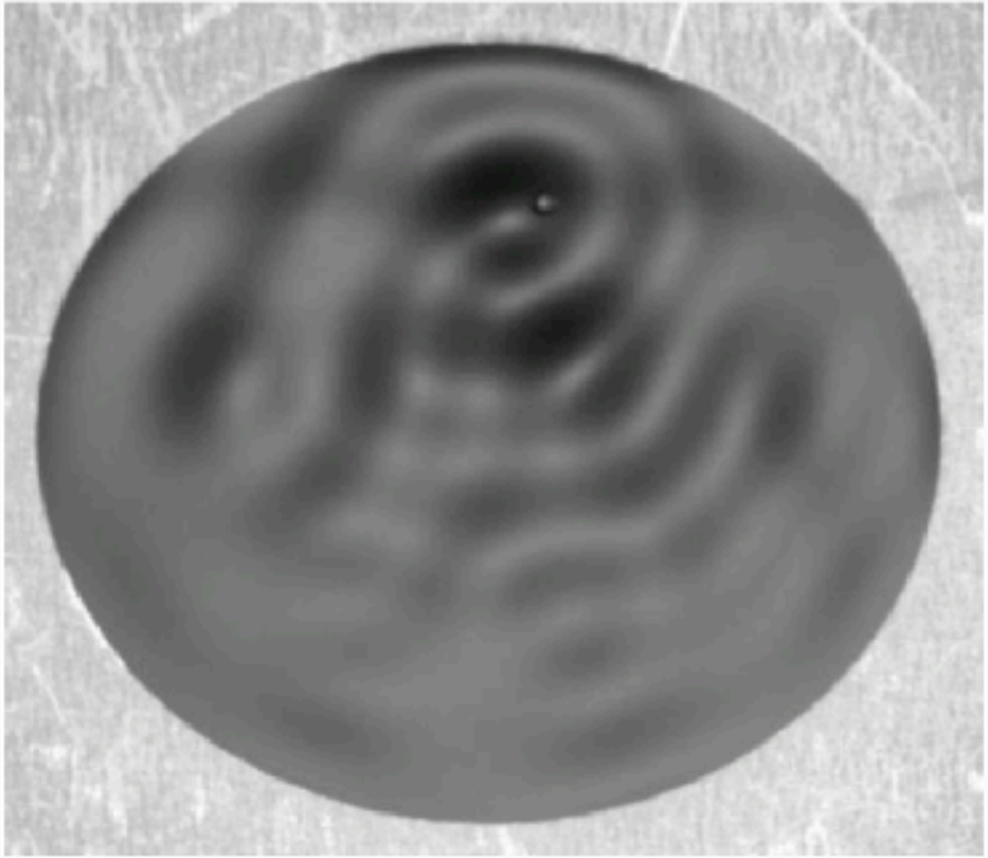

Phase variations, flips

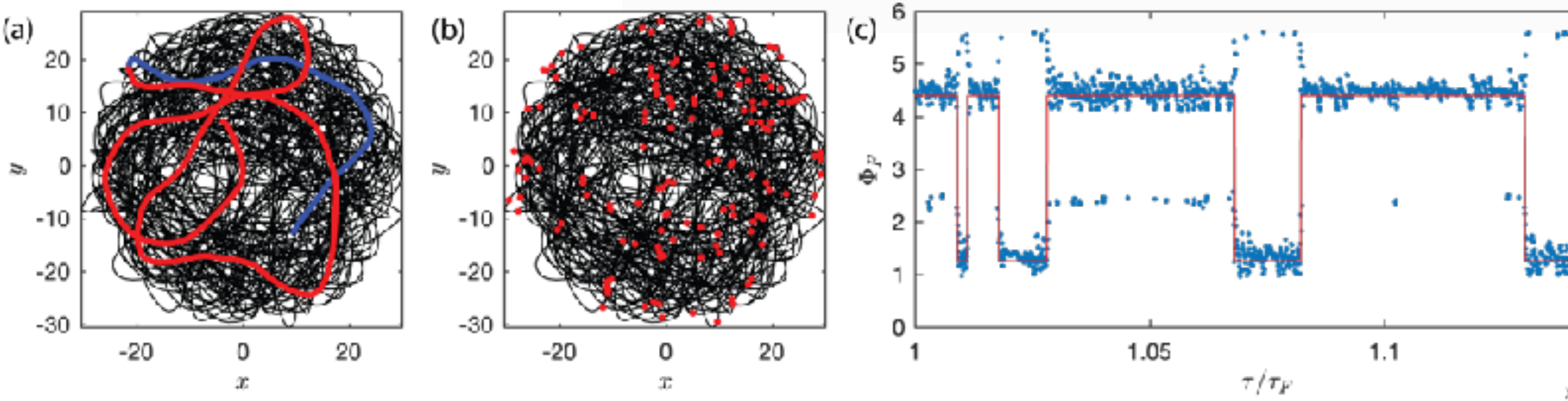

Wave modeling

- superposition of mean wave field (cavity mode) and local pilot wave

$$\eta(x,t) = \left(\varphi(x) + h[x,t;x_p(t)] \right) \times \cos(\omega t)$$

Interface height — Mean Wave — Local pilot wave — Faraday frequency

Standing wave
(above threshold)

OR

Mean wave induced by droplet
(below threshold)

$$h[x,t;x_p(t)] = \frac{A}{T_F}\int_{-\infty}^{t} J_0(k_F|x - x_p(s)|)\, e^{-(t-s)/T_M}\, ds$$

Stroboscopic Approximation (Oza 2013)

- the relative magnitude of these 2 wave components prescribes the system behavior

Stochastic walker dynamics

- consider parameter regime in which erratic, chaotic dynamics arises
- interpret the walker dynamics in terms of a stochastic process

Horizontal Linear Momentum Balance

$$m\ddot{x} + \zeta\dot{x} = \nabla h(x,t)\cos(\omega t)F_Z(t) + \nabla\varphi(x)\cos(\omega t)F_Z(t)$$

$$\zeta\dot{x} = \xi^{(1)}(t) + \nabla\varphi(x)\,\xi^{(2)}(t)$$

Long time scale: inertia << drag

Pilot Wave Force: White Noise 1

Background Force: White noise 2

Stochastic walker dynamics

- multiplicative noise induces an effective potential and a position-dependent diffusion coefficient

Horizontal Linear Momentum Balance

$$dX_t = \frac{\sigma_{XY}}{\zeta} dW_t^{(1)} + \frac{\sigma_Z}{\zeta} \nabla\varphi(X_t) \circ dW_t^{(2)}$$

Fokker-Planck Equation

$$\rho_t = -\mathrm{div}\left(\frac{1}{\zeta} U_P(x)\rho\right) + \mathrm{div}(\mathrm{div}(\mathsf{D}(x)\rho))$$

$$U_P(x) = \frac{\sigma_Z^2}{4\zeta} |\nabla\varphi(x)|^2$$

Ponderomotive potential

$$\mathsf{D}(x) = \frac{\sigma_Z^2}{\zeta^2}\left(\frac{\sigma_{XY}^2}{\sigma_Z^2}\mathbf{1} + \nabla\varphi \otimes \nabla\varphi\right)$$

Position-dependent diffusion tensor

where $\sigma_{XY} = F_0[\nabla h_c]\sqrt{\tau_1}$ $\quad$ $\sigma_Z = F_0\sqrt{\tau_2}$

$F_0 = < F(t)\ \cos\omega t >$, $[\nabla h_c]$ is the characteristic wave gradient,

and τ_1 and τ_2 are the autocorrelation times of the horizontal and vertical dynamics

Radial statistical signature

- predicted histograms now exhibit peaks every half-wavelength, as in experiment

Experiment

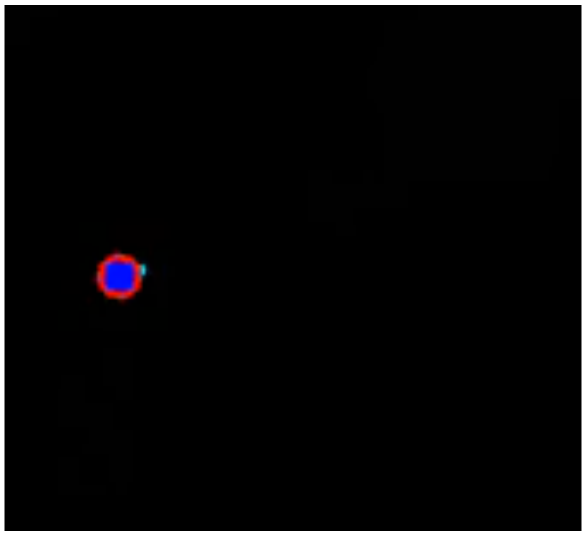

Histogram (Expt)

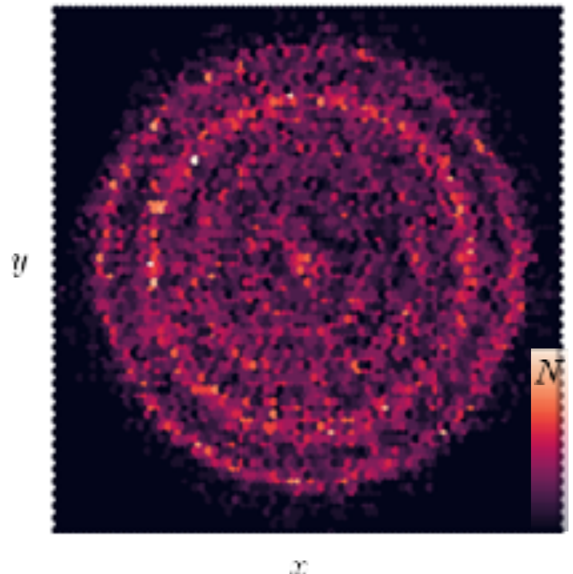

Simulation

$$\varphi(x) = J_0(x)$$

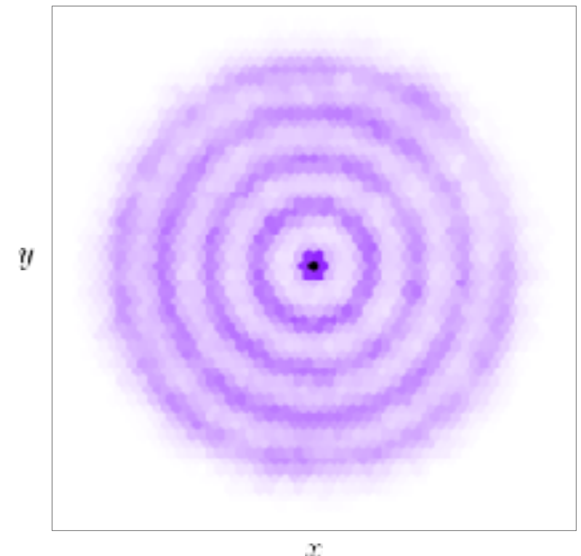

Steady-state *pdf* :

$$\rho_{SS}(x) = \frac{Z}{\sqrt{\frac{\sigma_{XY}^2}{\sigma_Z^2} + |\nabla\varphi|^2}}$$

- form depends on relative magnitudes of noise and background field

Radial statistical signature

Experiment

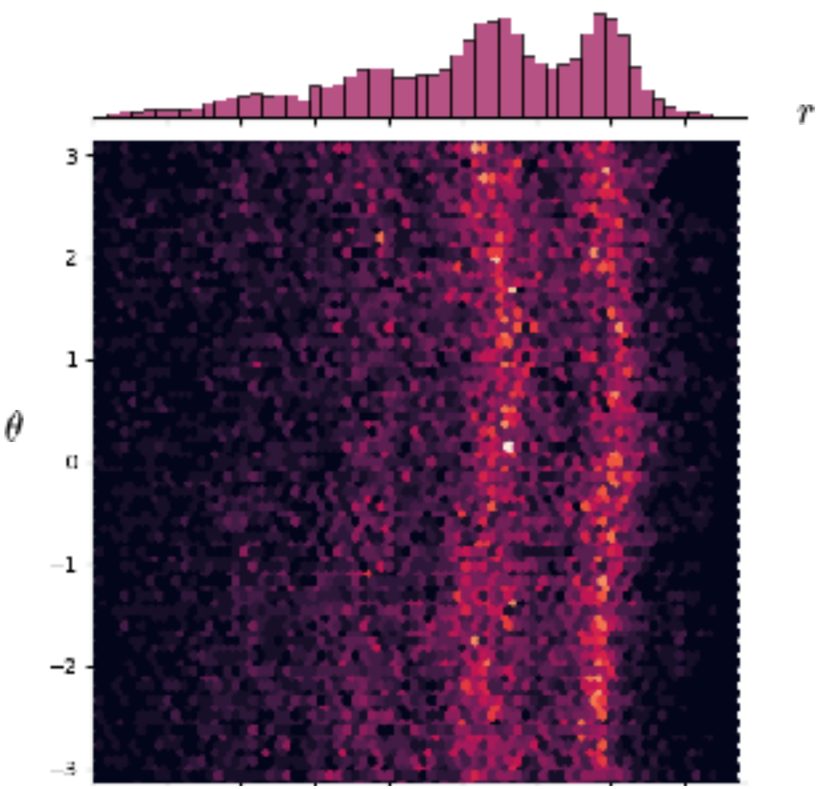

Simulation using $\varphi(x) = J_0(x)$

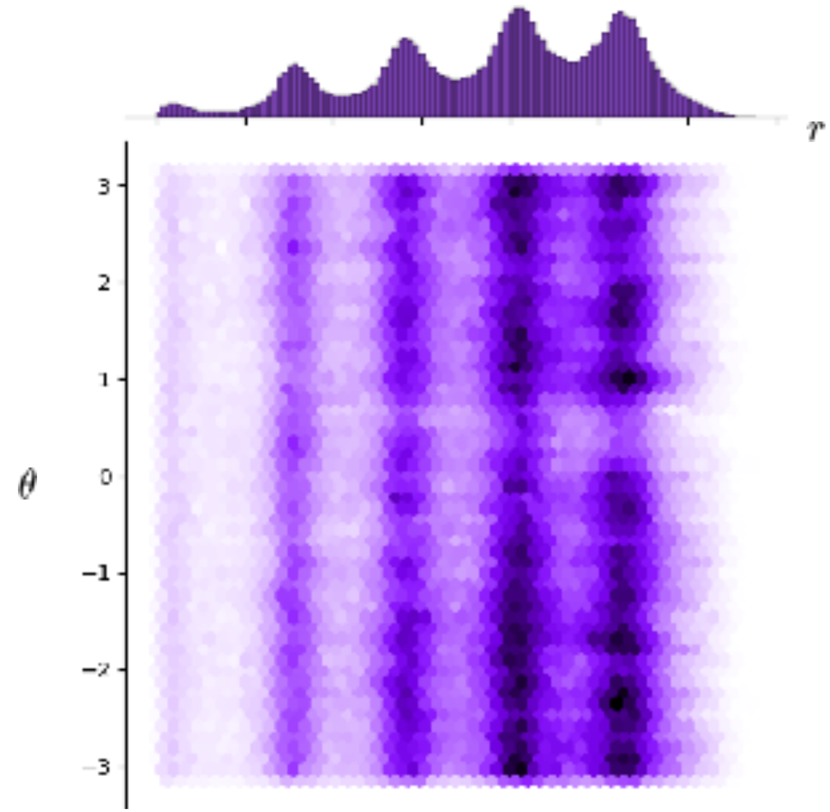

Ponderomotive potential:

$$U_P(x, y) = -\frac{\sigma_Z^2}{4\zeta} \,|\, \nabla \varphi(x, y) \,|^2$$

Anisotropic diffusion tensor:

$$\mathsf{D}(x) = \frac{\sigma_Z^2}{\zeta^2}\left(\frac{\sigma_{XY}^2}{\sigma_Z^2}\mathbf{1} + \nabla\varphi \otimes \nabla\varphi\right)$$

Paradigm III in HQA

- ponderomotive effects activated by non-resonant bouncing
- may arise above Faraday threshold, or below in high Me, closed systems
- above Faraday threshold, φ is the standing Faraday wave field
- below Faraday threshold, φ is the mean pilot-wave field

→ **A PONDEROMOTIVE SELF-POTENTIAL**

Future directions

- identify ponderomotive in other PWH systems; *e.g.* Talbot trapping
- characterize dependence on ratio of noise to mean pilot-wave field
- examine relation to Nelson's Stochastic Mechanics
- examine relation between ponderomotive and quantum potentials

	Bohmian mechanics	Walkers
WAVELENGTH	λ_B	λ_F
GUIDANCE	$m\,\ddot{\mathbf{x}}_p = -\nabla Q - \nabla V + \nabla\Phi_S$	$m\,\ddot{\mathbf{x}}_\mathbf{p} = -D\,\dot{\mathbf{x}}_\mathbf{p} + \nabla\eta(\mathbf{x},t) - \nabla V$
WAVE POTENTIAL	$\mathbf{Q} = -\frac{\hbar^2}{m^2}\frac{1}{\sqrt{\rho}}\nabla^2\sqrt{\rho}$ QUANTUM POTENTIAL	$\bar{\eta}(\mathbf{x}) = \eta_B * \mu(\mathbf{x})$ MEAN WAVE FIELD
STOCHASTIC FORCING	$\nabla\Phi_S$ ARBITRARY, *ad hoc*	$-\nabla\eta^*(\mathbf{x},t)$ PERTURBATION WAVE FIELD
WAVE ORIGIN	NONE	PARTICLE VIBRATION

HQA Corrals

$\gamma_F = 3.75g$

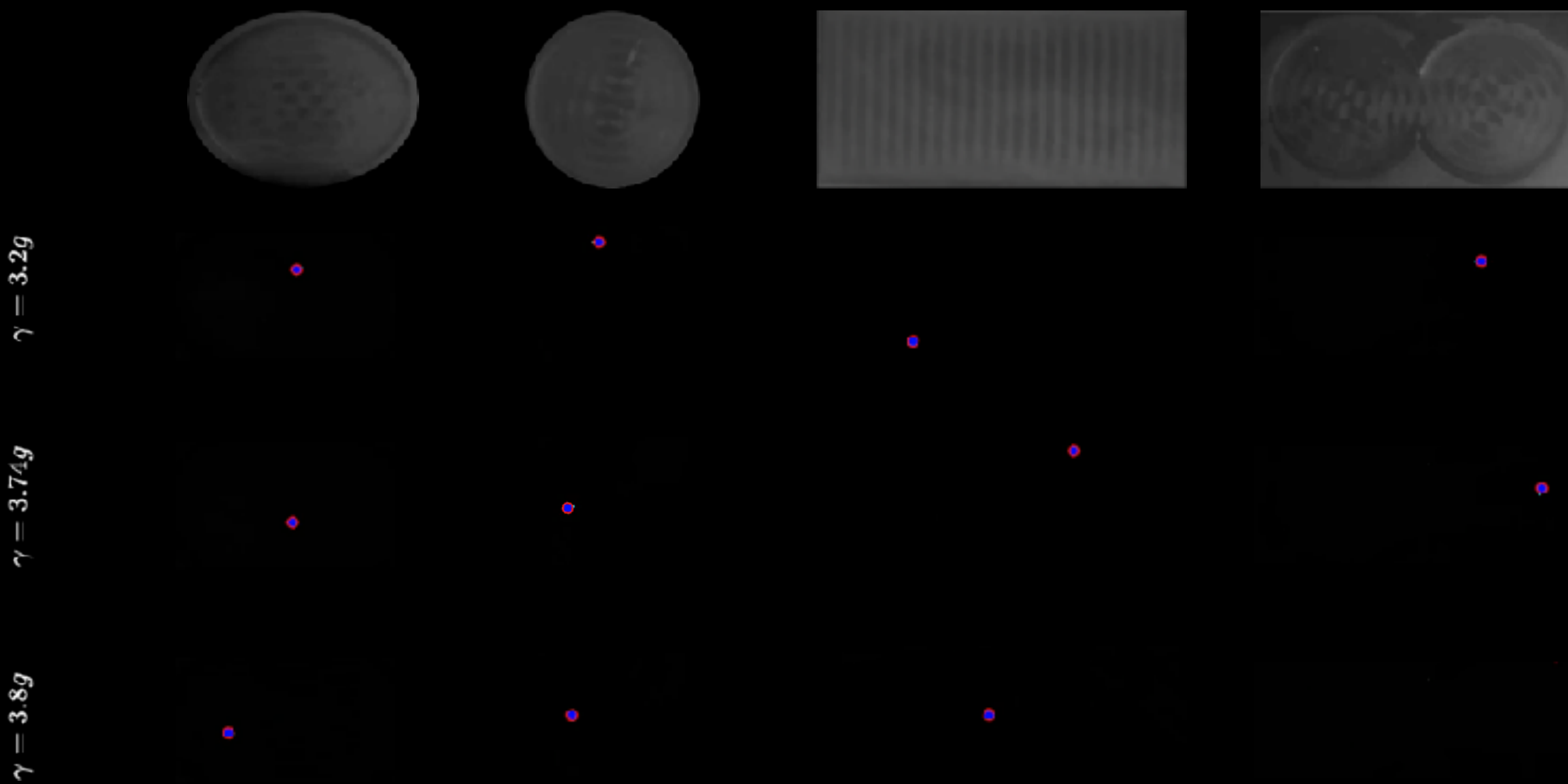

Histograms

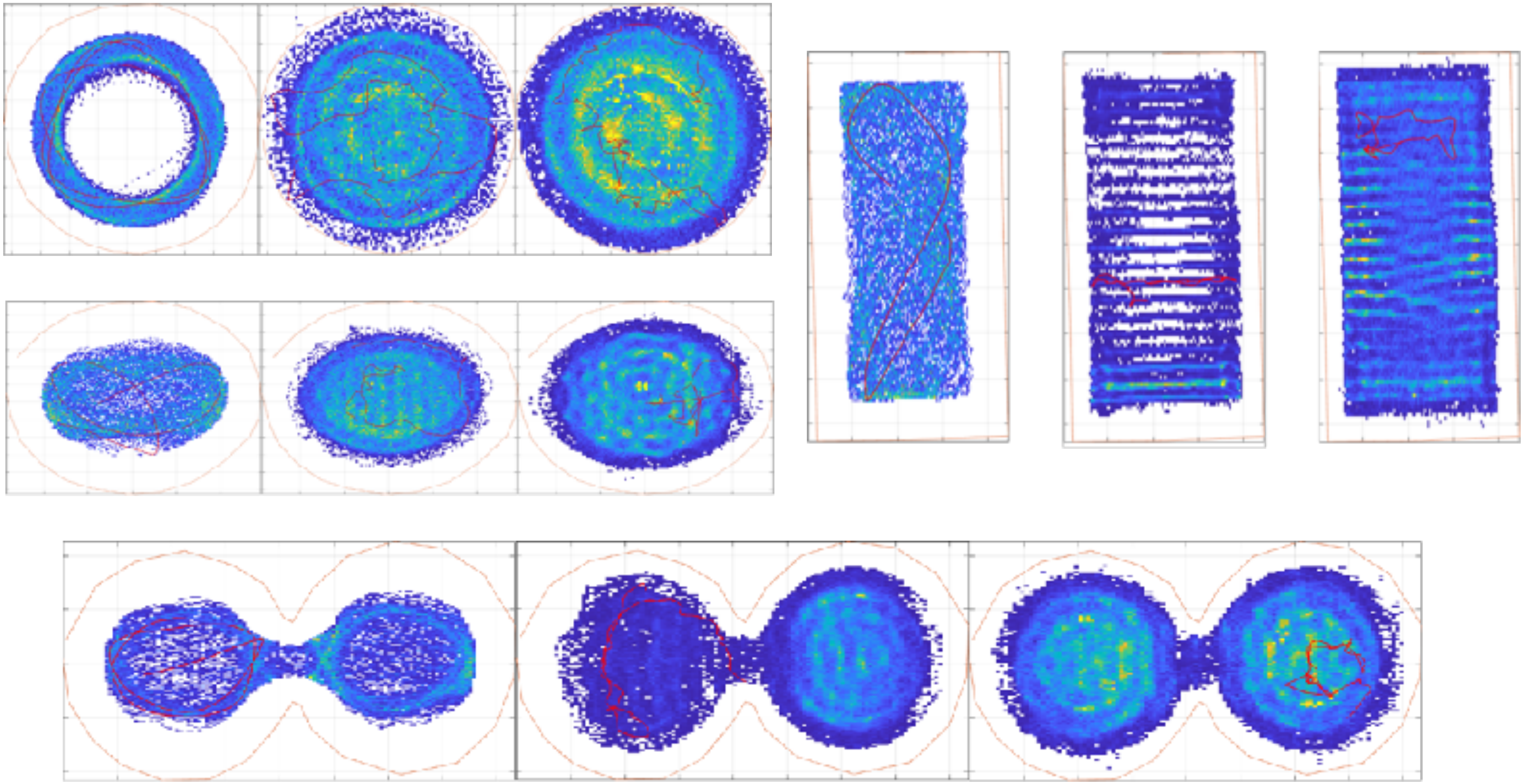

The distinction between just below and above the Faraday threshold is blurred:
the particle-induced mean pilot-wave acts as an imposed potential … like Q?

Chaos in quantum billiards: scars evident

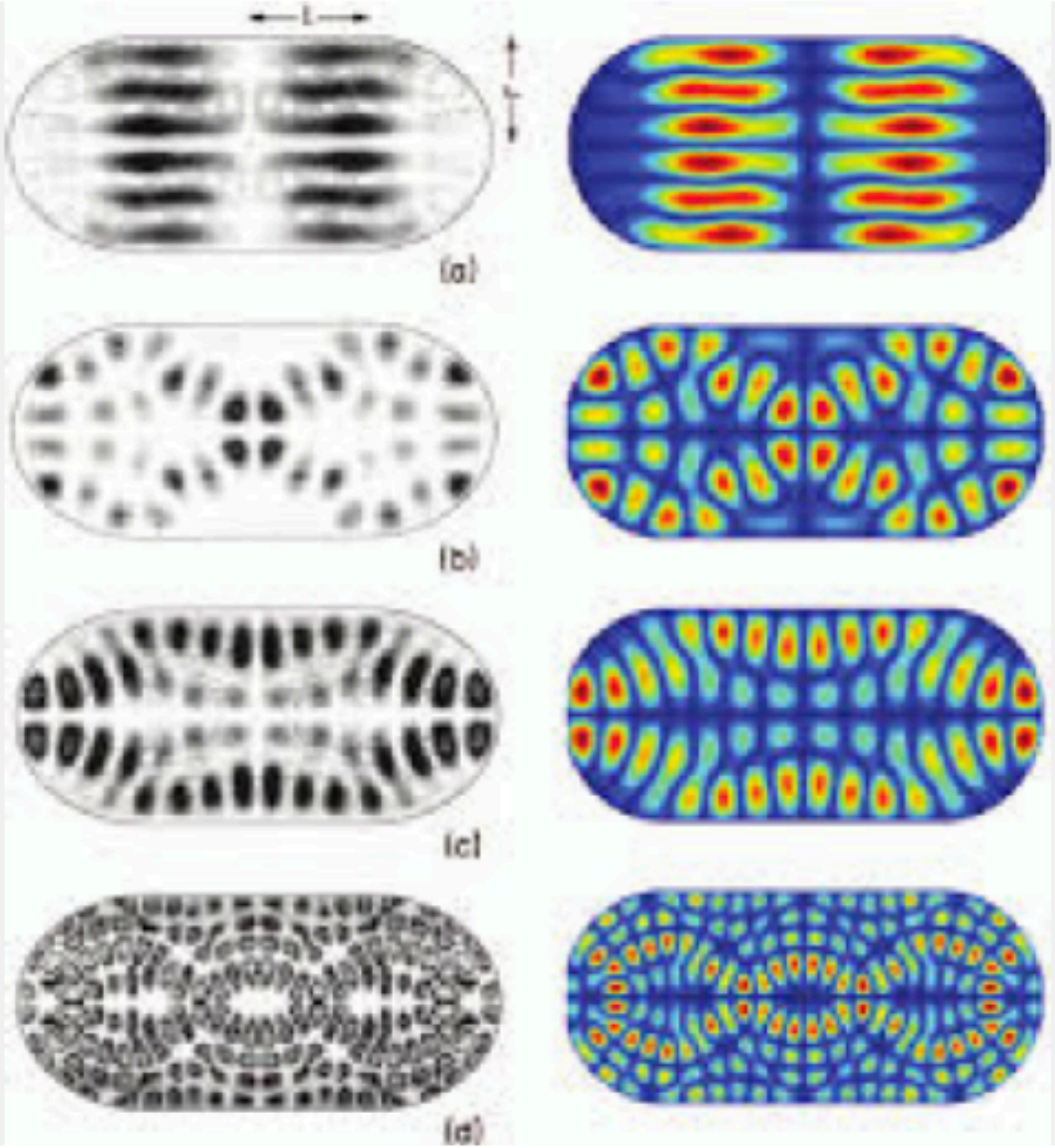

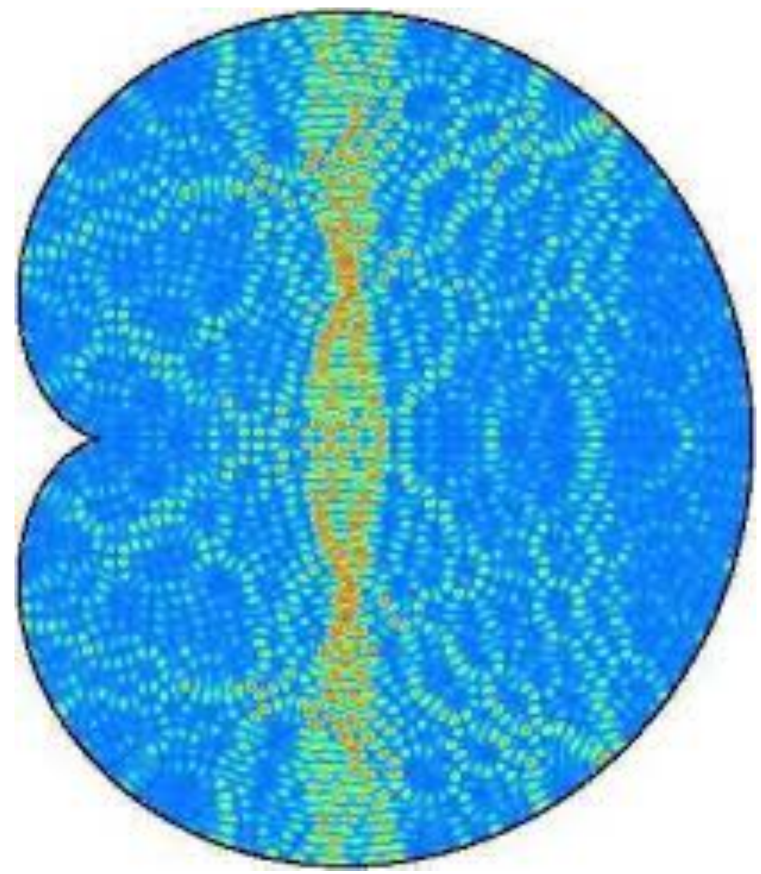

Scars in Faraday waves

PHYSICAL REVIEW E, VOLUME 63, 026208

Scarred patterns in surface waves

A. Kudrolli,[1,2,*] Mathew C. Abraham,[1] and J. P. Gollub[1,3,†]

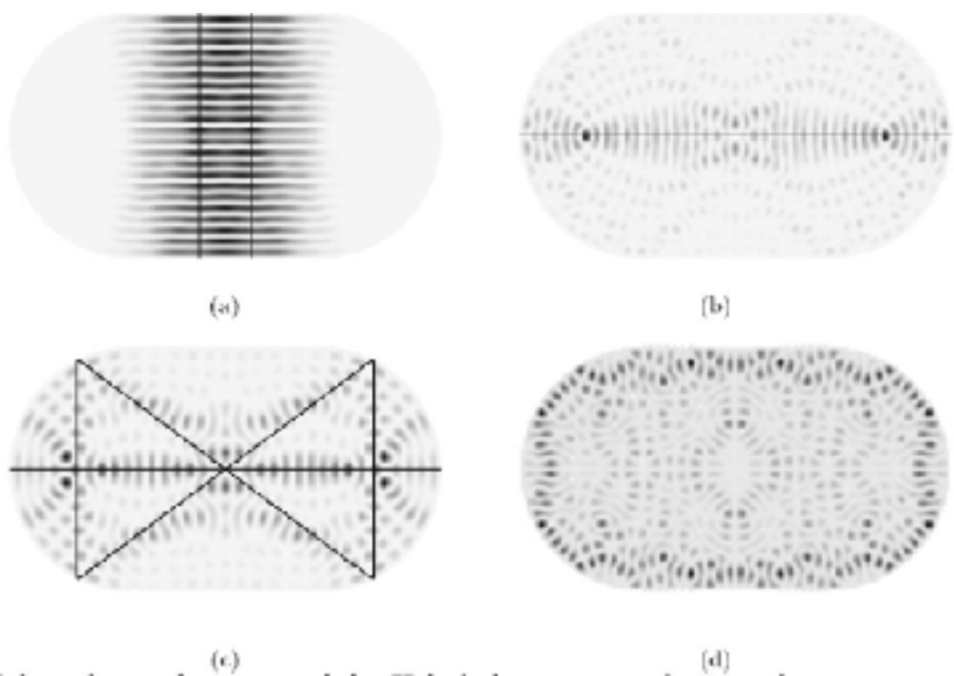

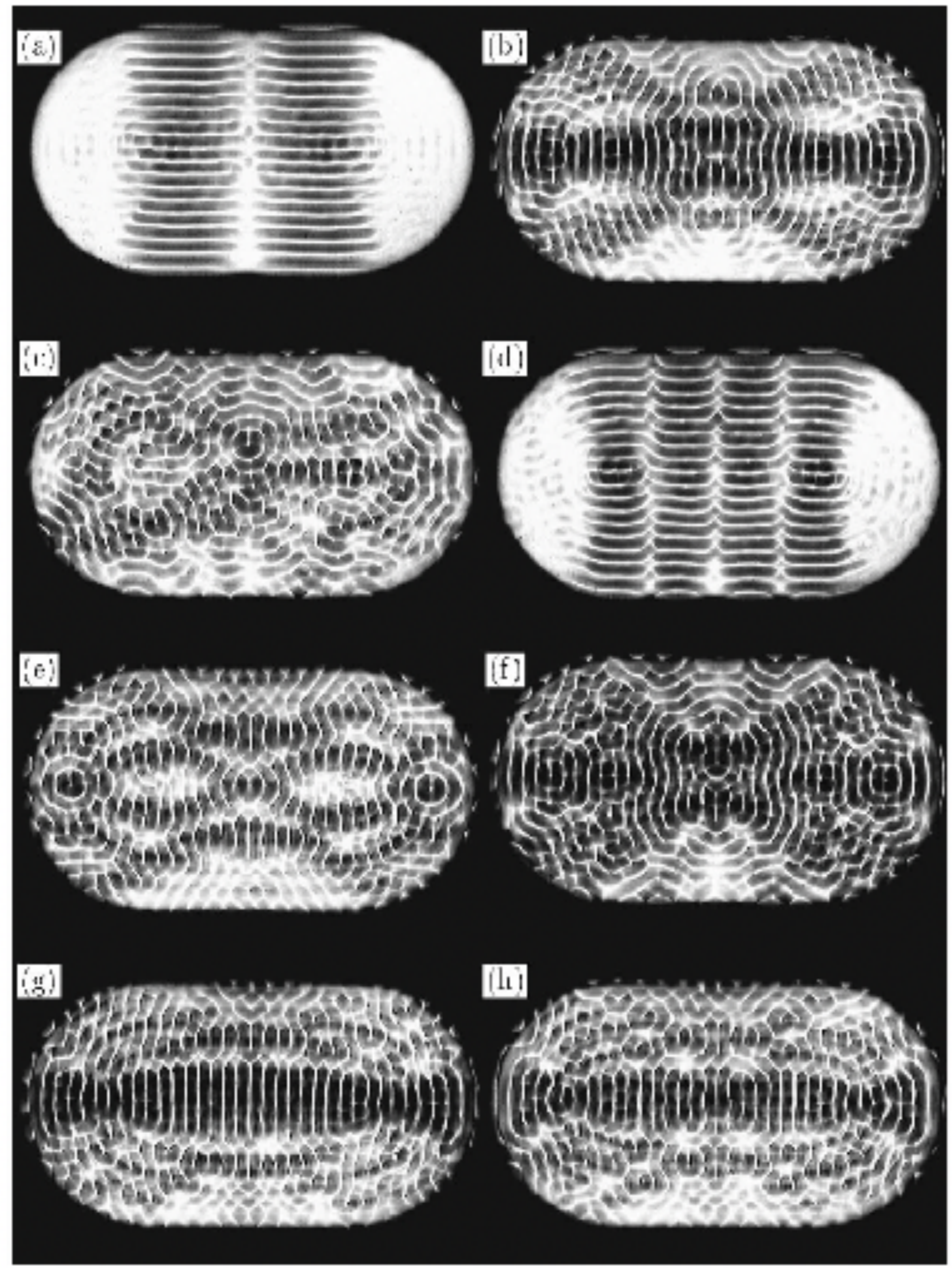

- can we see scars in walker *pdf*s ?

Scars in walker *pdf*s

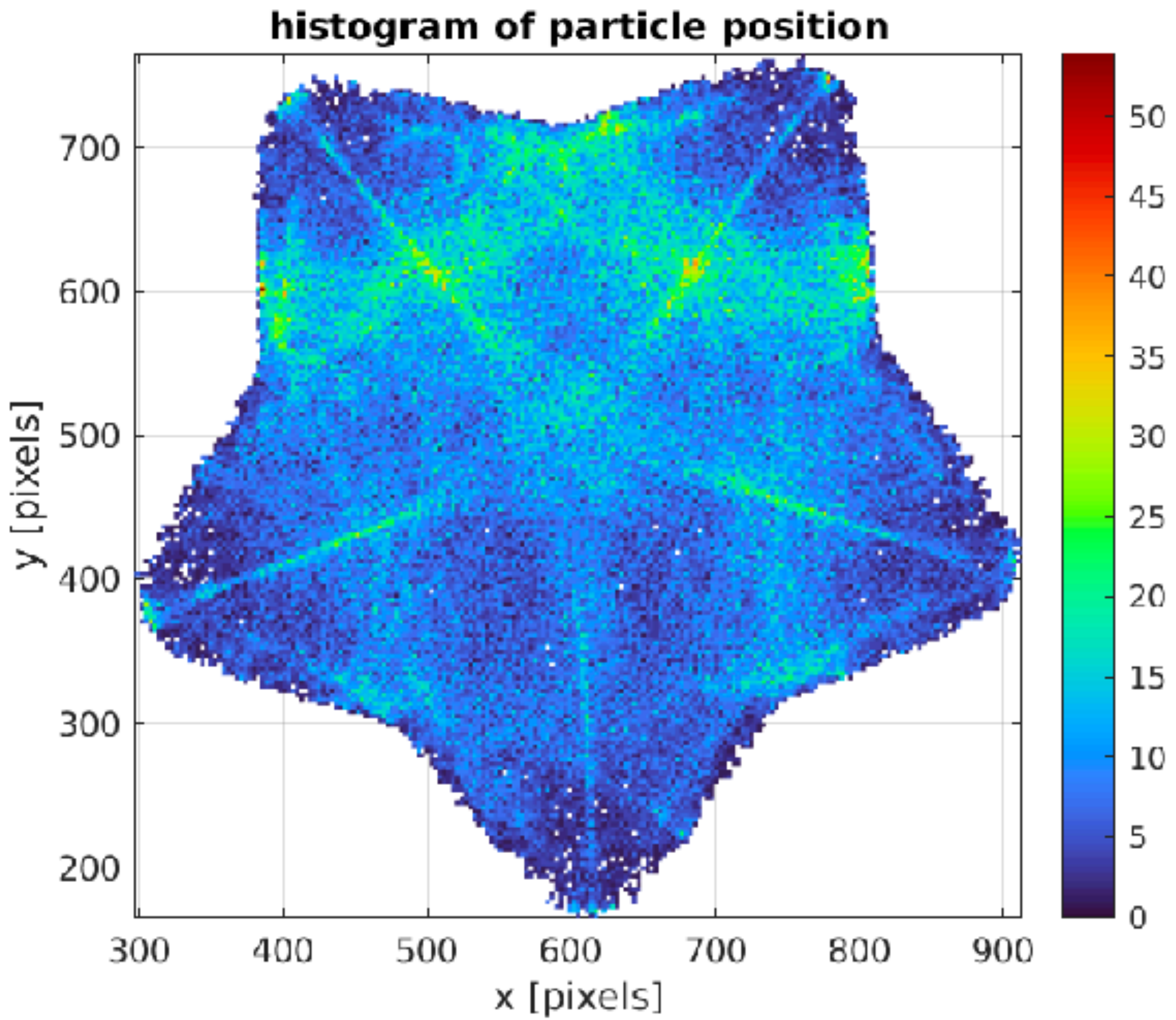

Scars in walker *pdf*s

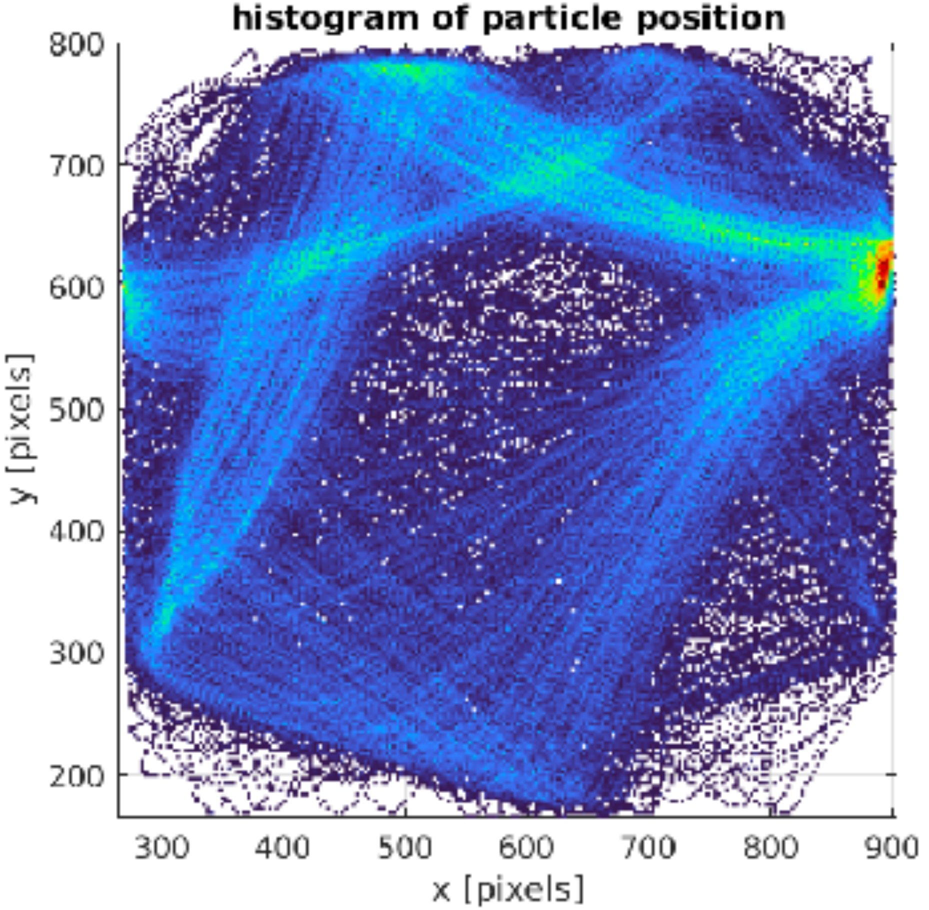

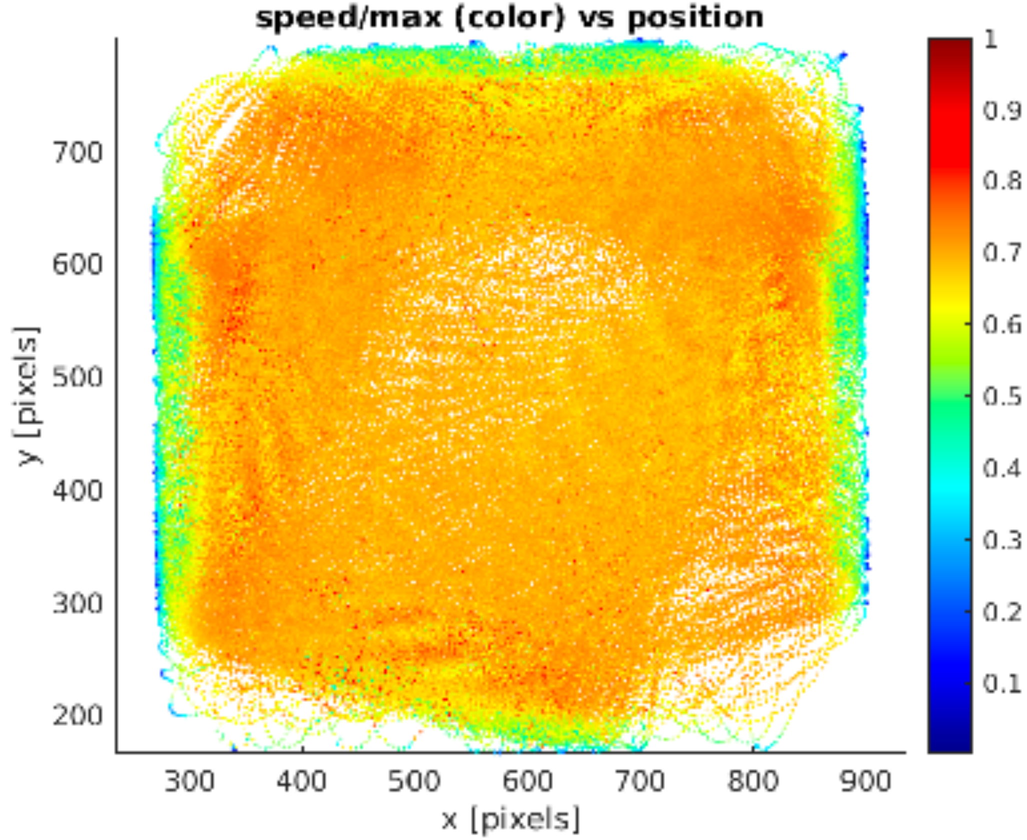

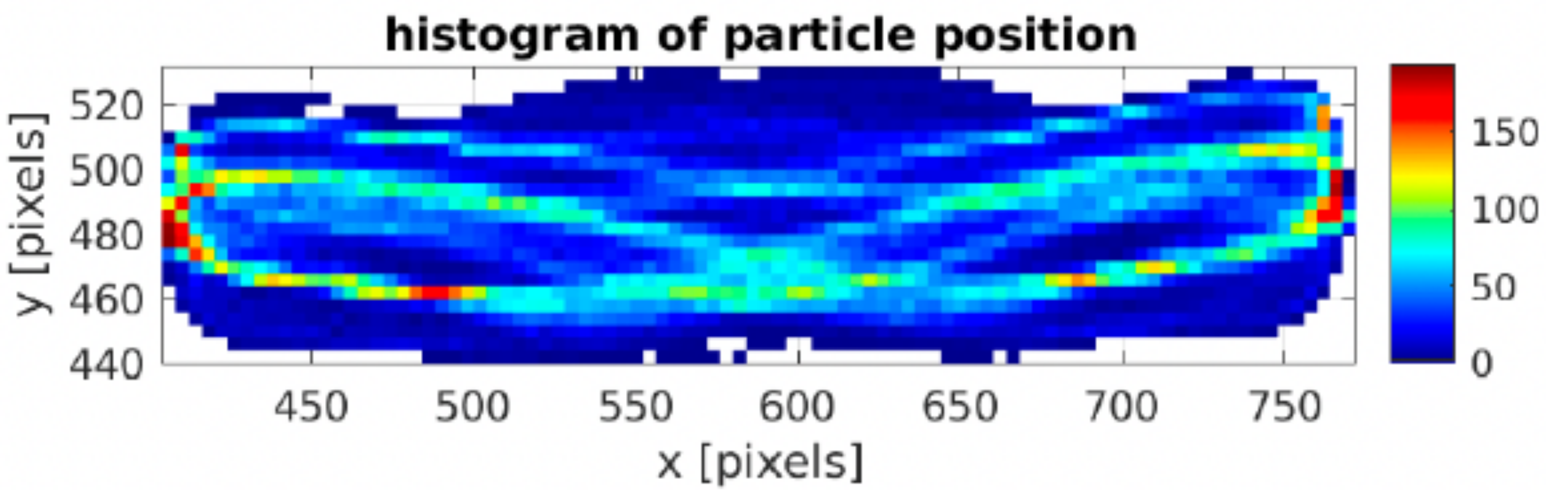

A generalized pilot-wave framework

PROCEEDINGS A

royalsocietypublishing.org/journal/rspa

Research

Check for updates

Speed oscillations in classical pilot-wave dynamics

Matthew Durey, Sam E. Turton and John W. M. Bush

Department of Mathematics, Massachusetts Institute of Technology, Cambridge, MA 02139, USA

Chaos

Classical pilot-wave dynamics: The free particle

Cite as: Chaos **31**, 033136 (2021); https://doi.org/10.1063/5.0039975
Submitted: 08 December 2020 . Accepted: 18 February 2021 . Published Online: 12 March 2021

Matthew Durey, and John W. M. Bush

A generalized pilot-wave framework

- retain key features of walker system

  (memory, resonance, quasi-monochromatic wave field)

- explore beyond the range of the hydrodynamic system

- connect to and inform quantum pilot-wave theories

(*Bush, ARFM, 2015*)

Pilot-wave dynamics: a parametric generalization

$$\kappa_0(1-\Gamma)\ddot{\mathbf{x}}_p + \dot{\mathbf{x}}_p = \frac{2}{(1-\Gamma)^2}\int_{-\infty}^{t} \frac{J_1(|\mathbf{x}_p(t)-\mathbf{x}_p(s)|)}{|\mathbf{x}_p(t)-\mathbf{x}_p(s)|}(\mathbf{x}_p(t)-\mathbf{x}_p(s))e^{-(t-s)}\,ds$$

INERTIA **DRAG** **WAVE FORCING**

where $$\Gamma = \frac{\gamma-\gamma_W}{\gamma_F-\gamma_W} \quad , \qquad \kappa_0 = (m/D)^{3/2} k_F \sqrt{gA/2T_F}$$

PROXIMITY TO THRESHOLD

$0 < \Gamma < 1$

CONTAINS ALL FLUID PARAMETERS: BOUNDED IN HYDRODYNAMIC SYSTEM

$0.8 < \kappa_0 < 1.6$ in lab

Question: For what values of (κ_0, Γ) does the system look most like QM?

Eg.1 When are hydrodynamic spin states stable?

Eg.2 When is walking state unstable to in-line oscillations?

Generalized pilot-wave theory

$$\Gamma = \frac{\gamma - \gamma_W}{\gamma_F - \gamma_W}$$

PROXIMITY TO THRESHOLD

$$\kappa_0 = (m/D)^{3/2} k_F \sqrt{gA/2T_F}$$

CONTAINS ALL FLUID PARAMETERS

When are hydrodynamic spin states stable? (*Oza, Rosales & Bush, 2018*)

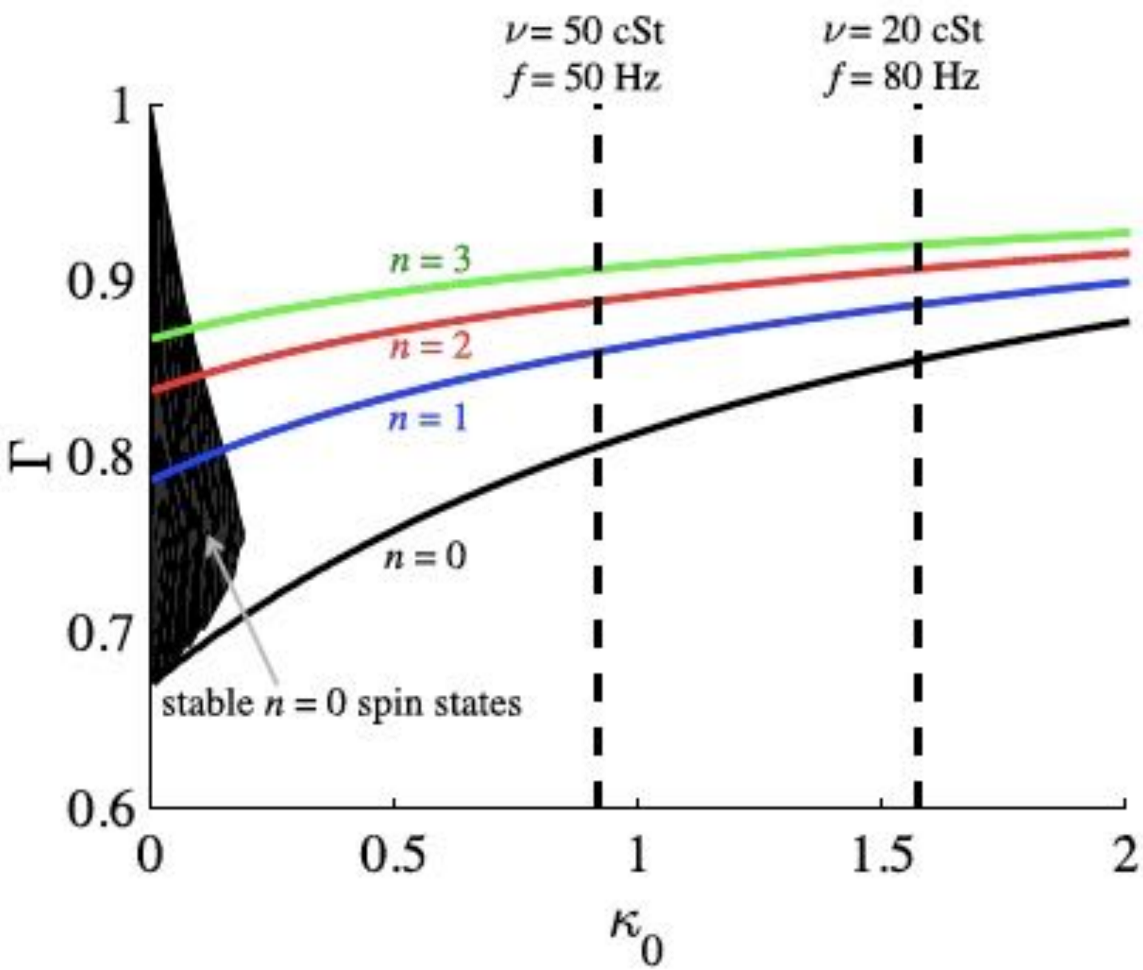

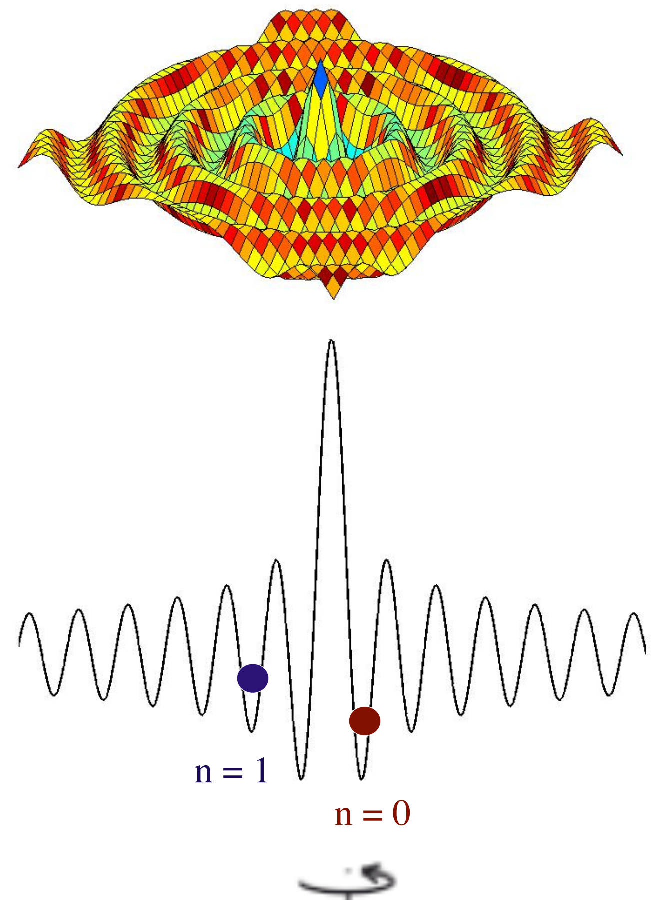

When is the walking state unstable to in-line oscillations?

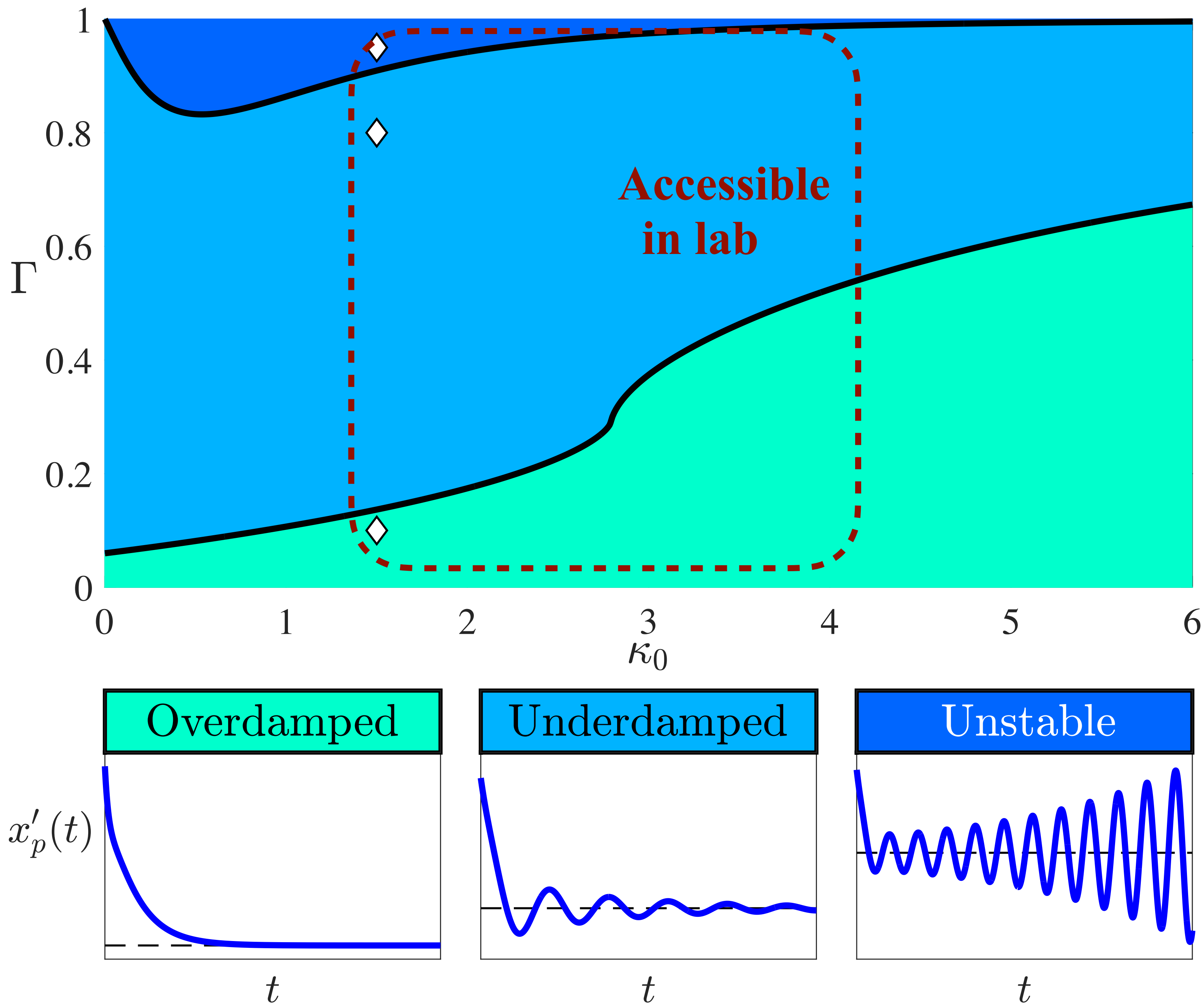

- walking state may be unstable to in-line oscillations with wavelength λ_F

Evidence of in-line oscillations

I. FREE WALKER

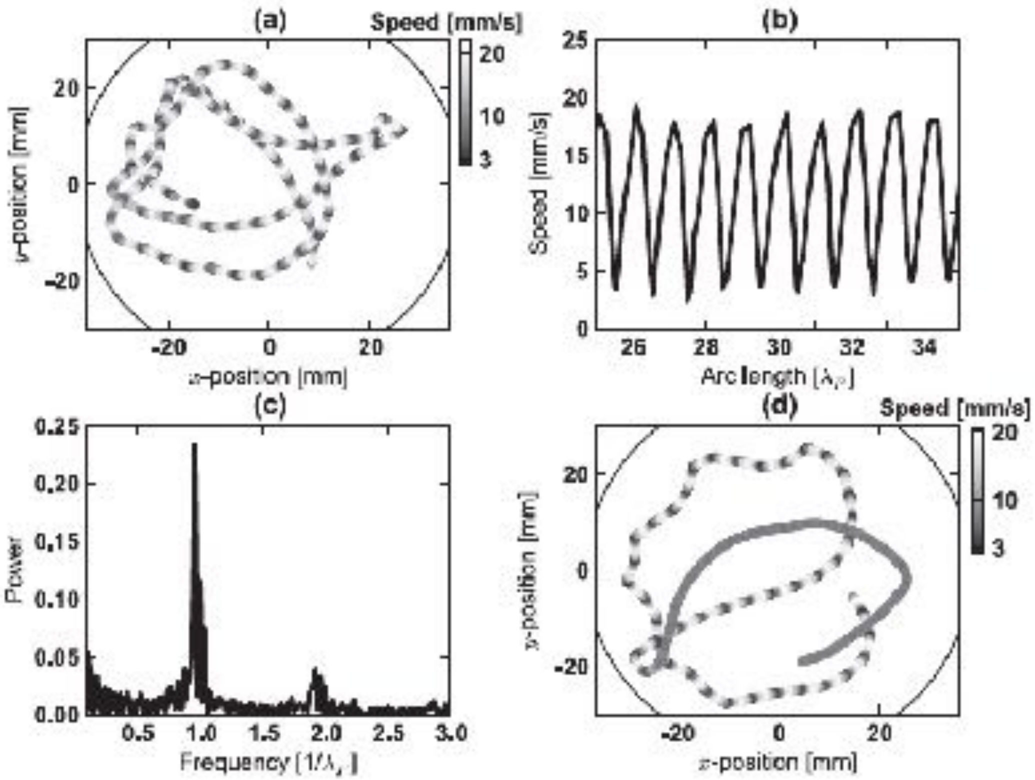

Wind-Willassen et al. (2013)

See also *Bacot et al. (2019)*

II. FRIEDEL OSCILLATIONS

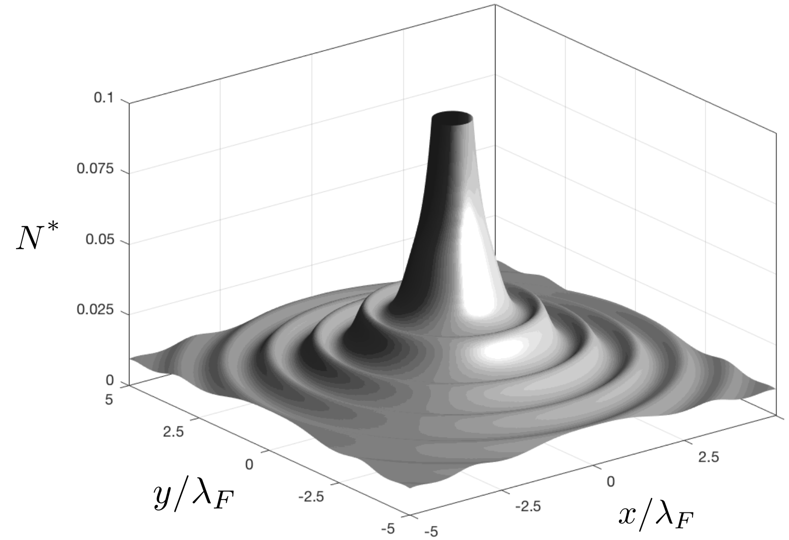

III. CORRALS

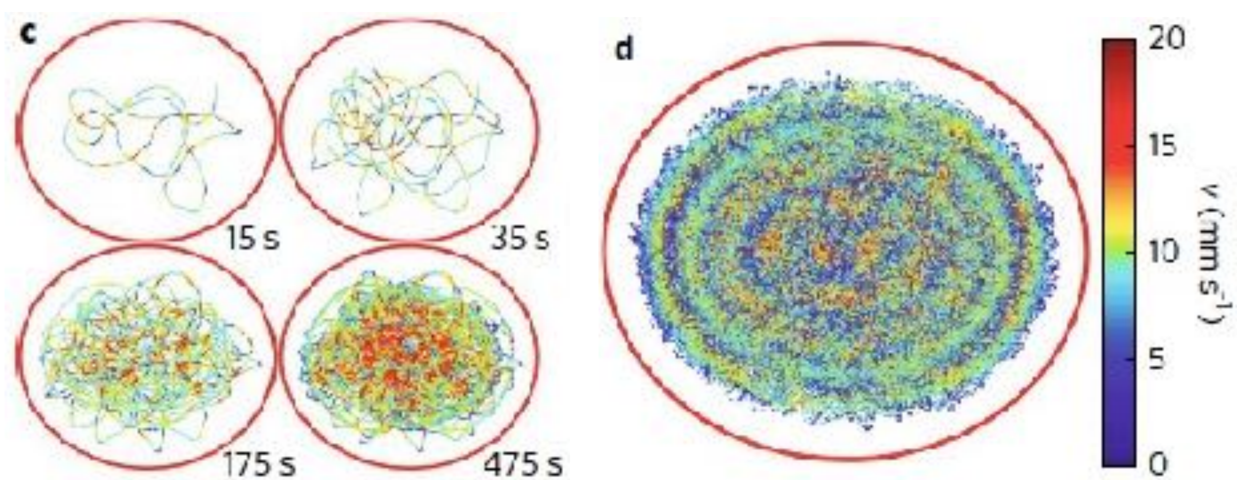

- provides mechanism for emergent statistics in the Friedel oscillations and corrals

When is the walking state unstable to in-line oscillations?

(*Durey, Turton & Bush, 2020*)

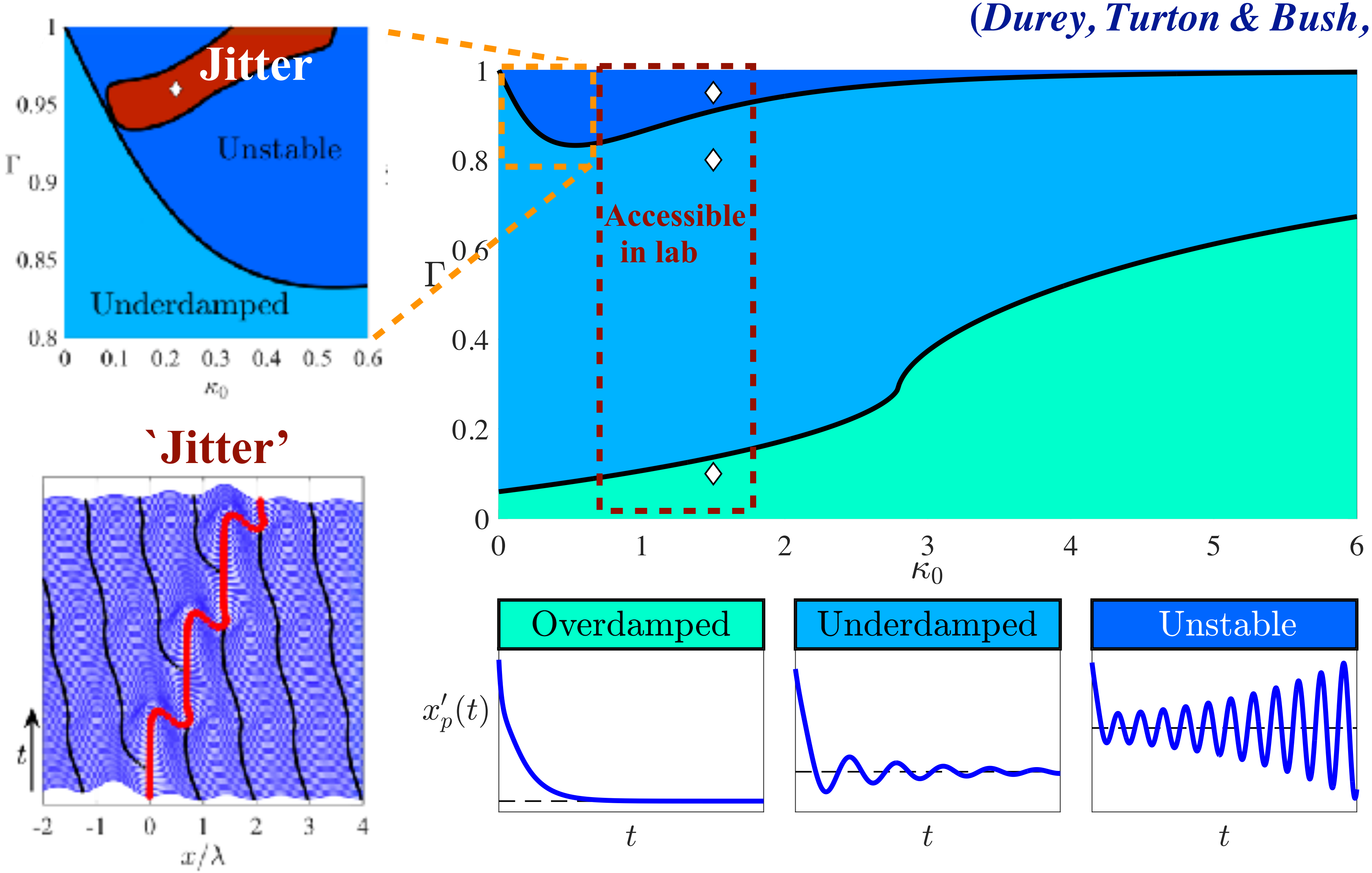

- walking state may be unstable to in-line oscillations with wavelength λ_F
- periodic and aperiodic *`jittering'* states may also obtain
- aperiodic jittering gives rise to random walk with diffusivity $D \sim U\lambda_F$

An aside: a nonlinear oscillatory `limping' state

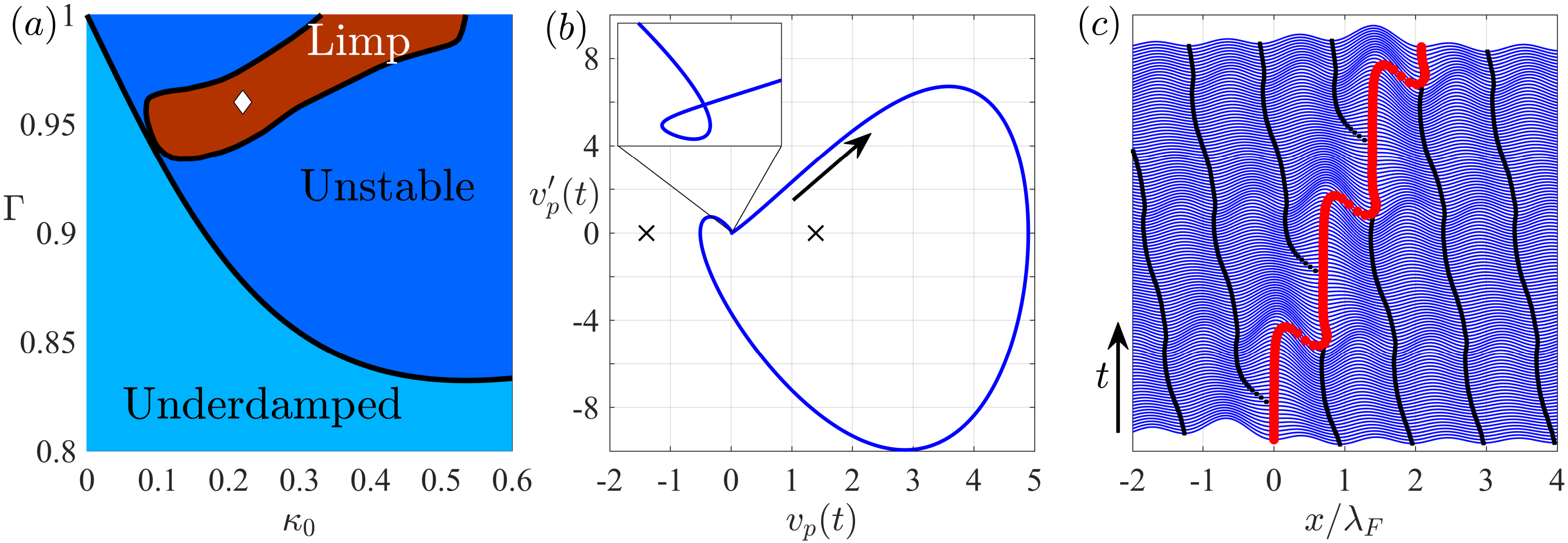

- in a certain regime, the particle may reverse direction, its motion be characterized in terms of a random walk with characteristic speed U and step size λ_F
- the characteristic diffusivity is thus $\mathrm{D} \sim \mathrm{U}\, \lambda_F$
- in his Stochastic Dynamics, Nelson (1966) asserted that QM may be understood in terms of a diffusive process with effective diffusivity $D_Q \sim \hbar/m$

NOTE: $$D_Q \sim \frac{\hbar}{m} \sim \frac{\hbar k_B}{m k_B} \sim U \lambda_B$$

Generalized pilot-wave theory: the free particle in 2D

(*Durey & Bush, 2020*)

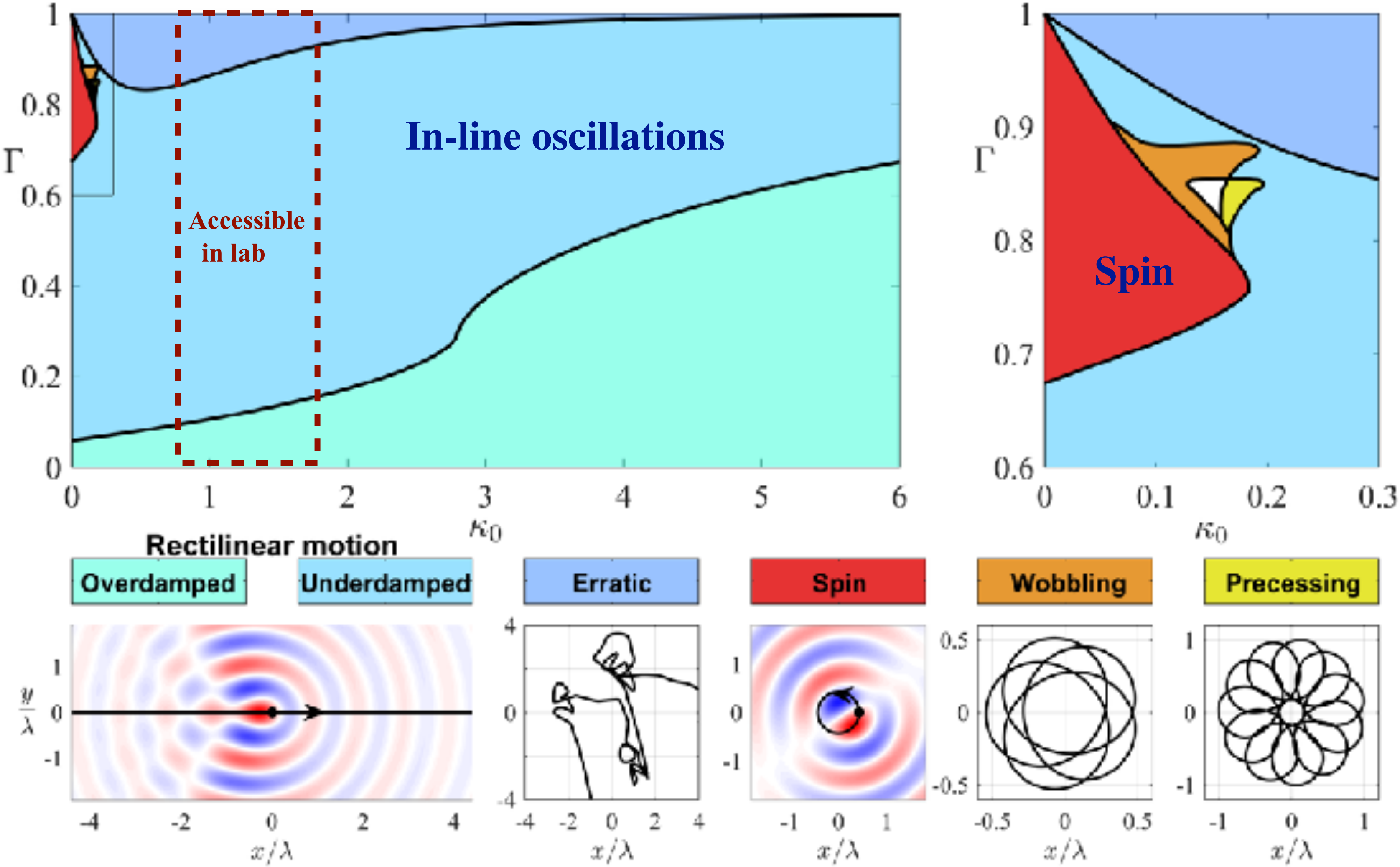

- stable, wobbling and precessing spin states may obtain
- walking state may be unstable to in-line oscillations with wavelength λ_F
- aperiodic `*jittering*' gives rise to random walk with diffusivity $D \sim U\lambda_F$

Bound states accessible in a generalized pilot-wave framework

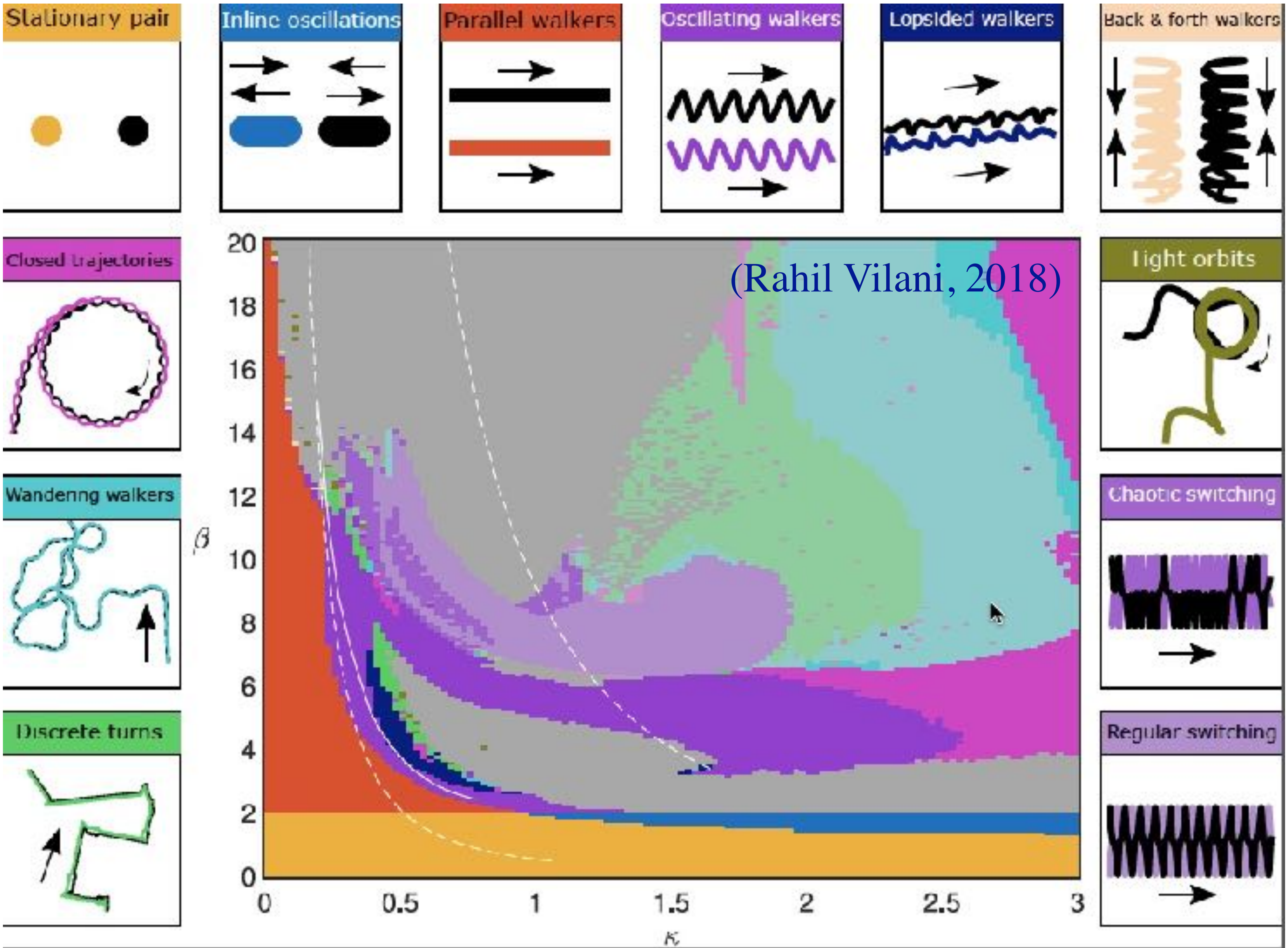

Newtonian pilot-wave dynamics

$$m\,\ddot{\mathbf{x}}_{\mathbf{p}} \; + \; D\,\dot{\mathbf{x}}_{\mathbf{p}} \; = \; A\,\nabla\eta$$

INERTIA DRAG WAVE FORCING

Three limits of interest

I. Hydrodynamic regime

II. Limping regime found in the GPWF

- resembles Stochastic Dynamics of Nelson (1966)

III. High memory, closed systems $\eta = \bar{\eta} + \eta^* \quad , \quad \bar{\eta} \gg \eta^*$

- resembles dynamics of Bohm & Vigier (1954)
    - mean pilot-wave field $\nabla\bar{\eta}$ acts as nonlocal potential
    - perturbation from mean $\nabla\eta^*$ plays role of stochastic forcing

Generalized pilot-wave theory

$$\kappa_0(1-\Gamma)\ddot{\mathbf{x}}_p + \dot{\mathbf{x}}_p = \frac{2}{(1-\Gamma)^2}\int_{-\infty}^{t} \frac{J_1(|\mathbf{x}_p(t)-\mathbf{x}_p(s)|)}{|\mathbf{x}_p(t)-\mathbf{x}_p(s)|}(\mathbf{x}_p(t)-\mathbf{x}_p(s))e^{-(t-s)}\,ds$$

INERTIA **DRAG** **WAVE FORCING**

where $$\Gamma = \frac{\gamma-\gamma_W}{\gamma_F-\gamma_W} \quad , \quad \kappa_0 = (m/D)^{3/2} k_F \sqrt{gA/2T_F}$$

PROXIMITY TO THRESHOLD

CONTAINS ALL FLUID PARAMETERS: BOUNDED IN HYDRODYNAMIC SYSTEM

Question: For what values of (κ_0, Γ) does the system look most like QM?

Further extensions

- consideration of alternative spatio-temporal damping, bouncing phase variations
- in our system, the wavelength is prescribed by the forcing, constant
- extend to 3D by treating particle as a source of spherically symmetric waves
- inspired by SED and Nelson (1958), we can also incorporate a stochastic forcing

Stochastic pilot-wave dynamics

$$\kappa_0(1-\Gamma)\ddot{\mathbf{x}}_p + \dot{\mathbf{x}}_p = \frac{2}{(1-\Gamma)^2}\int_{-\infty}^{t} \frac{J_1(|\mathbf{x}_p(t)-\mathbf{x}_p(s)|)}{|\mathbf{x}_p(t)-\mathbf{x}_p(s)|}(\mathbf{x}_p(t)-\mathbf{x}_p(s))e^{-(t-s)}\,ds \;+\; \mathbf{F_s(t)}$$

INERTIA **DRAG** **WAVE FORCING** **STOCHASTIC FORCING**

New control parameter: $\beta = \dfrac{\text{STOCHASTIC FORCE}}{\text{WAVE FORCE}}$

Approach

- tuning β should allow us to pass continuously between two traditionally disparate realist models of QM: pilot-wave theory and stochastic dynamics
- expect certain systems to change quantitatively (e.g. orbital dynamics) while others may change qualitatively (e.g. diffraction)

For what values of $(\Gamma, \kappa_0, \beta)$ **does the system look most like QM?**

Might stochastic forcing induce ponderomotive effects that stabilize spin states?

Exploring orbital dynamics and trapping with a generalized pilot-wave framework

Lucas D. Tambasco, and John W. M. Bush

Citation: Chaos **28**, 096115 (2018); doi: 10.1063/1.5033962
View online: https://doi.org/10.1063/1.5033962

Well-induced trapping

Sáenz *et al.* (2017) demonstrated that *pilot-wave dynamics are viable* in relatively *shallow water*, where the lower boundary affects the dynamics.

We here consider pilot-wave dynamics with a *central well* that induces a circularly-symmetric Faraday wave.

We then explore the dynamics with the general pilot-wave framework.

Well-induced trapping

EXPERIMENTS

SETUP

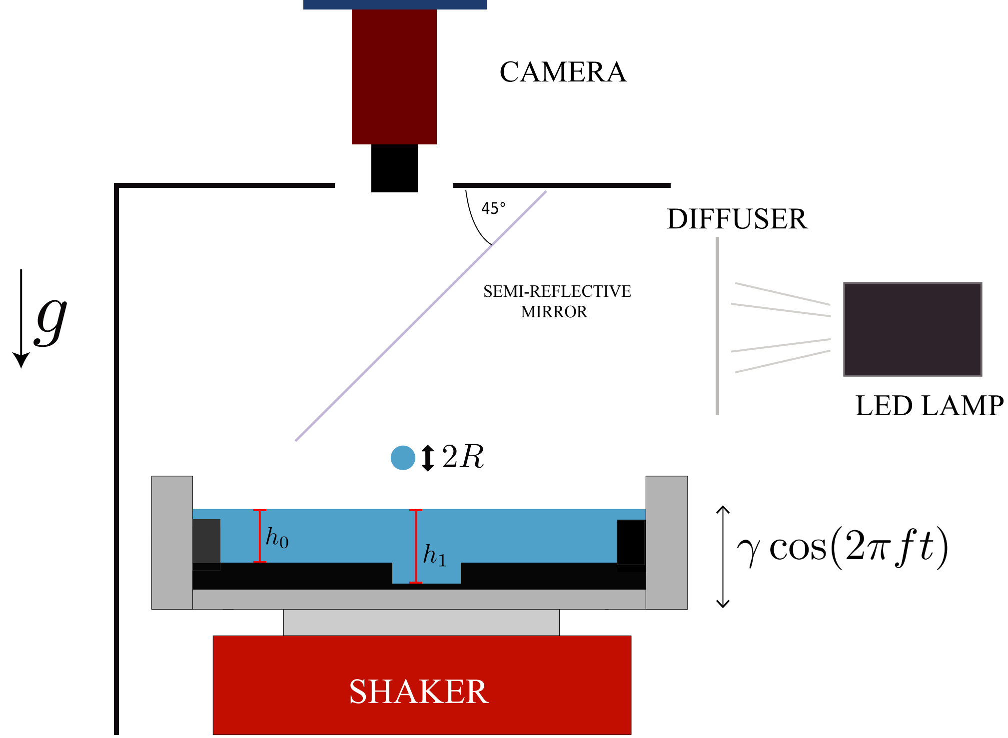

Well located in the middle of bath

WELL-INDUCED WAVEFIELD

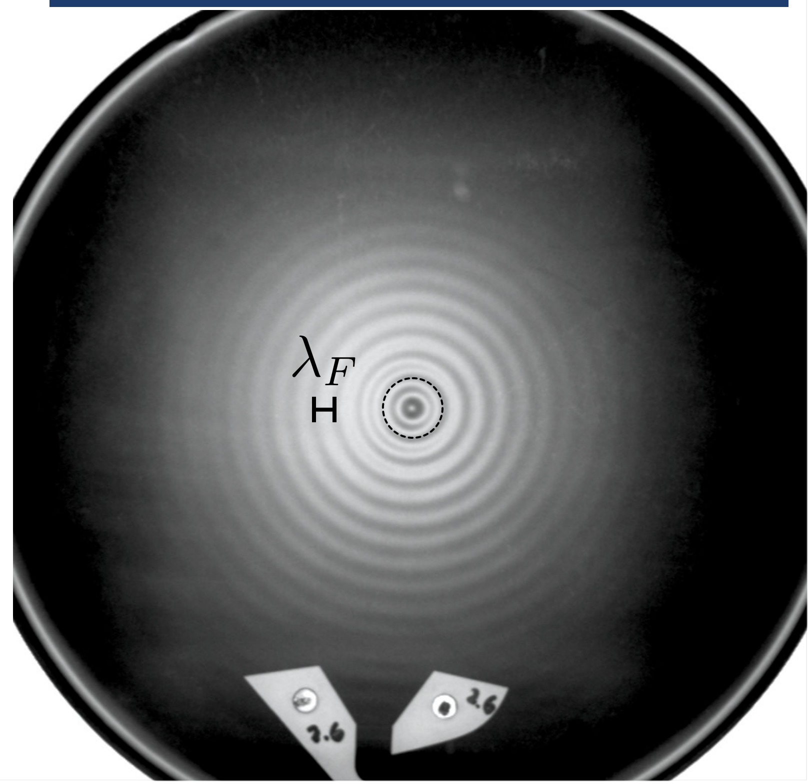

Central well excited above threshold.
Waves decay in shallower region

Well-induced trapping

EXPERIMENTS

TRAJECTORIES

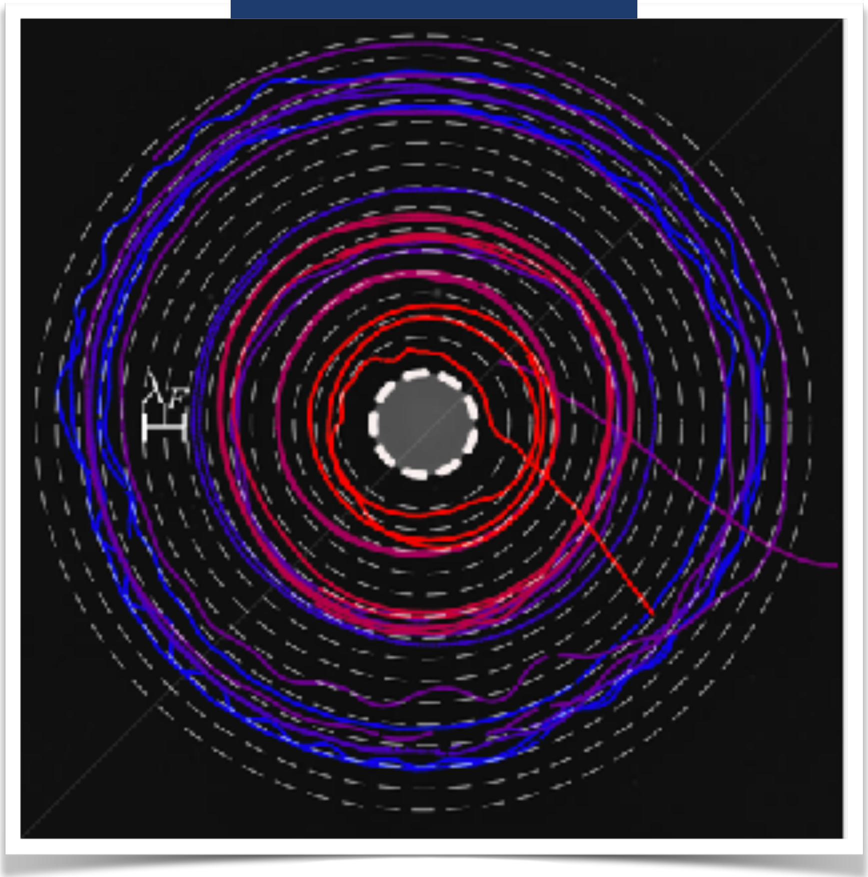

WELL-INDUCED WAVEFIELD

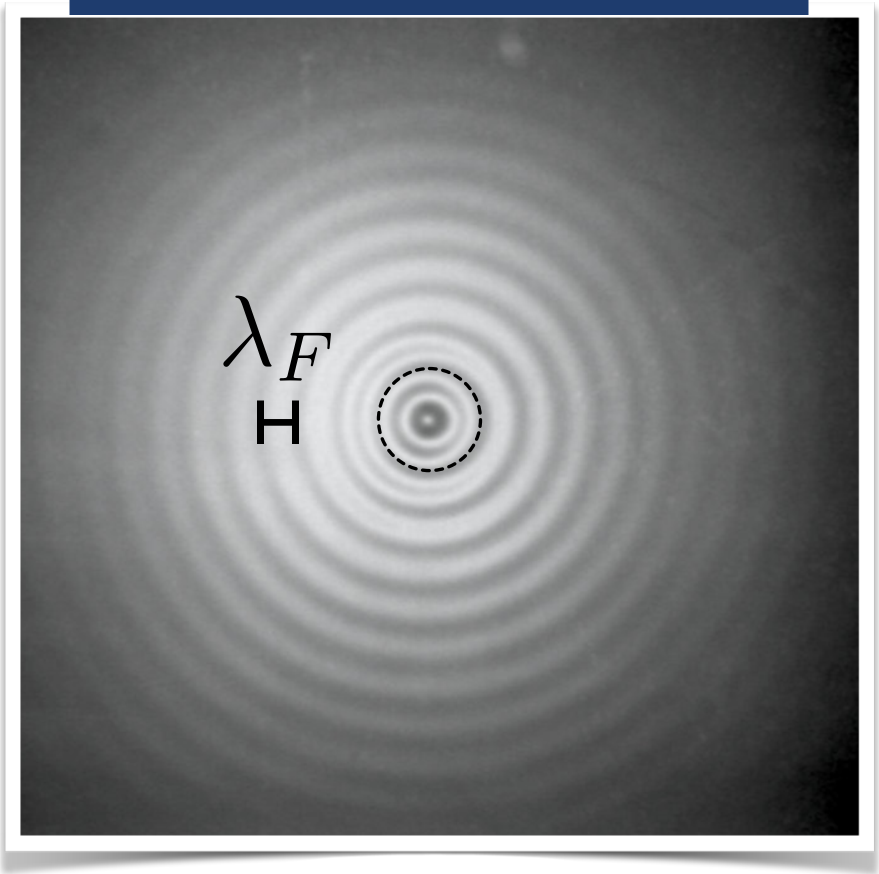

Conjecture: adjacent orbits have drops with alternating bouncing phase.

$$h_w(\mathbf{x},t) = A_w J_0\left(|k_F\mathbf{x}|\right)\sin(\pi f t)$$
$$\Rightarrow \mathcal{F} = -mg\nabla h_w$$

Simulated trajectories

$$m\ddot{\mathbf{x}}_p + D\dot{\mathbf{x}}_p = A\left(\underbrace{\int_{-\infty}^{t} \frac{J_1\left(k_F\left|\mathbf{x}_p(t)-\mathbf{x}_p(s)\right|\right)}{\left|\mathbf{x}_p(t)-\mathbf{x}_p(s)\right|}\left(\mathbf{x}_p(t)-\mathbf{x}_p(s)\right)e^{-(t-s)/(T_F M_e)}\,ds}_{\text{Drop-generated wave}} - \underbrace{\sigma J_1(k_F\mathbf{x}_p(t))}_{\text{Standing wave}}\right)$$

Circular solutions are quantized at troughs and crest of the standing wave field. All other radii are unstable.

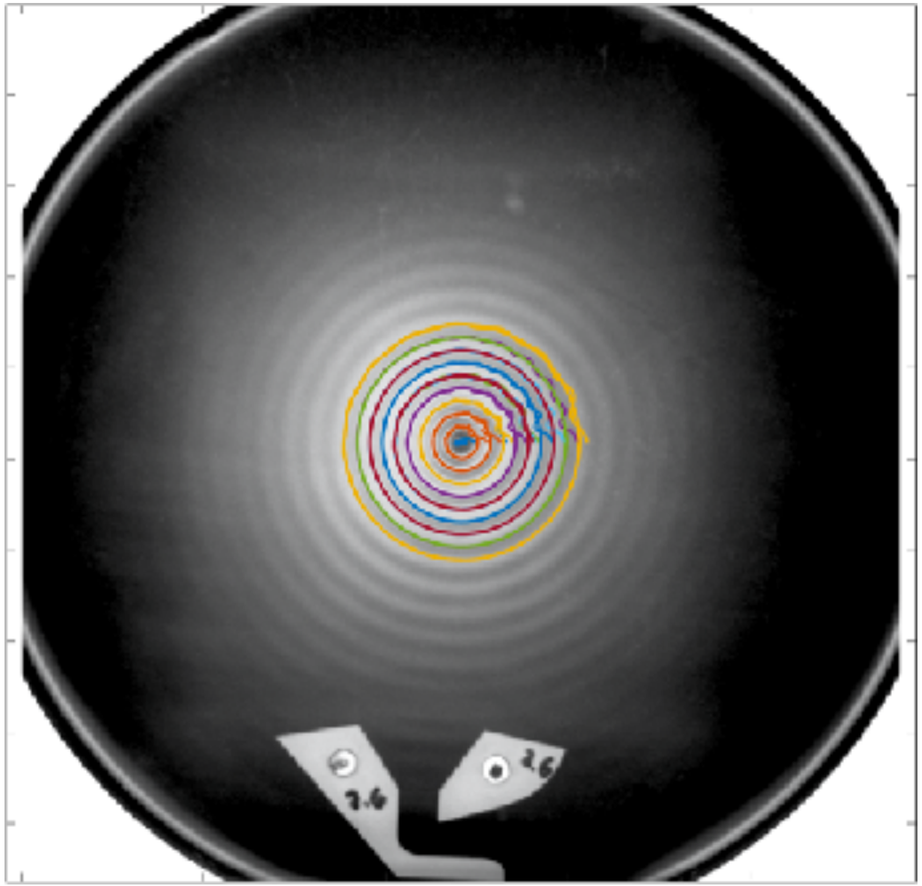

Simulated trajectories, overlaid on experimental photo

Well-induced trapping

EXPERIMENTS

TRAJECTORIES

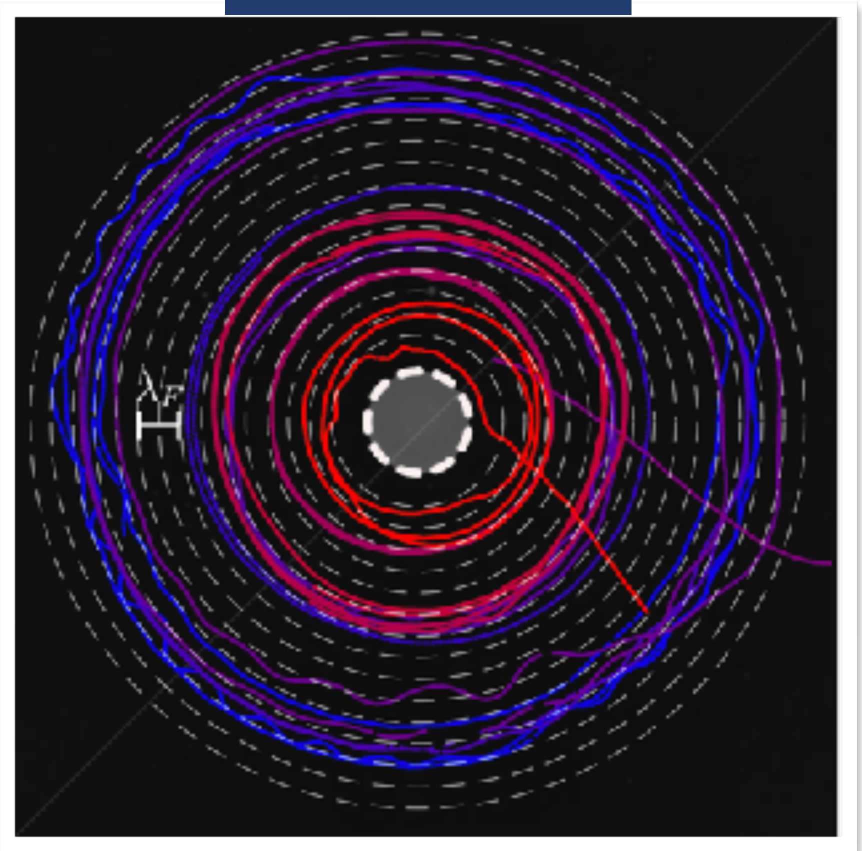

SIMULATIONS

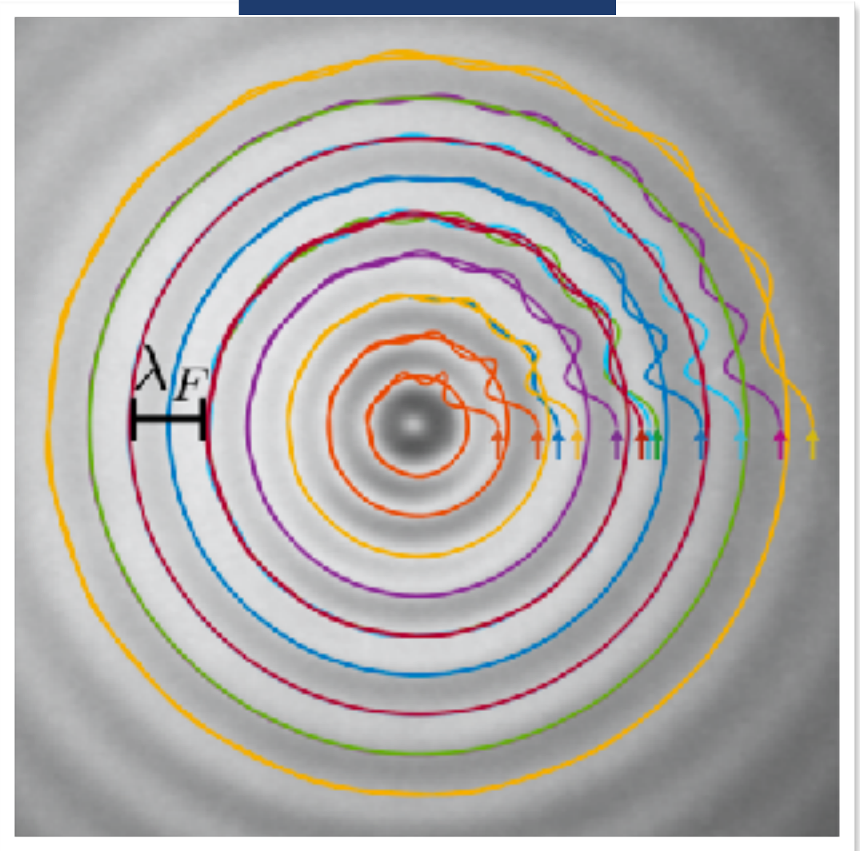

$$\kappa \ddot{\mathbf{x}}_p + \dot{\mathbf{x}}_p = \beta \int_{-\infty}^{t} \frac{J_1\left(|\mathbf{x}_p(t) - \mathbf{x}_p(s)|\right)}{|\mathbf{x}_p(t) - \mathbf{x}_p(s)|} \left(\mathbf{x}_p(t) - \mathbf{x}_p(s)\right) e^{-(t-s)}\, \mathrm{d}s + Q J_1(|\mathbf{x}_p(t)|)\hat{\mathbf{r}}$$

For fluid-like parameters, *quantized circular orbits are stable.*

Can we find more interesting dynamics in the GPWF?

Generalized pilot-wave framework

TRAJECTORY EQUATION

$$\kappa \ddot{\mathbf{x}}_p + \dot{\mathbf{x}}_p = \beta \int_{-\infty}^{t} \frac{J_1\left(|\mathbf{x}_p(t) - \mathbf{x}_p(s)|\right)}{|\mathbf{x}_p(t) - \mathbf{x}_p(s)|} \left(\mathbf{x}_p(t) - \mathbf{x}_p(s)\right) e^{-(t-s)}\, \mathrm{d}s + \tilde{\mathcal{F}}$$

Parameters κ, β may be tuned independently in this framework.

We also consider different applied forces to constrain dynamics.

$$\tilde{\mathcal{F}} = \tilde{\mathcal{F}}_O + \tilde{\mathcal{F}}_H$$

$$\text{Oscillatory: } \tilde{\mathcal{F}}_O(\mathbf{x}_p) = Q J_1(|\mathbf{x}|)\hat{\mathbf{r}}$$

$$\text{Harmonic: } \tilde{\mathcal{F}}_H(\mathbf{x}_p) = -k\mathbf{x}$$

Transient switching to stable orbit

$\kappa = 0.14, \beta = 252.8$

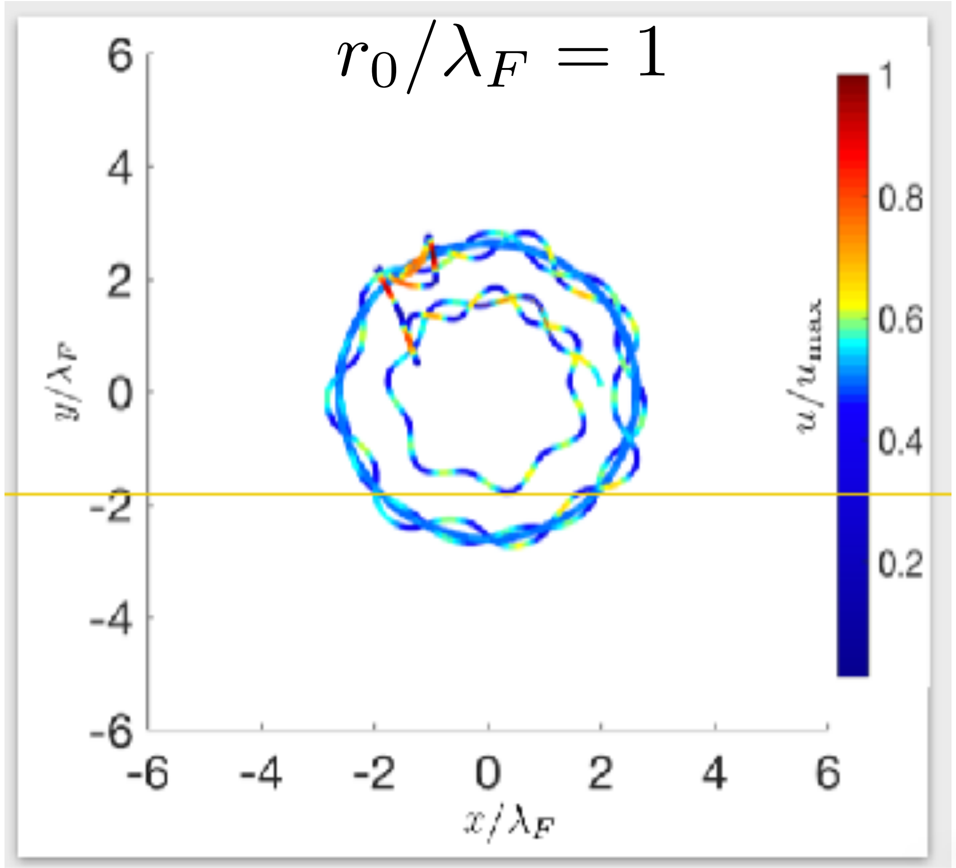

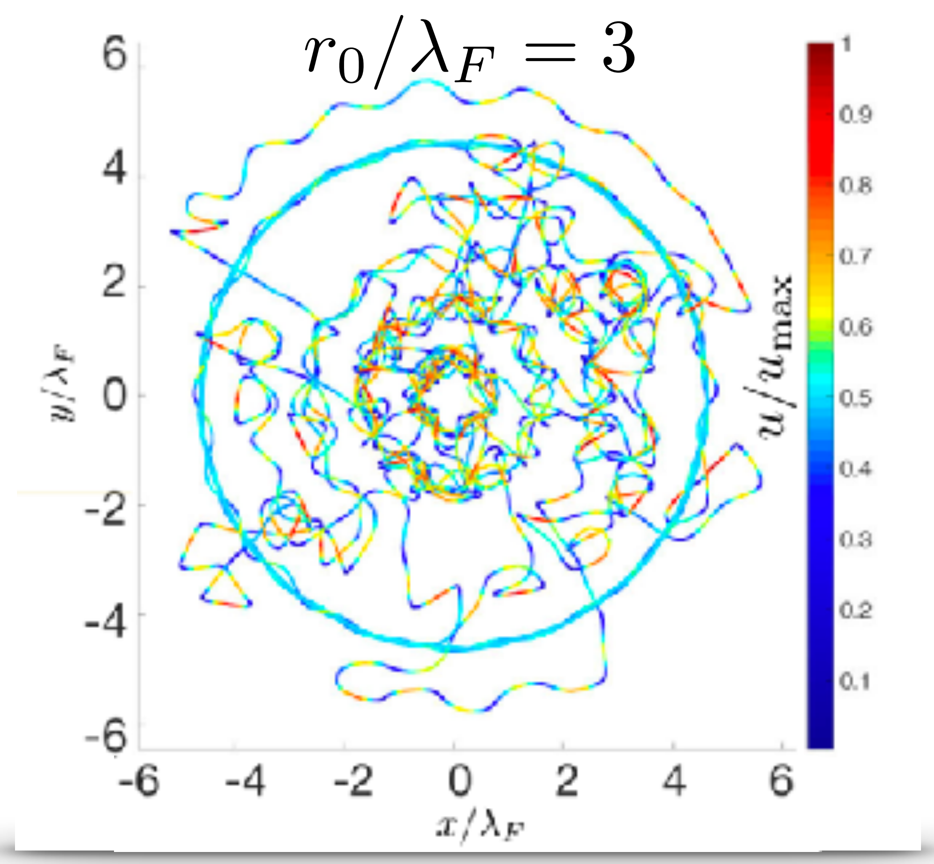

$$\kappa \ddot{\mathbf{x}}_p + \dot{\mathbf{x}}_p = \beta \int_{-\infty}^{t} \frac{J_1\left(|\mathbf{x}_p(t) - \mathbf{x}_p(s)|\right)}{|\mathbf{x}_p(t) - \mathbf{x}_p(s)|} \left(\mathbf{x}_p(t) - \mathbf{x}_p(s)\right) e^{-(t-s)}\,\mathrm{d}s + \tilde{\mathcal{F}}$$

Transient switching, then trapping

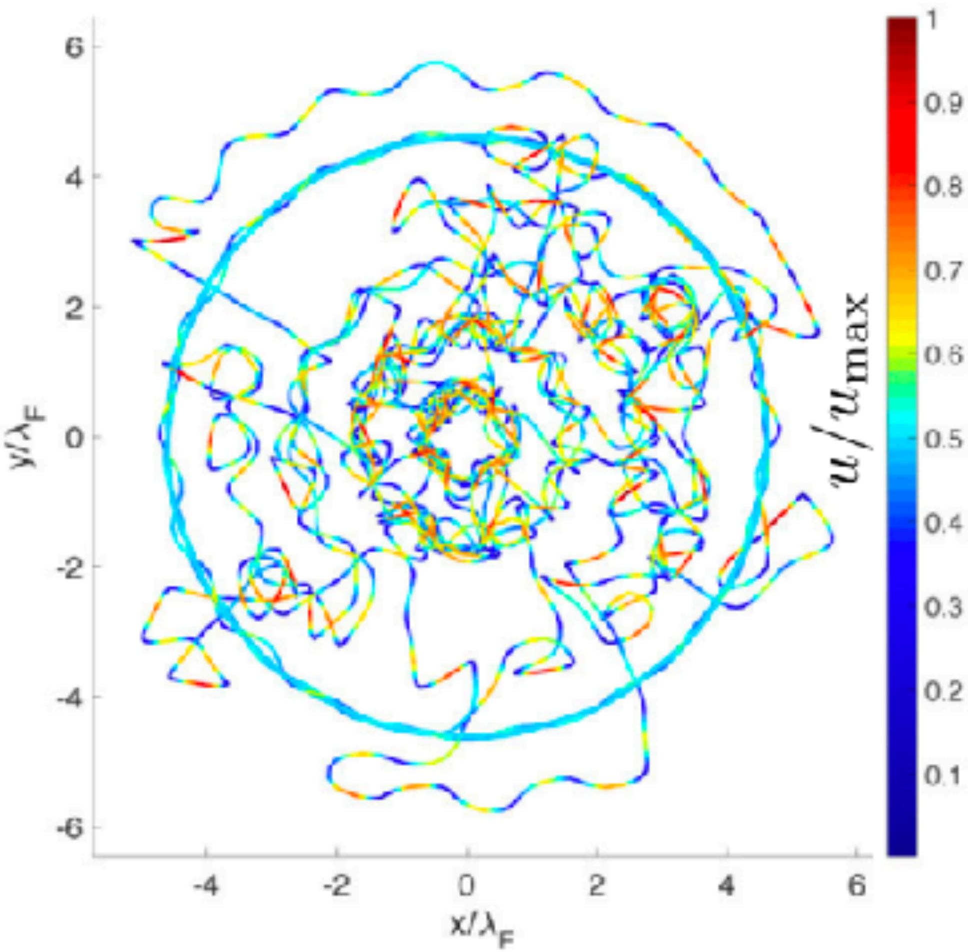

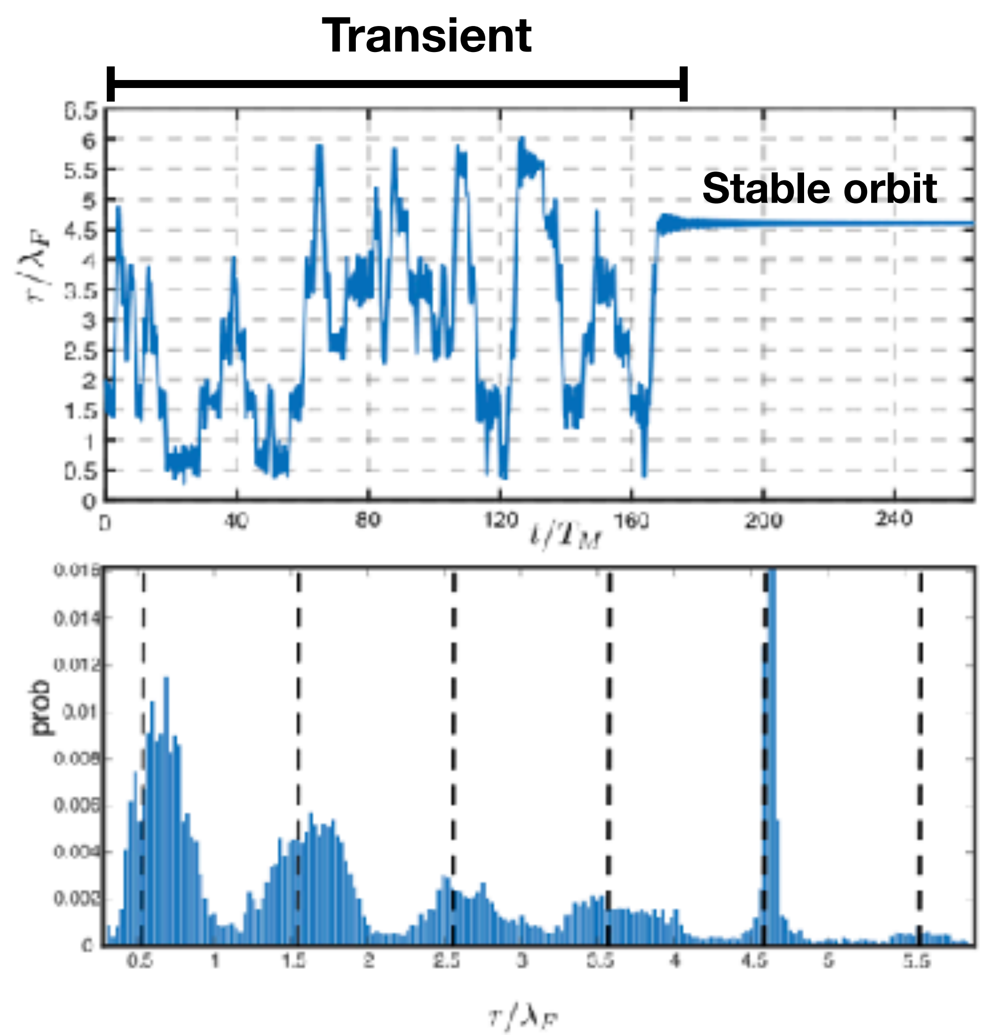

Transient switching between unstable orbits

$\tilde{\kappa} = 0.042, \beta = 152.8$

y/λ_F

x/λ_F

Achieves chaotic, statistically steady state

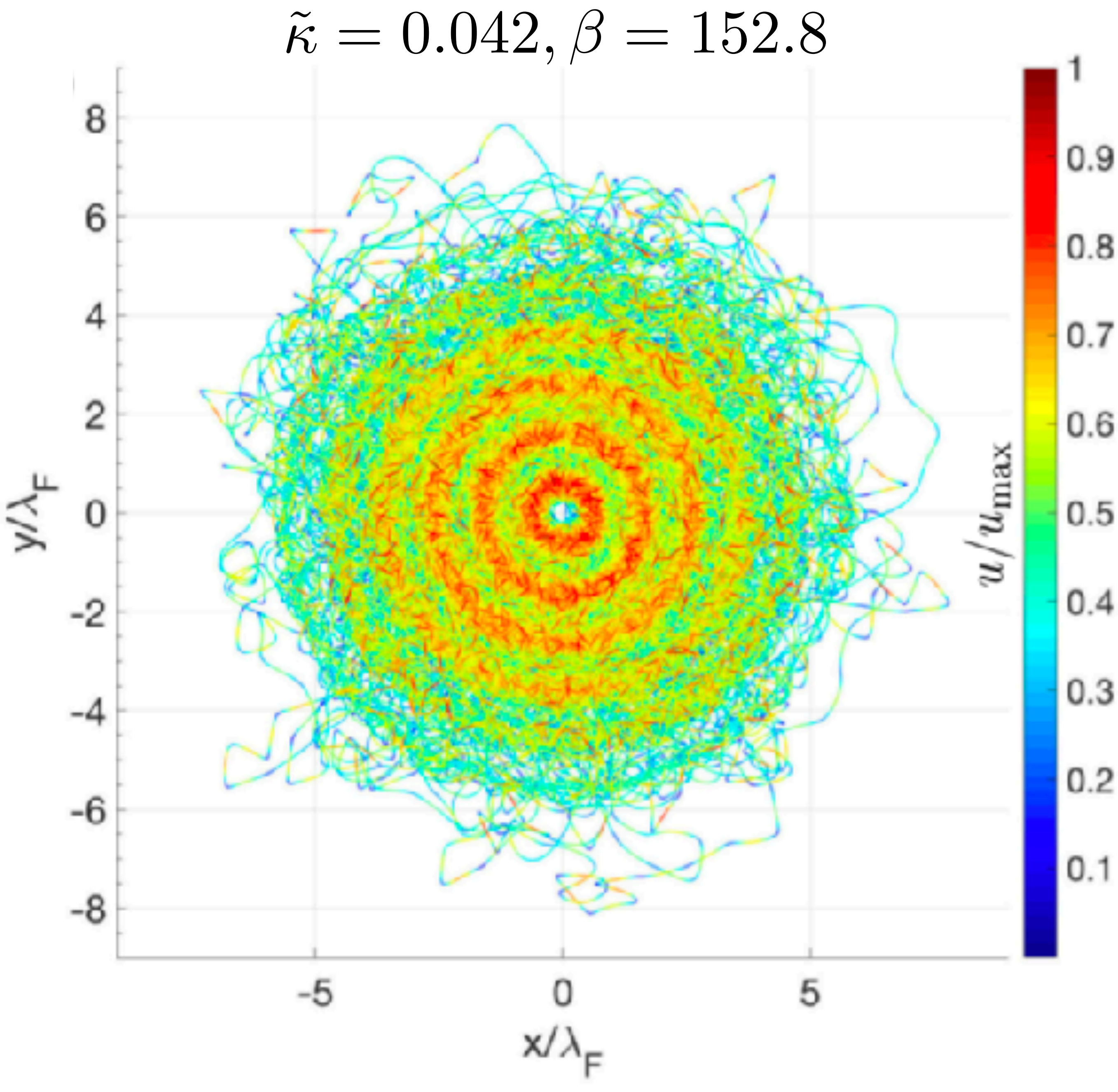

Chaotic switching between accessible unstable orbits

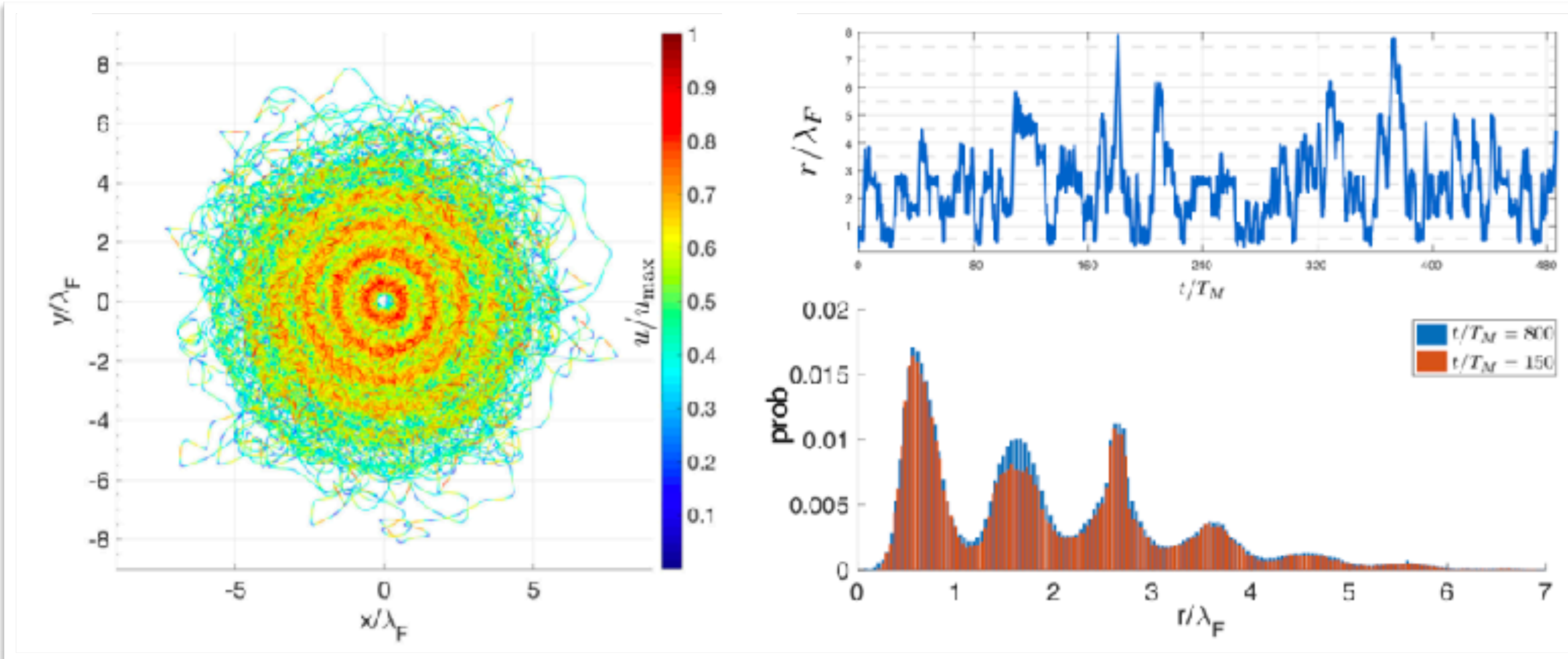

Statistical relaxation time: $\tau_S \sim 200T_M$

- characterized by chaotic switching between unstable circular eigenstates
- converges to a statistically steady state over a statistical relaxation time
- suggests *two unresolved timescales in QM: that of convergence of the pilot-wave field to its mean, and that of statistical convergence*

Rapid convergence of the instantaneous to the mean pilot wave

(Tambasco & Bush, 2018)

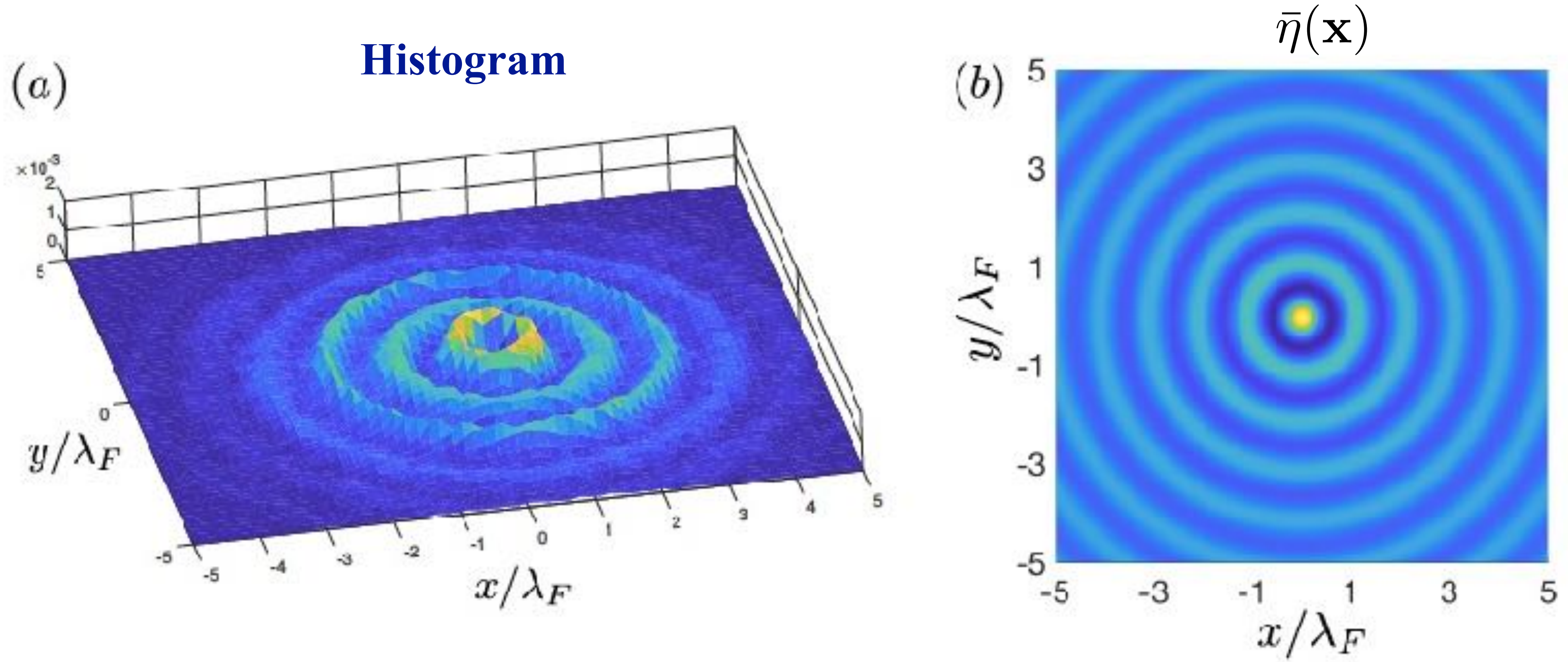

- mean wave field rapidly converges to convolution result $\bar{\eta}(\mathbf{x}) = \eta_B * \mu(\mathbf{x})$
- thereafter, the system approaches a statistically steady state
- the particle feels the mean pilot-wave potential long before statistical convergence

→ **the mean pilot-wave field acts as an imposed potential**

Rapid convergence of the instantaneous to the mean pilot wave

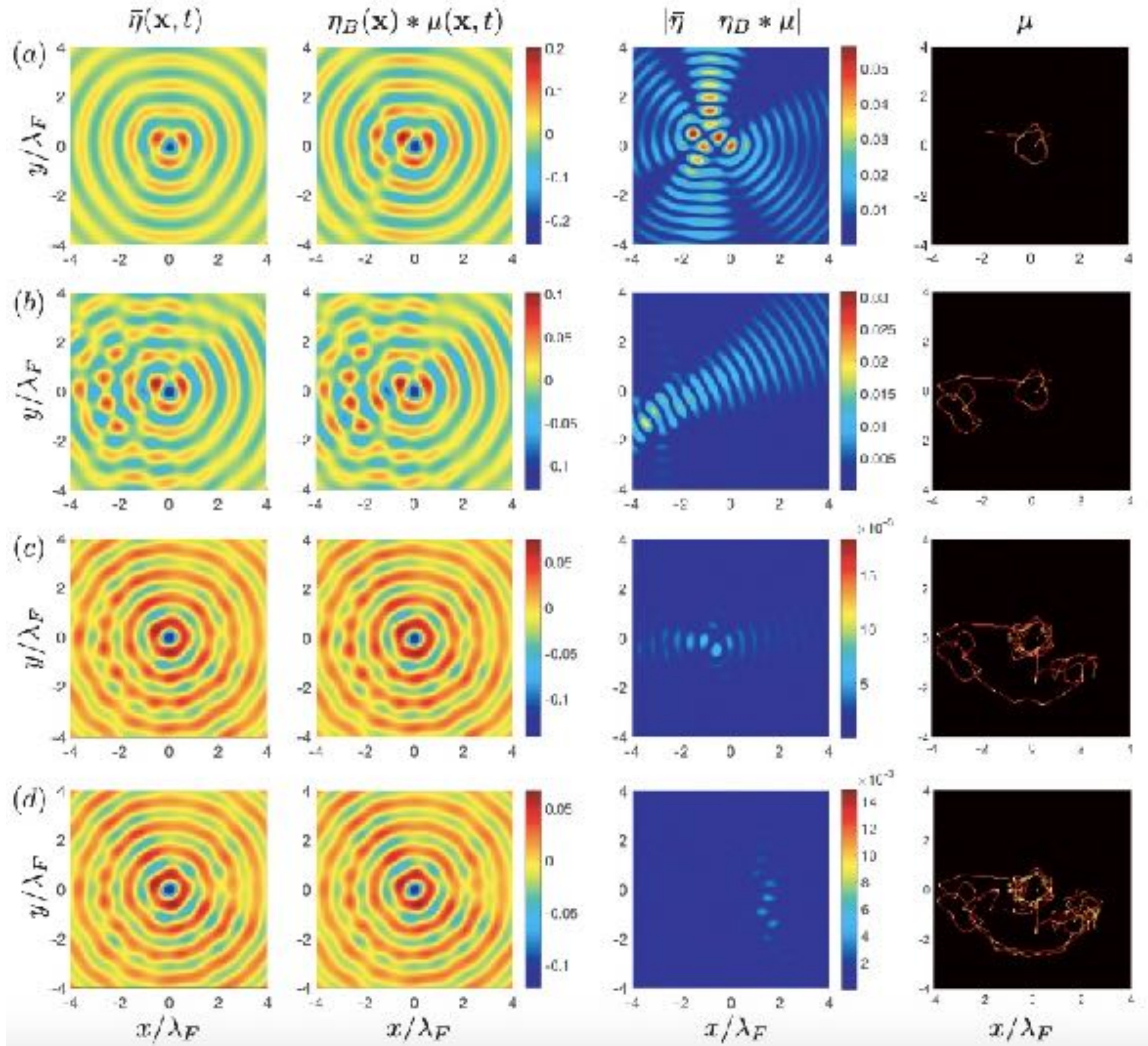

$t/T_M = 3.5$

$t/T_M = 8.2$

$t/T_M = 22.3$

$t/T_M = 34.0$

Summary

- used an underlying well-induced wavefield to achieve orbital trapping
- considered the generalized pilot-wave framework to reveal a richer dynamics, including *chaotically switching states*
- demonstrated that *the mean wavefield* (as deduced by Durey's Theorem) is established well before the statistics have converged
- the *statistical relaxation time* is much longer than the timescales of establishment of the mean pilot-wave field
- beyond the establishment of the mean wave field, the droplet feels this *self-induced potential*

3D Pilot-Wave Dynamics

with Adam Kay, Matt Durey

- does the discontinuity in drop-bath interaction in 2D preclude pilot-wave modeling in 3D?

Physical picture

Particle is source of spherically symmetric waves

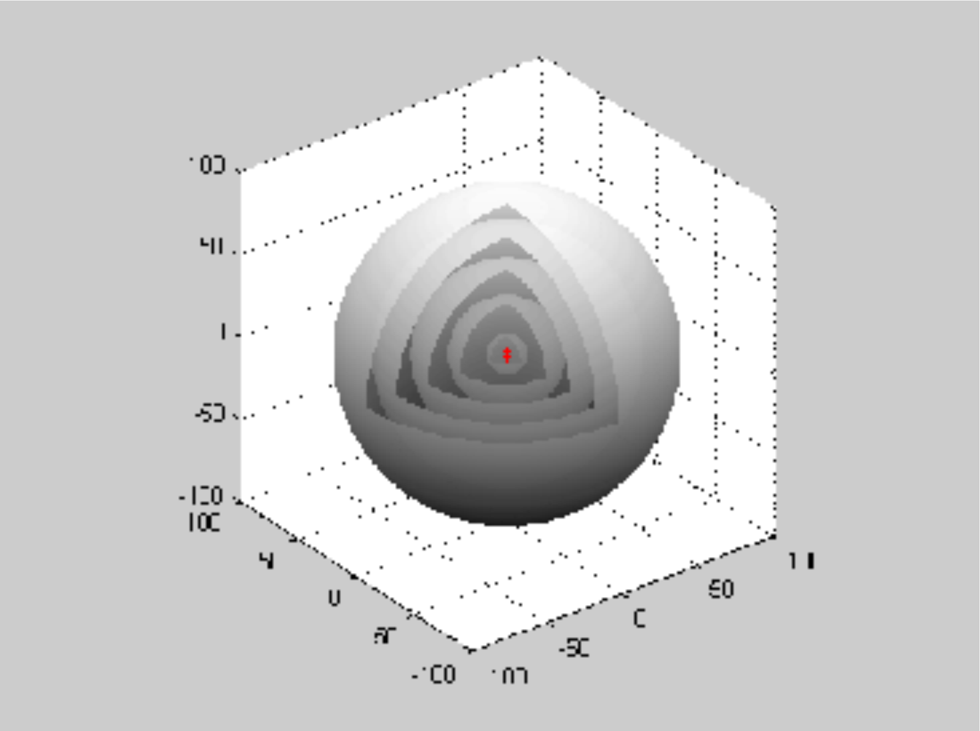

Wave field may destabilize stationary particle

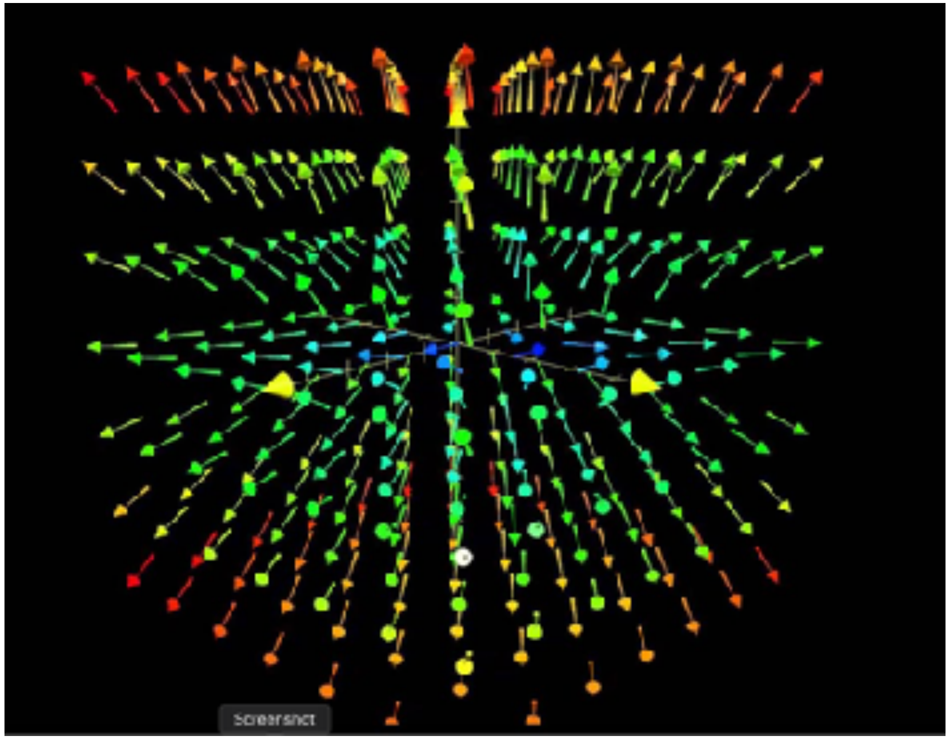

Generalized Pilot-Wave Dynamics: moving to 3D

- a mathematical bridge between macroscopic and microscopic pilot-wave theories

Trajectory equation:

$$\kappa_0 \ddot{\mathbf{x}}_p + \dot{\mathbf{x}}_p = -3\nabla h(\mathbf{x}_p, t)$$

Pilot waveform:

$$h(\mathbf{x}, t) = \int_{-\infty}^{t} \mathcal{H}(k|\mathbf{x} - \mathbf{x}_p(s)|) e^{-\mu(t-s)} ds$$

Wave kernel:

$\mathcal{H} = \cos(x)$ **in 1D**

$\mathcal{H} = J_0(x)$ **in 2D**

$\mathcal{H} = j_0(x)$ **in 3D**

Two dimensionless parameters:

Magnitude of inertial force
(i.e. dimensionless mass)

$$\kappa_0 = \frac{m}{\tau_0 D}$$

Magnitude of wave force
(i.e. dimensionless memory)

$$\mu = \frac{\tau_0}{\tau} = 1 - \Gamma$$

Walking threshold	High memory
$\Gamma = 0$	$\Gamma = 1$
$\mu = 1$	$\mu = 0$

The 3D pilot-wave field

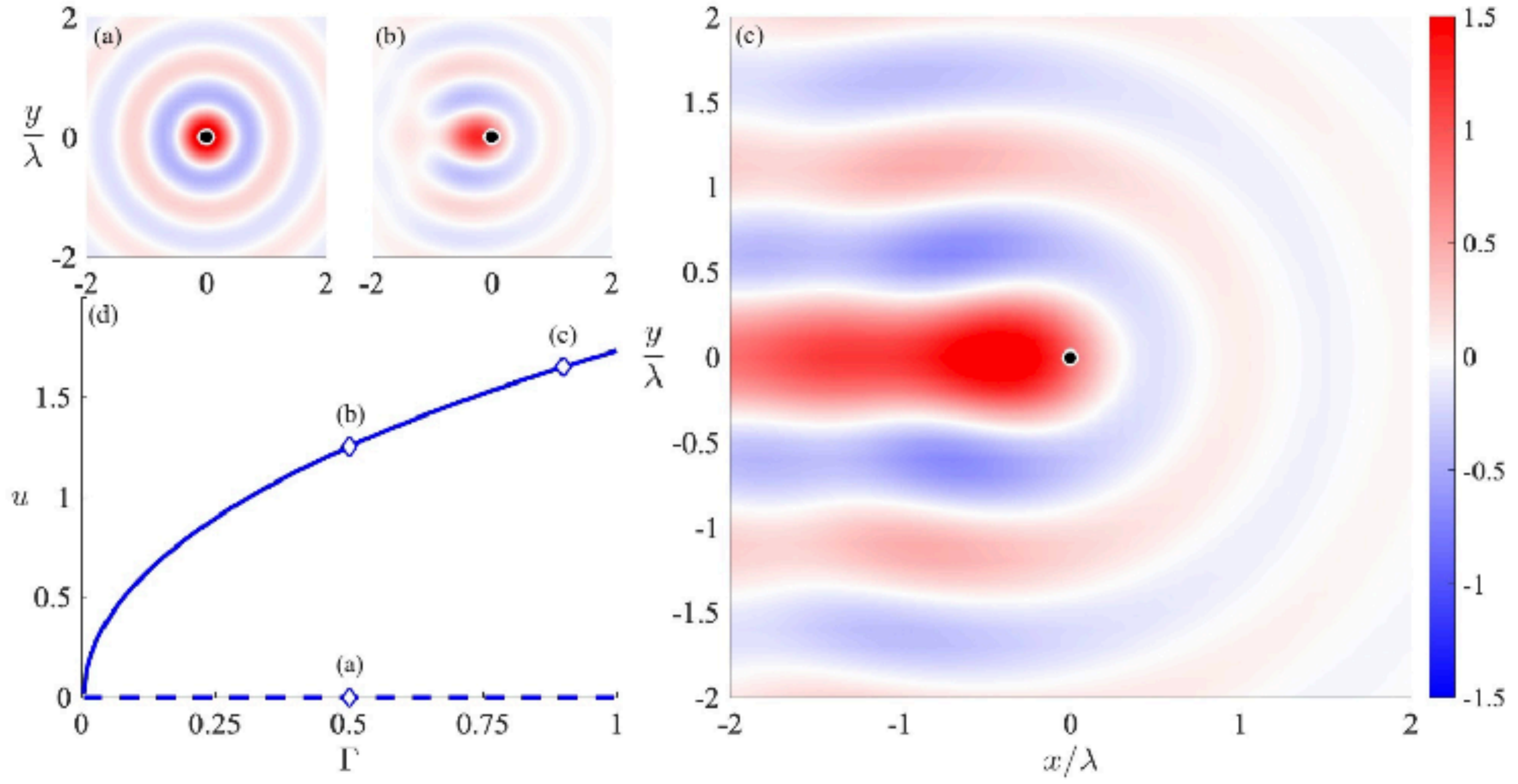

Helical spin states

$$\mathbf{x}(t) = r\cos\omega t\ \mathbf{i} + r\sin\omega t\ \mathbf{j} + vt\ \mathbf{k}$$

- may exist provided:

$$-\kappa_0\omega_0^2 = 3\int_0^\infty \frac{j_1(D)}{D}\left(1-\cos\omega_0\tau\right)e^{-\mu\tau}d\tau$$

$$\omega_0 = 3\int_0^\infty \frac{j_1(D)}{D}\sin(\omega_0\tau)e^{-\mu\tau}d\tau$$

$$1 = 3\int_0^\infty \frac{j_1(D)}{D}\tau e^{-\mu\tau}d\tau$$

where $D = \sqrt{4r^2\sin^2\frac{\omega\tau}{2} + v^2\tau^2}$

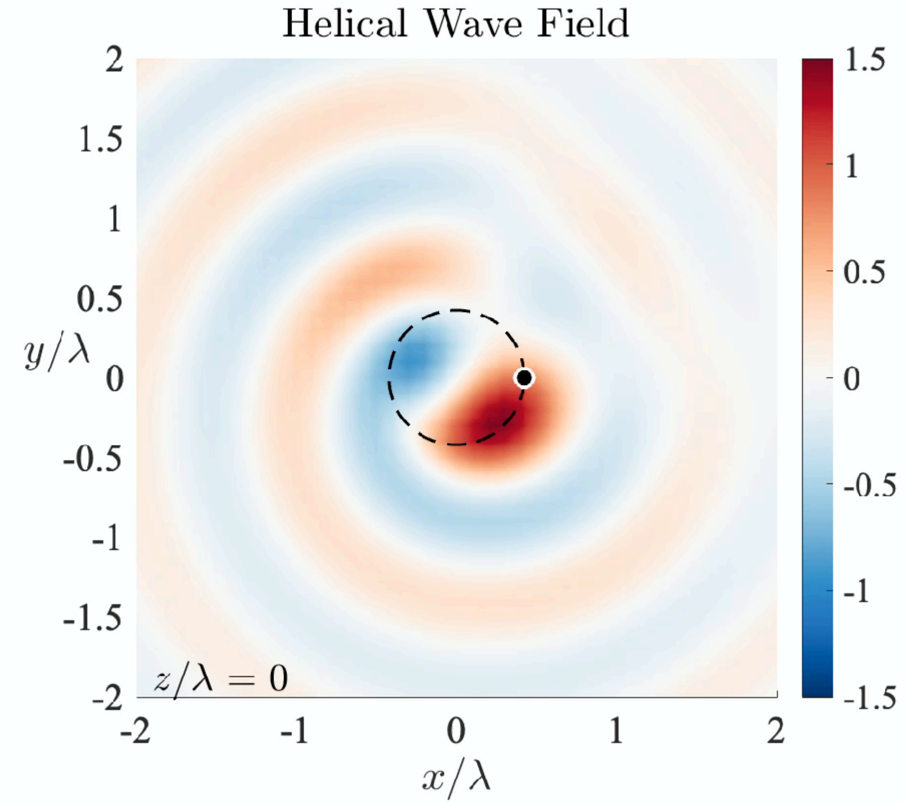

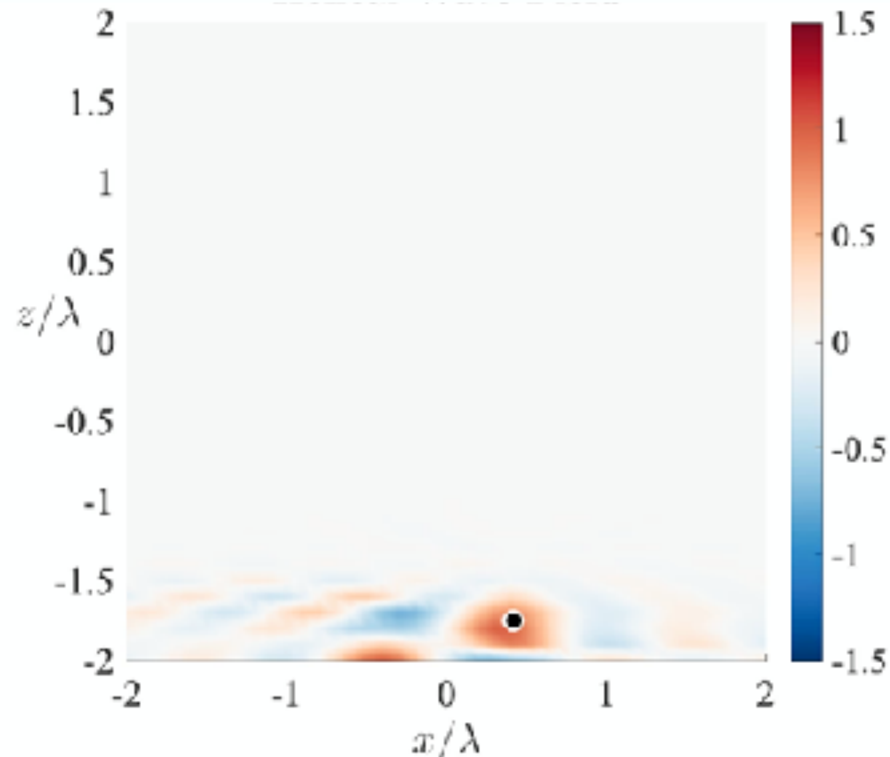

Helical spin states

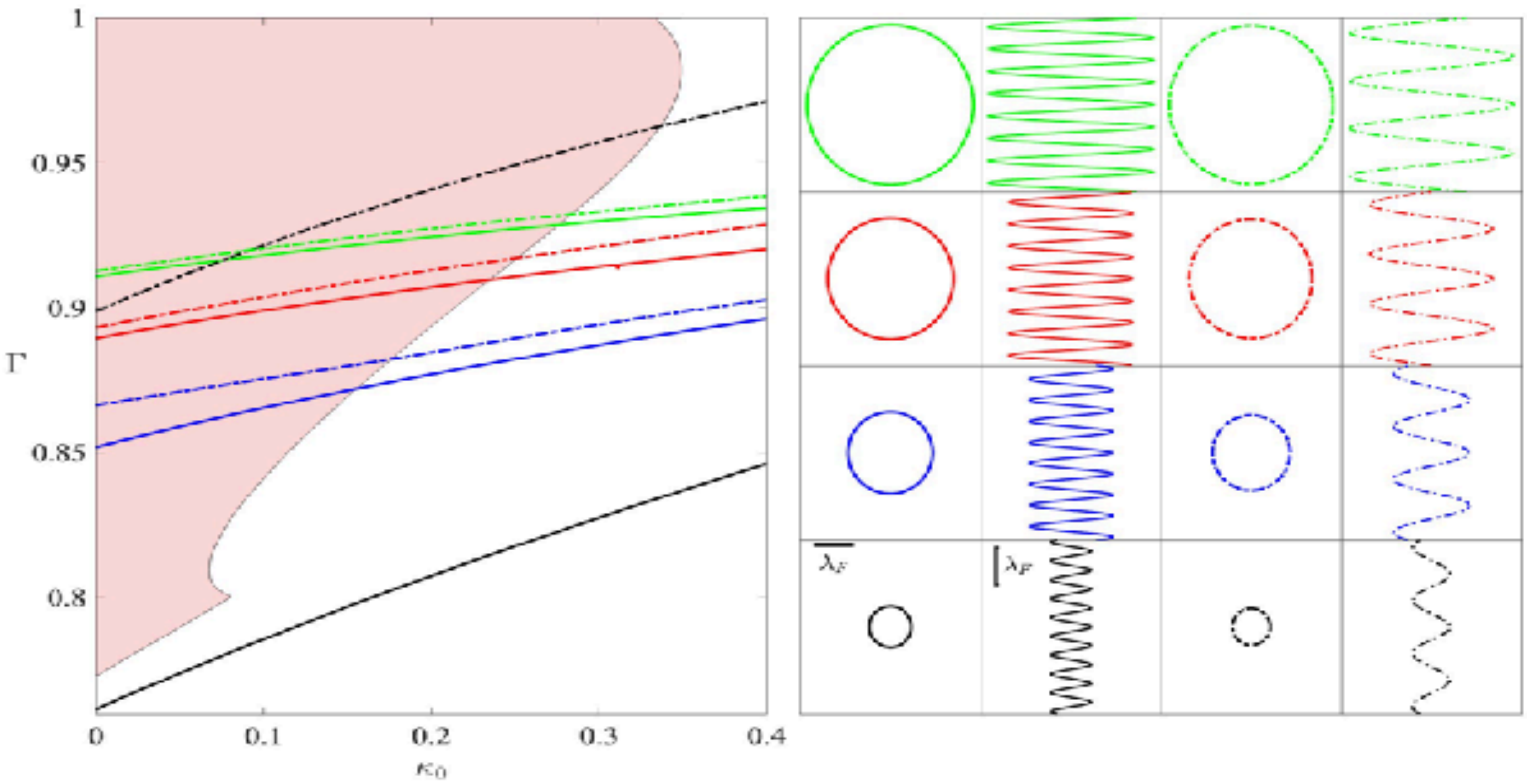

- double quantization, with discrete solutions in both radius, and pitch angle.

Regime diagram in 3D

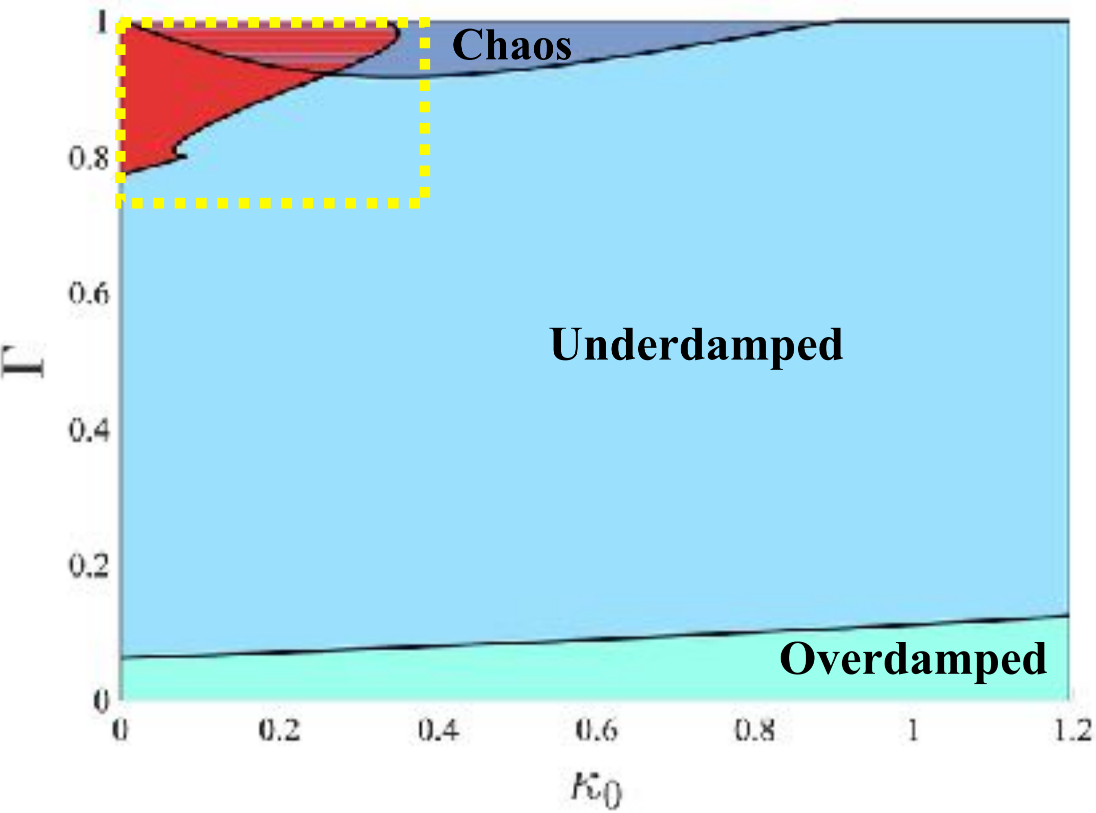

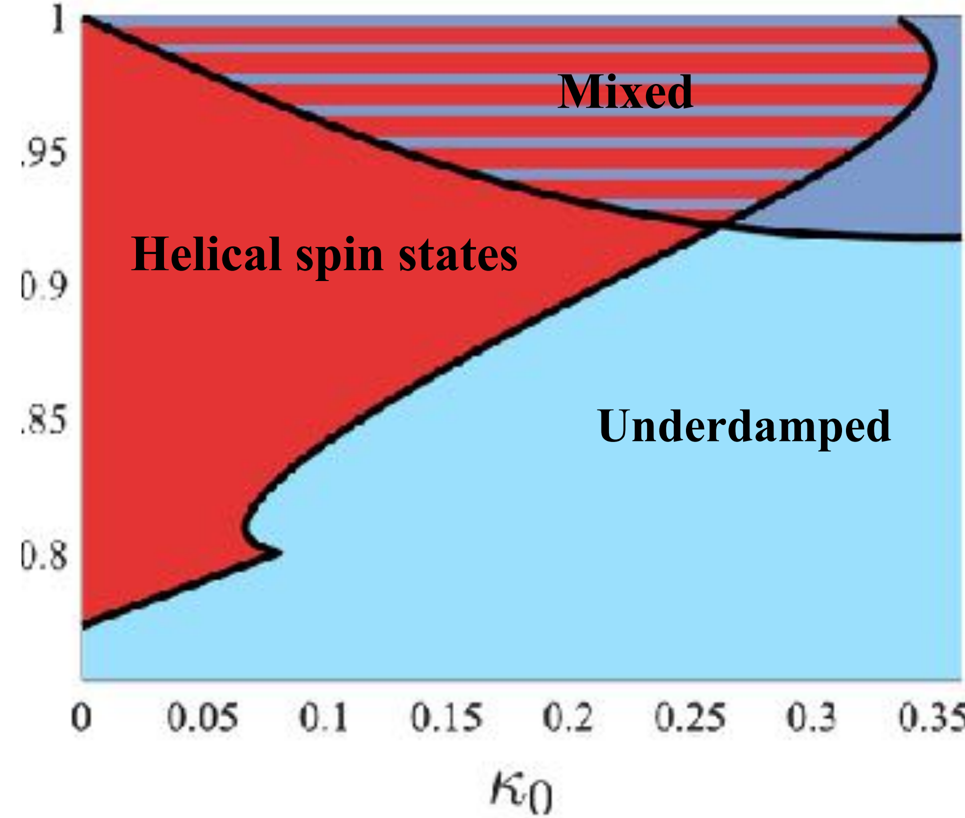

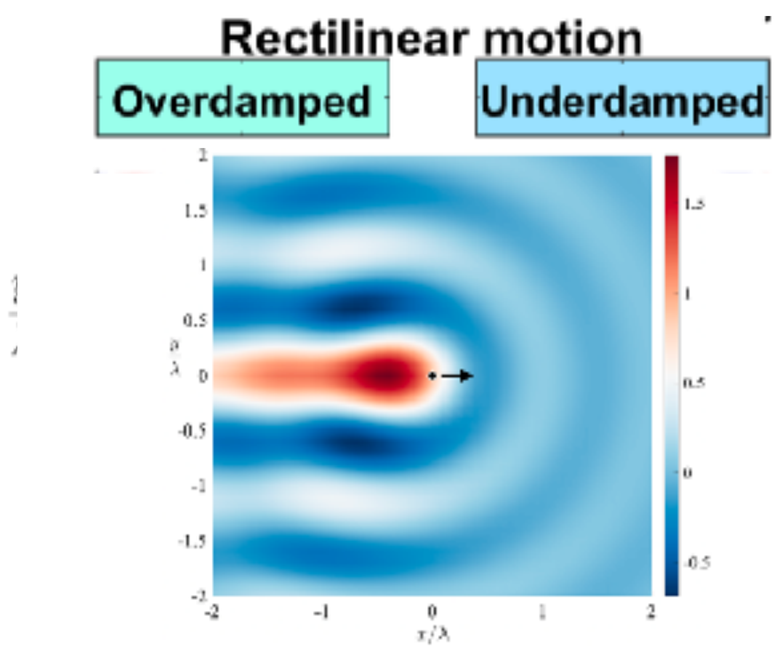

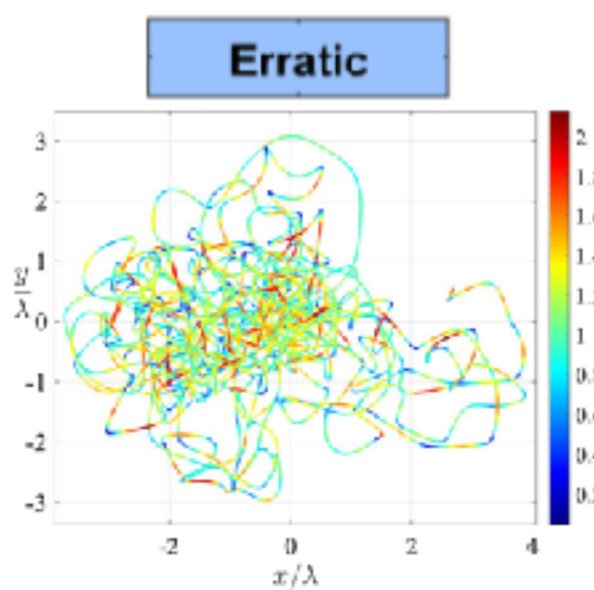

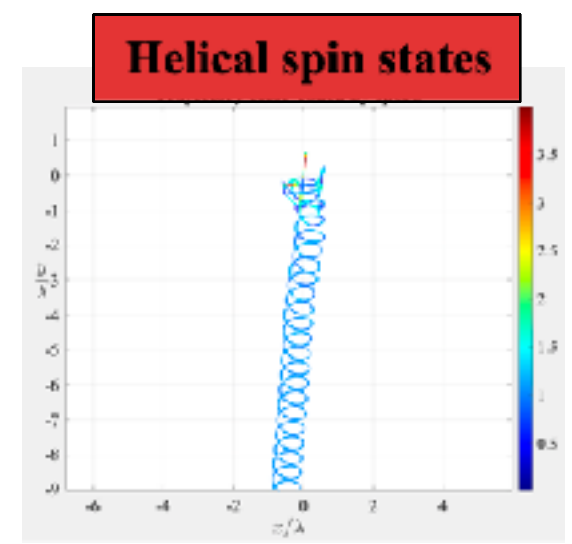

A generalized pilot-wave framework

(Bush ARFM 2015, *Durey & Bush, 2020*)

- retain key features of walker system

  (memory, resonance, quasi-monochromatic wave field)

- explore beyond the range of the hydrodynamic system

- discovered new quantum features

  - *stable spin states, purely stochastic regime, in-line oscillations*

- extended to 3D, where helical spin states were found

- connect to and inform quantum pilot-wave theories

BIG PICTURE

- the landscape before PWH: classical mechanics and quantum mechanics

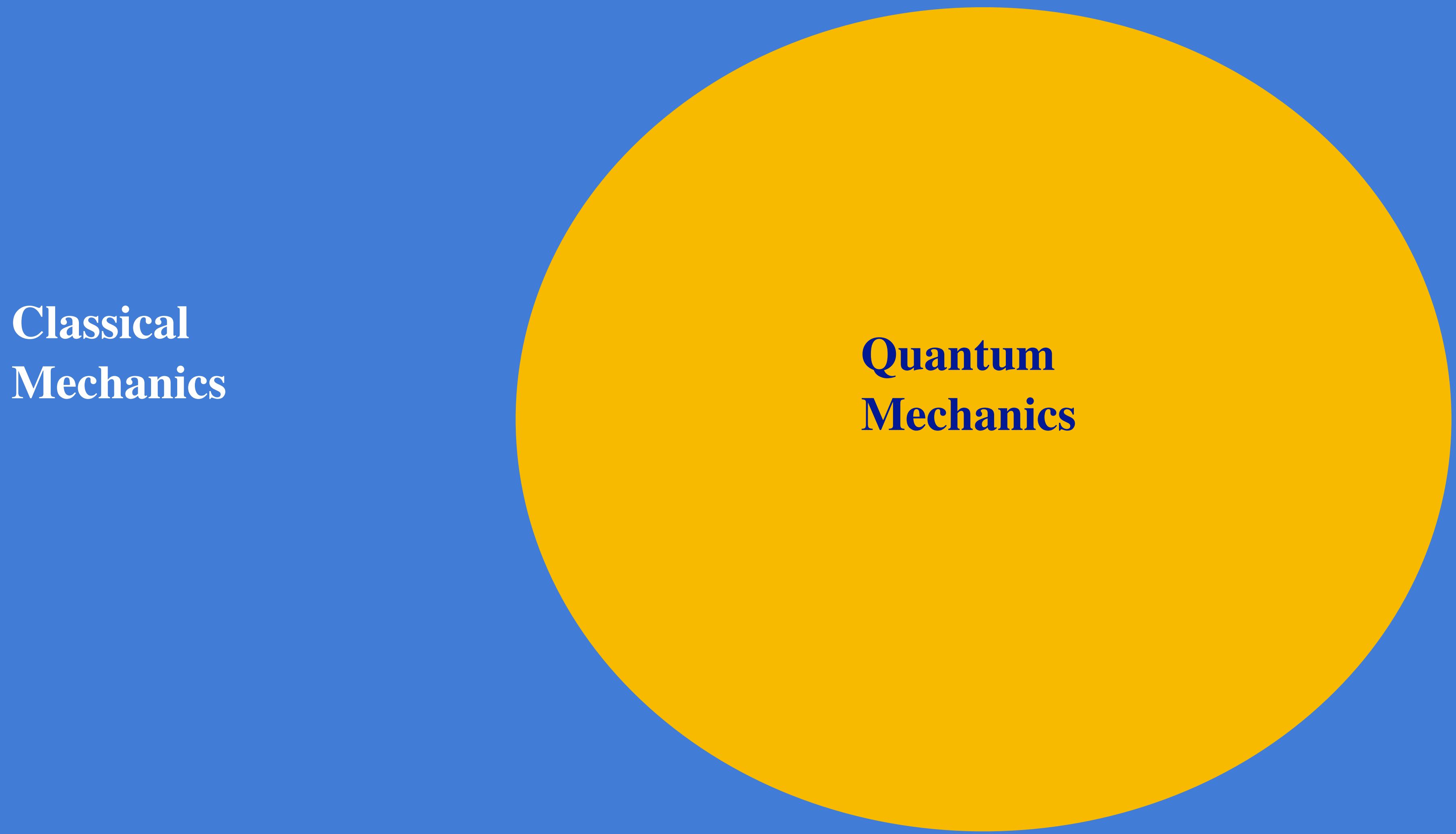

BIG PICTURE

- enter pilot-wave hydrodynamics

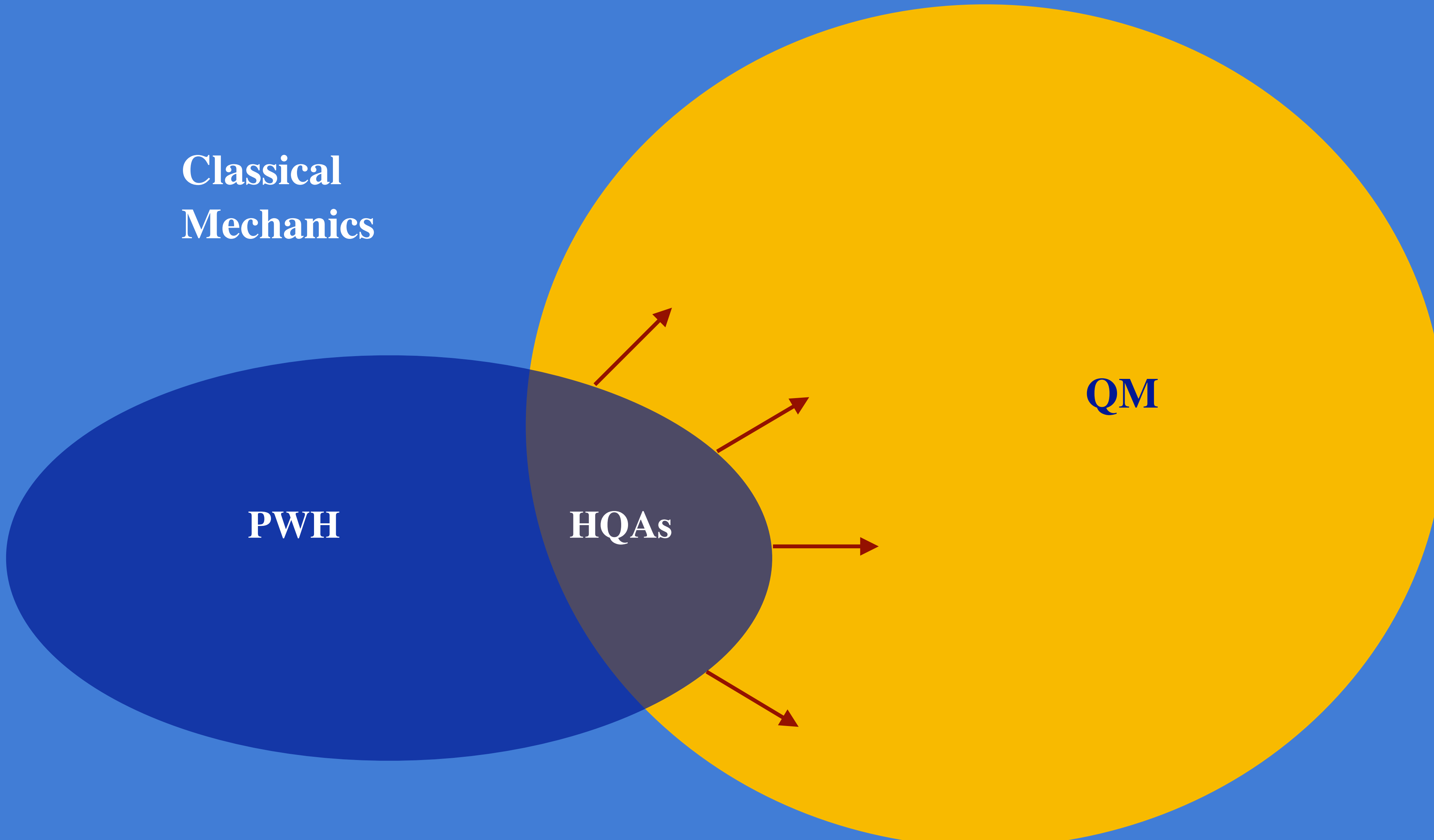

BIG PICTURE

- has motivated exploration of the Generalized Pilot-wave Framework